Genetic architecture of phenotypic differences between endangered hybridizing *Arabis* floodplain species



Inaugural-Dissertation

zur

Erlangung des Doktorgrades der Mathematisch-Naturwissenschaftlichen Fakultät der Universität zu Köln

vorgelegt von

Neda Rahnamae

aus Maschhad, Iran

Köln, 2025

Reviewer 1: Prof. Dr. Juliette de Meaux

Reviewer 2: Prof. Dr. George Coupland

Assessor (Beisitzer): Dr. Margarita Takou

Tag der Disputation: 05.02.2025

List of Figures

Figure	Page
Figure 1. Dry root-to-shoot ratio distribution in <i>Arabis</i> species.	29
Figure 2. Dry biomass distribution in <i>Arabis</i> species.	30
Figure 3. Dry biomass distribution in <i>Arabis</i> species of the Rhine population.	31
Figure 4. Phenotypes distribution of the mapping population.	35
Figure 5. Correlation network of phenotypic traits.	37
Figure 6. Correlation heatmap of phenotypic traits.	38
Figure 7. Synteny and rearrangement plot between <i>A. nemorensis</i> and <i>A. sagittata</i> genomes.	40
Figure 8. Correlation between SNPs genetic and physical distance.	42
Figure 9. Mosaic plot of SNP distribution along the genome in the <i>Arabis</i> mapping population.	43
Figure 10. Segregation distortion and strength of selection along the genome.	44
Figure 11. Genetic map with QTLs for ecologically relevant traits.	45
Figure 12. QTLs LOD score distribution.	46

Figure	Page
Figure 13. Genetic architecture of fertility score.	47
Figure 14. Distribution of flowering time in <i>Arabis</i> F3 hybrids.	51
Figure 15. Fine-mapping of flowering time QTL #1, which explains 22.7% of flowering time variation.	53
Figure 16. Phenotypic correlations between Inflorescence Height and Flowering Time in <i>Arabis</i> F3 plants.	54
Figure 17. Phenotypic correlations between Rosette Diameter and Flowering Time in <i>Arabis</i> F3 plants.	55
Figure 18. Phenotypic correlations between Number of Shoots and Flowering Time in <i>Arabis</i> F3 plants.	56
Figure 19. Phenotypic correlations between Stem Height and Flowering Time in <i>Arabis</i> F3 plants.	57
Figure 20. Expression patterns of <i>PEP1</i> , <i>TFL1</i> , and <i>LFY</i> in response to seasonal changes in young and old <i>A. alpina</i> plants.	65
Figure 21. Phenotypic variation in fitness-related traits in <i>Arabis</i> .	67

List of Tables

Table	Page
Table 1. Overview of samples in the dry root-to-shoot ratio experiment in <i>Arabis</i> species.	28
Table 2. Statistical analysis of species effects on different traits under nutrient-limiting conditions.	30
Table 3. Phenotypic traits differences between parents.	32
Table 4. Results of reciprocal cross effect analysis on phenotypic traits.	34
Table 5. Assembly statistics of <i>Arabis</i> genomes.	39
Table 6. Genetic map overview.	41
Table 7. QTLs of ecologically relevant traits in the <i>Arabis</i> mapping population.	48
Table 8. Overview of <i>Arabis</i> F3 families' mean flowering time.	52

Abstract

Deciphering the genetic basis of ecological differences among hybridizing species is essential for

predicting their adaptive responses to climate change and human activities. Previous studies

identified a hybridization hotspot on the Rhine River, highlighting episodic gene flow between

Arabis nemorensis and A. sagittata. I quantified interspecific differences in 22 phenotypic traits

between these closely related species. To investigate the genetic architecture underlying these

differences, I constructed a genetic map for A. nemorensis and A. sagittata using an interspecific

F2 population of 742 individuals derived from reciprocal crosses of sympatric parents. The genetic

map, comprising 2,082 SNPs across eight linkage groups, provided a genetically validated

genome assembly for both species.

Using this map, I identified the genetic basis of 20 phenotypic traits, uncovering 58 quantitative

trait loci (QTLs) distributed across the genome. Analysis of fertility variation and segregation

distortions revealed six large-effect QTLs associated with significant fitness loss in hybrids. While

F2 hybrids generally exhibited lower seed production than parental lines, some hybrids displayed

extreme trait values and patterns of transgressive segregation. Incompatibility QTLs had a simple

genetic basis, and several ecologically relevant QTLs were independent of incompatibility loci,

indicating potential for hybrid offspring to combine novel trait combinations absent in either parent.

Fine mapping of the largest-effect QTL, associated with flowering time and explaining 23% of

phenotypic variation, conducted on 410 F3 individuals, identified TFL1 as a regulator close to age

pathway, excluding FLC and CO as contributors within this QTL region. Lastly, contrary to our

expectations, A. nemorensis showed a larger biomass. Also unexpectedly, the root-to-shoot ratio

did not differ significantly between the species. These observations suggest potential genetic

similarities in their nutrient allocation strategies. However, I recommend further experiments under

varying soil conditions to validate these findings.

Keywords: introgression, RAD sequencing, QTL mapping, incompatibilities, *TFL1*.

7

Zusammenfassung

Die Entschlüsselung der genetischen Grundlagen ökologischer Unterschiede zwischen hybridisierenden Arten ist wesentlich, um ihre adaptiven Reaktionen auf den Klimawandel und menschliche Aktivitäten vorherzusagen. Frühere Studien identifizierten Hybridisierungshotspot am Rhein, der episodischen Genfluss zwischen Arabis nemorensis und A. sagittata hervorhebt. Ich quantifizierte interspezifische Unterschiede in 22 phänotypischen Merkmalen zwischen diesen eng verwandten Arten. Um die genetische Architektur, die diesen Unterschieden zugrunde liegt, zu untersuchen, erstellte ich eine genetische Karte für A. nemorensis und A. sagittata unter Verwendung einer interspezifischen F2-Population von 742 Individuen, die aus reziproken Kreuzungen sympatrischer Eltern abgeleitet wurden. Die genetische Karte, die 2.082 SNPs über acht Kopplungsgruppen umfasst, lieferte eine genetisch validierte Genomassemblierung für beide Arten.

Mit dieser Karte identifizierte ich die genetische Basis von 20 phänotypischen Merkmalen und entdeckte 58 quantitative Trait-Loci (QTLs), die über das Genom verteilt sind. Die Analyse der Fruchtbarkeitsvariation und der Segregationsverzerrungen zeigte sechs QTLs mit großer Wirkung, die mit signifikanten Fitnessverlusten bei Hybriden assoziiert sind. Während F₂-Hybriden im Allgemeinen eine geringere Samenproduktion als die Elternlinien aufwiesen, zeigten einige Hybriden extreme Merkmalswerte und Muster transgressiver Segregation. Inkompatibilitäts-QTLs hatten eine einfache genetische Grundlage, und mehrere ökologisch relevante QTLs waren unabhängig von Inkompatibilitätsloci, was auf das Potenzial der Hybridnachkommen hinweist, neuartige Merkmalskombinationen zu kombinieren, die in keinem der Eltern vorhanden sind.

Die Feinkartierung des QTL mit der größten Wirkung, das mit der Blütezeit assoziiert ist und 23 % der phänotypischen Variation erklärt, durchgeführt an 410 F3-Individuen, identifizierte *TFL1* als Regulator nahe dem *Altersweg* und schloss *FLC* und *CO* als Beitragende innerhalb dieser QTL-Region aus. Letztlich zeigte *A. nemorensis* entgegen unseren Erwartungen eine größere Biomasse. Auch unerwartet unterschied sich das Wurzel-Spross-Verhältnis zwischen den Arten nicht signifikant. Diese Beobachtungen deuten auf potenzielle genetische Ähnlichkeiten in ihren Strategien zur Nährstoffverteilung hin. Allerdings empfehle ich weitere Experimente unter unterschiedlichen Bodenbedingungen, um diese Ergebnisse zu validieren.

Contents

List of Figures	4
List of Tables	6
Abstract	7
Zusammenfassung	8
Contents	9
1. Introduction	11
1.1. Species responses to rapid environmental changes	11
1.1.1. Adaptive Phenotypic Plasticity	11
1.1.2. Dispersal to Other Habitats	12
1.1.3. Selection of New Mutations	13
1.1.4. Introgression of Pre-adapted Alleles	13
1.2. Interspecific hybridization	14
1.3. Study system	16
1.4. Thesis aims	16
1.4.1. Chapter 1: Growth variation under nutrient-limiting condition	ons16
1.4.2. Chapter 2: Genetic architecture of phenotypic differences hybridizing <i>Arabis</i> floodplain species	_
1.4.3. Chapter 3: Flowering time QTL fine-mapping	17
2. Materials and Methods	19
Chapter 1: Growth variation under nutrient-limiting conditions	19
Nutrient Limitation Experiment and Phenotyping	19
Statistical Analyses	19
Chapter 2: Genetic architecture of phenotypic differences between Arabis floodplain species	
Common Garden Experiment and Phenotyping	20
Phenotypic Analyses	21
DNA Extraction and RAD-seq Library Construction	22
Genome Assembly	22
Analysis of RAD-seq Data and SNP Calling	22
Linkage Map Construction, Genotype Correction, Segregation D Coefficient	istortion, and Selection

QTL Mapping	24
Chapter 3: Flowering time QTL fine-mapping	26
Common Garden Experiment and Phenotyping	26
Primer Design, PCR, and Statistical Analyses	26
3. Results	28
Chapter 1: Growth variation under nutrient-limiting conditions	28
Chapter 2: Genetic architecture of phenotypic differences between end Arabis floodplain species	, ,
Phenotypic Differences of Ecologically Relevant Traits	32
Genome Assembly	39
Genetic Map and Segregation Distortion	41
Genetic Architecture of Ecologically Relevant Traits	45
Chapter 3: Flowering time QTL fine-mapping	51
Flowering Time Responsible Genes	51
4. Discussion	58
Chapter 1: Growth variation under nutrient-limiting conditions	58
Chapter 2: Genetic architecture of phenotypic differences between end Arabis floodplain species	, ,
Chapter 3: Flowering time QTL fine-mapping	64
5. Conclusion	68
Bibliography	70
Data Availability	87
Acknowledgments Error! E	Bookmark not defined.

1. Introduction

"Does species richness

bear on gene diversity?

We ask the meadow."

-Jochen Wolf

(Eisenhauer et al. 2019)

Biodiversity is crucial for the structure and functioning of ecosystems (Staudinger et al. 2012). The direct impact of human activity and the escalating threat of climate change have initiated the sixth Mass Extinction (Cochrane et al. 2016; Ceballos et al. 2020; Cowie et al. 2022; IPCC 2023). The consequences of biodiversity loss have sparked global concern (Hooper et al. 2002; Eichenberg et al. 2021; Theissinger et al. 2023) and prompted investigations into how species may cope with these challenges (Moore & Hendry 2009; Bontrager & Angert 2018; Schlaepfer and Lawler 2022). Rapid shifts in the environment bring out four responses: 1) adaptive phenotypic plasticity (a near-term solution), 2) dispersal to more suitable habitats (a long-term solution), 3) genetic adaptation via selection of new mutations, and 4) introgression of preadapted alleles via interspecific hybridization (Hansen et al. 2012; Anderson et al. 2012; Chunco 2014; Brauer et al. 2023). Among these four potential responses, the acquisition of pre-adapted alleles could be the fastest way to rescue endangered species.

1.1. Species responses to rapid environmental changes

1.1.1. Adaptive Phenotypic Plasticity

Phenotypic plasticity in plants refers to their ability to exhibit new phenotypes in response to environmental conditions, altering growth, development, morphology, or physiology. This variation can influence adaptive evolution over time (Anderson et al. 2012; He et al. 2021; Stotz et al. 2021; Adams III et al. 2023). While plasticity has its limitations for adaptation, it enables plants to optimize survival and reproduction in diverse and often unpredictable environments (He

et al. 2024). For example, in response to varying light availability, many plants exhibit shade avoidance syndrome, elongating stems, petioles, and lamina to compete for light in dense canopies (Ballaré & Pierik 2017; Yin et al. 2024). Similarly, roots adjust their growth patterns to explore nutrient-rich soil, a response commonly observed in heterogeneous nutrient environments (Lynch 2019; Lynch et al. 2023). This flexibility allows plants to maximize resource use efficiency and adapt to changing conditions within short time scales.

Phenotypic plasticity also presents in traits such as leaf morphology. For instance, semi-aquatic plants exhibit heterophylly, producing distinct leaf types depending on whether they grow submerged or above water. Submerged leaves, such as those in *Potamogeton*, lack stomata and cuticles, are thinner, and are better suited for aquatic environments, whereas aerial leaves are thicker, covered by cutin, and equipped with stomata for gas exchange (Wells & Pigliucci 2000). Additionally, plants exposed to herbivory demonstrate various strategies to reduce stress. For example, grazing by herbivores can drive evolutionary or ecological shifts in grass species, favoring low-growth habits that minimize damage (Didiano et al. 2014; Ohgushi 2016). These examples highlight phenotypic plasticity as a critical survival mechanism across diverse ecosystems, emphasizing its role in plant ecological success and adaptive potential.

1.1.2. Dispersal to Other Habitats

Dispersal, defined as the unidirectional movement of organisms, primarily occurs during the early stages of plant life (Levin et al. 2003; Nathan 2006; Lososová et al. 2023; van Leeuwen et al. 2022). Dispersal to more suitable habitats is important for shaping the spatial dynamics of plants (van Leeuwen et al. 2014). It is one of the key strategies plants employ to ensure survival, reproductive success, range expansion, and genetic variability in response to changing environments (Nathan et al. 2008; van Leeuwen et al. 2022; Wu et al. 2023). By dispersing seeds or spores, plants reduce competition, avoid localized environmental stress, colonize favorable habitats, and escape the risks of inbreeding (Nathan et al. 2008; Wu et al. 2023).

For example, in the genus *Rorippa* (Brassicaceae), Han et al. (2023) observed that these plants originated in Eurasia and North America before undergoing long-distance dispersal (LDD) to other continents. Their findings also revealed that polyploidy enhances dispersal, and together with LDD, has significantly shaped the biogeography of these plants. Dispersal in *Rorippa* is often facilitated by flooding and migrating shorebirds, leveraging the seeds' high tolerance to flooding. These mechanisms highlight the importance of dispersal in providing plants with resilience against habitat fragmentation and environmental variability (Wu et al. 2023).

1.1.3. Selection of New Mutations

Genetic adaptation in plants involves the rapid increase in the frequency of advantageous alleles or the emergence of mutations with significant effects (e.g., pesticide resistance), enabling populations to better withstand environmental pressures (Anderson et al. 2012; Martin & Orgogozo 2013; Kreiner et al. 2018). The speed of adaptation is influenced by factors such as the occurrence rate of adaptive mutations, the fixation rate of new advantageous alleles, and the time required for fixation (Charlesworth 2020; Korfmann et al. 2023).

A notable example of genetic adaptation is the evolution of herbicide resistance in plants. Research using candidate gene sequencing has elucidated that target-site resistance (TSR) mutations alter proteins, preventing herbicides from binding to their target site (Baucom 2019). These genetic changes, often caused by major-effect mutations, confer survival advantages, allowing plants to thrive despite herbicide application.

Another example is the adaptation of *Arabidopsis thaliana* to diverse climatic conditions across its geographical range. Studies have identified allelic variations in the *FRIGIDA* (*FRI*) gene that regulate flowering time which is crucial for plant fitness (Johanson et al. 2000; Le Corre et al. 2002; Korves et al. 2007). Mutations or recombination events within the *FRI* region lead to early flowering in *fri* mutants (loss-of-function of *FRI*). This early flowering trait provides a selective advantage in regions with shorter growing seasons, demonstrating a clear example of positive selection (Le Corre et al. 2002; Maple et al. 2024).

1.1.4. Introgression of Pre-adapted Alleles

Adaptive introgression is the process by which beneficial, pre-adapted alleles from one species or population are transferred to another through hybridization, facilitating adaptation (Anderson & Hubricht 1938; Olson-Manning et al. 2012; Hedrick 2013). This genetic exchange enables recipient populations to rapidly acquire advantageous traits without relying on the independent occurrence and fixation of mutations (Mallet et al. 2015; Schmickl et al. 2017). In plants, adaptive introgression has played a critical role in driving ecological and evolutionary success in response to both biotic and abiotic factors (Hedrick 2013; Mallet et al. 2015).

A notable example of adaptive introgression is the transfer of abiotic tolerance traits through hybridization between sunflower species (*Helianthus*). Traits from *H. debilis* were initially thought to be favored during hybridization due to their contribution to higher growth rates and fitness

before the onset of hot and dry seasons (Whitney et al. 2010). Later, Todesco et al. (2020) demonstrated that early flowering adaptive alleles in non-recombining haplotype blocks originated from *H. argophyllus*, and were enriched among locally adapted introgressed genomic fragments in *H. annuus*. However, subsequent studies by Owens et al. (2021) revealed that the introgressed regions from *H. argophyllus* were not responsible for adaptation. Instead, they showed that the adaptive alleles originated from incomplete lineage sorting (ILS).

This underscores the complexities in identifying the source and adaptive value of introgressions. Demonstrating whether the alleles are adaptive is challenging, as both positive selection (e.g., *Gasterosteus*: Aguirre et al. 2022) and negative selection (e.g., *Xiphophorus*: Schumer et al. 2014) leave similar effects and signatures in the genome. Both processes result in heterogeneous introgression patterns along the genome, complicating interpretations.

In the next section, I delve deeper into the concept of interspecific hybridization.

1.2. Interspecific hybridization

Hybridization, the interbreeding of individuals from genetically distinct populations or species, occurs frequently among close relatives (Blanckaert et al. 2023; Peñalba et al. 2024; Rosser et al. 2024). It can have both advantageous and detrimental consequences on the species receiving gene flow (Todesco et al. 2016; Ma et al. 2019; Dittberner et al. 2022; Blanckaert et al. 2023; Nocchi et al. 2023; Thawornwattana et al. 2023; Theissinger et al. 2023). First, interspecific hybridization can enable the transfer of locally adapted alleles across species barriers and thus enhance the adaptive potential of species (Seehausen 2004; Pfennig et al. 2016; Abbott 2017). Indeed, if hybridization occurs between populations with different ecological specializations, it can give rise to new, viable, and fertile hybrids equipped with novel trait combinations. Such combinations may improve the fitness of the population or even enable the colonization of previously untapped habitats (Buerkle et al. 2000; Rieseberg et al. 2003; Mallet 2007; Abbott et al. 2013; Blanckaert et al. 2023). This process can contribute to rescue endangered species and thus maintains diversity. For example, the genus *Pachyclasdon* appears to have survived the Last Glacial Maximum thanks to genetic information transferred through hybridization in alpine refugia of New Zealand's South Island (Becker et al. 2013). Hybrid populations between generalists and narrow range endemic rainbowfishes (Melanotaenia spp.) were well adapted to environmental changes under the effects of introgression (Brauer et al. 2023). Hybridization has been even proposed to promote the formation of new species, a phenomenon referred to as "hybrid

speciation", which nevertheless remains controversial (Anderson & Stebbins 1954; Ellstrand & Schierenbeck 2000; Schumer et al. 2015).

The deleterious effects of hybridization are easier to detect. Indeed, allelic incompatibilities can cause massive fitness effects, when gene pools reunite after years of evolution in isolation (e.g., *Drosophila* [Masly & Presgraves 2007; Cooper et al. 2018]; *Mimulus* [Zuellig & Sweigart 2018]; *Mus* [White et al. 2011; White et al. 2012; Wang et al. 2015]; *Xiphophorus* [Schumer et al. 2014; Schumer and Brandvain 2016; Powell et al. 2020; Moran et al. 2024]; Bomblies & Weigel 2007; Presgraves 2010; Coughlan & Matute 2020; Li et al. 2022). The overall fitness of the hybridizing population will be reduced if a significant amount of resources is used to produce poorly performing hybrids (Rhymer & Simberloff 1996; Todesco et al. 2016; Goulet et al. 2016). This phenomenon, sometimes described as demographic swamping, elevates the risk of extinction or selects for allelic variation reinforcing species isolation (Goulet et al. 2016; Ma et al. 2019; Brauer et al. 2023).

Despite the interest for the positive consequences of hybridization and the abundant evidence for allelic incompatibilities (Bomblies & Weigel 2007), little is known about how the positive or the negative effects of hybridization interact and condition the emergence of a genotype carrying adaptive alleles in a background, where detrimental effects have been recombined out. Such "super genotypes", although rare in the offspring of the first generation of poorly performing hybrids, may be the new and exceptional combination of adaptive alleles that determines the evolutionary success of hybridization.

The goal of this thesis is to investigate how the positive and negative effects of hybridization can be genetically disentangled in offspring populations, with a focus on *A. nemorensis* and *A. sagittata*, two endangered hybridizing floodplain species. By examining growth variation under nutrient-limiting conditions, the genetic architecture of phenotypic differences, and the genetic basis of flowering time variation, this research aims to understand the balance between detrimental and adaptive effects of alleles in hybrid offspring. Specifically, it seeks to determine whether "super genotypes," which combine advantageous traits while minimizing deleterious effects, can emerge through hybridization. Through the integration of phenotypic analyses, quantitative trait locus (QTL) mapping, and fine-mapping approaches, this study addresses fundamental questions about the evolutionary potential of hybridization, providing insights into how hybrid genotypes may drive adaptation and evolutionary success in natural populations.

1.3. Study system

Here, we focused on a hybridization hotspot located along the banks of the Rhine near Mainz, Germany, where two endangered floodplain species hybridize (Dittberner et al. 2019; Dittberner et al. 2022). *Arabis nemorensis*, a species within the Brassicaceae family (*Arabis hirsuta* tribe), inhabits flood meadows and is currently in a critical state in Central Europe, requiring special attention from conservation authorities (Schnittler & Günther 1999; Burmeier et al. 2011). *A. nemorensis* is self-pollinating and exhibits low levels of nucleotide diversity. Its endangered status is further intensified by its unique ecological requirements, and the loss of its natural habitat (Hölzel 2005; Burmeier et al. 2011; Mathar et al. 2015; Dittberner et al. 2019). It hybridizes with *A. sagittata*, another member of the same *phylogenetic* tribe (Karl & Koch 2014), that is morphologically very similar, but is commonly found in calcareous grasslands and thus possibly more tolerant to drought (Dittberner et al. 2022). *A. sagittata* was recently observed in floodplains, where it naturally hybridizes with *A. nemorensis* (Dittberner et al. 2019; Dittberner et al. 2022).

Introgression analysis has revealed that gene flow between *A. nemorensis* and *A. sagittata* is not restricted to the sympatric population (Dittberner et al. 2022). According to Dittberner et al. (2019; 2021), introgression between these species occurred heterogeneously in the past and in both directions. However, contemporary gene flow is more frequent from *A. nemorensis* to *A. sagittata* and confined to a narrow area on the Rhine, where intraspecific genetic variation is extremely low (Dittberner et al. 2019; Dittberner et al. 2022). Additionally, population genetics analyses estimated the divergence between *A. nemorensis* and *A. sagittata* around 900 000 generations ago (Dittberner et al. 2022). During the last glaciation, populations were mostly isolated from each other (Dittberner et al. 2022).

1.4. Thesis aims

1.4.1. Chapter 1: Growth variation under nutrient-limiting conditions

To study the growth variation under nutrient-limiting conditions, I conducted an experiment with 159 plants from 10 accessions of *Arabis nemorensis* and *A. sagittata*, representing four populations (AdI-1, Con-1, Lob, and Rhine). Seeds were stratified, germinated, and grown under controlled conditions in a growth chamber. Seedlings were then transplanted into pots containing a nutrient-limited soil-sand mixture. Plant growth was monitored through periodic photography,

and fresh and dry weights of shoots and roots were measured to calculate the dry root-to-shoot ratio.

Statistical analyses, including a linear mixed-effects model and ANOVA, revealed no significant difference in dry root-to-shoot ratios between the two species (*p*=0.263). These findings suggest that nutrient allocation strategies in these hybridizing species may be more similar than expected, with *A. sagittata* not exhibiting a stronger investment in root formation compared to *A. nemorensis* under nutrient-limiting conditions.

1.4.2. Chapter 2: Genetic architecture of phenotypic differences between endangered hybridizing *Arabis* floodplain species

I investigated the genetic basis of interspecific differences between two endangered hybridizing *Arabis* floodplain species, *A. nemorensis* and *A. sagittata*. Using an F2 progeny from a reciprocal cross between *A. nemorensis* and *A. sagittata* collected from the natural hybridizing hotspot, I mapped loci controlling interspecific differences. My research aimed to address the following questions:

What are the phenotypic differences in relevant ecological traits?

What is the genetic architecture of interspecific differences in this hybridizing hotspot?

Can a "super-genotype" arise, combining ecologically relevant traits with higher fitness?

The study confirmed significant phenotypic differences between the two species. While some F2 hybrids exhibited extreme trait values and patterns of transgressive segregation, most produced fewer seeds compared to their parental lines. Genetically based differences were detected for several ecologically relevant traits, revealing that incompatibility QTLs have a simple genetic basis. Furthermore, some ecologically relevant QTLs were independent of the incompatibility QTLs and segregation distortion regions, suggesting the potential for recombination to create favorable trait combinations. Thus, these findings indicate that a small fraction of hybridization offspring has the potential to harbor a genotype totalling properties that none of the parents have.

1.4.3. Chapter 3: Flowering time QTL fine-mapping

From the 58 QTLs identified for 20 ecologically relevant traits, the largest QTL was associated with flowering time, explaining 22.7% of the variation. To investigate the genetic basis of flowering

time variation in *Arabis* hybrids, I conducted a fine-mapping experiment targeting this major QTL, located on chromosome 8. Fifteen F2 lines heterozygous for the target QTL and homozygous for other flowering QTLs were selected, and 30 F3 seeds per line were grown across two common garden trials.

Using species-specific PCR markers, I identified 138 recombinants among 410 individuals, refining the QTL region to a ~300 kb interval containing 64 genes, 38 of which have orthologs in *Arabidopsis thaliana*. The study revealed that TFL1, a gene associated with the photoperiod flowering pathway, regulates flowering time independently of other traits such as plant height and stem leaf density. This fine-mapping experiment provided key insights into the genetic basis of flowering time variation in the *Arabis* F3 population.

2. Materials and Methods

Chapter 1: Growth variation under nutrient-limiting conditions

Nutrient Limitation Experiment and Phenotyping

On January 20, 2022, I stratified seeds from different accessions of *Arabis nemorensis* and *Arabis sagittata* from various populations, as described in Dittberner et al. (2022). Seeds were stratified at 4°C for four days in darkness. On January 25, 2022, I sowed three seeds per accession per pot in seedling trays filled with 'Topferde' soil (Einheitserde, Sinntal-Altengronau, Germany). Accessions were randomly distributed within the seedling trays. The trays were then placed in a growth chamber for two weeks to allow germination (20°C during the day / 16°C at night; 60% relative humidity; 10 hours of light / 14 hours of darkness).

On February 9, 2022, I transferred the germinated seedlings to 9x9 cm pots filled with a mixture of 5% 'Topferde' and 95% quartz sand, and randomly distributed them across 13 trays. The trays were placed in a growth chamber for seven weeks to measure plant growth under nutrient-limiting conditions (20°C during the day / 16°C at night; 50% relative humidity; 12 hours of light / 12 hours of darkness). Plants were watered as needed.

On March 30, 2022, I measured the fresh weight of each pot. I then washed the plants to remove sand, separated the shoots from the roots, and placed each in separate paper bags (one bag per plant part: shoot and root). I recorded the fresh weight of each plant's shoot and root by weighing the bags both empty and with the plant material. The bags were then dried for four days at 40°C, after that I measured the dry weight of each.

Statistical Analyses

Using the fresh and dry weights of each plant's shoots and roots, I calculated the root-to-shoot ratio. I employed a linear mixed-effects model (Imer) from the ImerTest package in R (version 3.1-3), controlling for tray and pot positions within trays, to assess the effect of species on variation in the dry root weight, dry shoot weight, and dry root-to-shoot ratio. Finally, I also performed an ANOVA to determine if species had a significant effect on these traits.

Chapter 2: Genetic architecture of phenotypic differences between endangered hybridizing *Arabis* floodplain species

Common Garden Experiment and Phenotyping

In 2019, Dr. H. Dittberner crossed sympatric *Arabis nemorensis* and *Arabis sagittata* plants which had been collected from the banks of the Rhine near Mainz in Riedstadt, Hessen, Germany and fully sequenced (Dittberner et al. 2019; Dittberner et al. 2022). Since nucleotide diversity within the population is very low (Dittberner et al. 2019), we assume here that differences between these genotypes reflect species differences. Plants were reciprocally crossed to generate F1s, and seedlings were grown in the greenhouse at the Experimental Garden of the University of Cologne. The seeds of the first generation of selfing (F2) were harvested.

On October 5, 2019, Dr. H. Dittberner and Y. Özoglan sowed F2 seeds (two seeds per line) in seedling trays. After two weeks of vernalisation and germination, they transplanted seedlings into 7x7 cm pots filled with 'Topferde' soil (Einheitserde, Sinntal-Altengronau, Germany), always placing one seedling per pot. In total, 1204 individual plants (both hybrids and parents replicates) were distributed across 43 trays, which were put in cold frames to accelerate growth and prevent frost damage from November 8 to December 13, 2018. Photographs of each tray were taken on November 19, 2018, using a Canon EOS camera, and plant rosette sizes were measured using ImageJ.

On December 13, 2019, trays were transferred to bird-protected cages under semi-natural conditions. Leaf harvesting was done on December 19, 2019, for plants that had reached sufficient size (~50 mg of leaves per plant), and continued through January, February, and March 2019. Harvested rosette leaves were stored at -80°C for DNA extraction.

On March 1, 2019, eight trays were moved to cold frames for a 10-day recovery period of potential stress. A total of 199 F2 individual plants, seven *A. nemorensis*, and seven *A. sagittata* individuals were submerged in transparent boxes containing 17 L of water each for seven weeks. Plants were randomized and distributed across eight boxes, which were kept in cold frames throughout the submergence experiment. After seven weeks of complete submergence, plants were removed from water and left to recover. Then, their survival status was documented. Following a two-week recovery period, Dr. H. Dittberner and Y. Özoglan again recorded the survival status of plants,

categorizing plants as either died, survived with new leaf growth, or survived and bolted. During recovery, pots remained in cold frames and watered as needed.

For dry biomass measurement, roots were separated from the soil with a gentle water flow. Each plant was photographed with a Canon EOS camera for further analysis, then dried in a VWR Dry-Liner. Roots and shoots were subsequently weighed separately.

In total, Dr. H. Dittberner, Y. Özoglan, and I phenotyped plants for more than 20 traits grouped into five categories: 1) Fitness: seed mass from 10 randomly selected siliques or fertility score, and submergence survival status; 2) Growth: rosette diameter at four time points (November 19, 2018; January 8, 2019; February 7, 2019; March 13, 2019), inflorescence height, side and ground shoot number, and dry root/shoot ratio; 3) Timing: bolting and flowering times; 4) Leaf Traits: stem leaf number, leaf length, petiole length, lamina length, lamina length/width ratio, leaf margin type (serrated or smooth), leaf width, and petal length; and 5) Stem Traits: stem leaf density, stem leaf length and width, and stem height.

Phenotypic Analyses

To assess phenotypic differences between the two species, I used a generalized linear model (glm) with a quasi-Poisson family structure in a loop to analyze each trait, controlling for environmental effects, in R. A t-test from the stats package in R (version 3.6.2) was then applied to the residuals of the models to calculate the significance of differences (p-value < 0.05) between the two groups (*A. nemorensis* and *A. sagittata*, each with 35 replicates) for each trait. I used ggplot2 (version 3.5.1; Wickham 2016) to visualize the distribution of phenotypes for both F2 and parental replicates in a single plot per trait, helping in the understanding of transgressive segregation within the F2 population.

For phenotypic correlations in the F2 population, I employed a mixed-effects model approach (glm, family = quasi-Poisson) to account for random variation attributed to experimental blocks, cross direction due to reciprocal cross. Residuals were extracted for each trait, and pairwise Spearman correlations were calculated using the cor function from the stats package in R (version 3.6.2), applying pairwise deletion to handle missing data. This resulting correlation matrix was used to generate both a network structure and a clustered heatmap, representing the significance of correlations. I used the qgraph package (version 1.9.5-2), with edges illustrating significant correlations in the network structure, and ggcorrplot function from the ggcorrplot package (version 0.1.4.1) to visualize the heatmap.

DNA Extraction and RAD-seq Library Construction

In March 2021, DNA was extracted from leaves stored at -80°C using the NucleoSpin® 8 Plant II protocol. I genotyped 801 F2 individuals following the restriction-site-associated DNA sequencing (RAD-seq) protocol described in Dittberner et al. (2019). DNA quantification was performed using the Qubit® 3.0 Fluorometer. For each sample, a total of 250 ng of genomic DNA were digested with the KpnI-HF restriction enzyme (New England Biolabs).

Each digested sample was then ligated with one individually barcoded modified Illumina P1 adapter, containing 5 bp random nucleotides to allow for the removal of PCR duplicates in later processing steps. A total of 20 different barcodes were used, and 52 pools of 20 barcoded individuals each were constructed, with all pools standardized to equal volume and concentration. Library sequencing was conducted in four separate runs at the Cologne Center for Genomics (CCG) on an Illumina NovaSeq platform. For 46 pools, sequencing length was 2x100 bp, generating approximately 3 million reads per individual, while the remaining six pools were sequenced at 2x150 bp, yielding approximately 6 million reads per individual.

Genome Assembly

In order to improve previous genome assemblies, the DNA of both parental lines was sequenced with PacBio HiFi technology and Hi-C data. Dr. T. Ali used Jellyfish (version 2.3.0; Marcais & Kingsford 2011) to count k-mers of size 21 in the 2.18 and 1.98 million reads obtained for *Arabis nemorensis* and *A. sagittata*, respectively. The k-mer histogram generated by Jellyfish was then processed with GenomeScope (version 2.0; Ranallo-Benavidez et al. 2020) to estimate genome size, heterozygosity, and repetitiveness. HiFiAdapterFilt (version 2.0.0; Sim et al. 2022) was used to remove residue PacBio adapter sequences from the HiFi reads. Then, hifiasm was used again to assemble the filtered HiFi reads (version 0.16.1; Cheng et al. 2021; Cheng et al. 2022) with integration of Hi-C data. To scaffold the primary assembly produced by hifiasm, Dr. T. Ali employed RagTag (version 2.1.0; Alonge et al. 2022), using the *A. alpina* assembly as a reference.

Analysis of RAD-seq Data and SNP Calling

To assess the quality of RAD-seq reads, I used FastQC (version 0.11.9; Andrews 2010). PCR duplicates were removed using the clone_filter module in Stacks (version 2.59; Catchen et al. 2013), based on a 5 bp random nucleotide sequence at the end of each adapter. Adapter trimming

and removal of reads shorter than 60 bp were performed using Cutadapt (version 1.18; Martin 2011). I demultiplexed samples and filtered out reads with ambiguous barcodes (allowing one mismatch), cut sites, uncalled bases, and low-quality reads (default threshold) using the process_radtags module in Stacks (version 2.59). Reference-based mapping and read filtering were conducted with BWA (version 0.7.17; Li & Durbin 2009) using default settings against the A. nemorensis reference genome, along with SAMtools (version 1.10; Li et al. 2009) and bash scripts from Rivera-Colón & Catchen (2022).

Variant calling for 801 individuals was performed using BCFtools mpileup and call (version 1.18; Li et al. 2009) under specific criteria: a base quality score greater than 30, base quality recalculation (-E option), and SNP calling with a significance threshold of p-value < 0.05. Genotyped loci were filtered using VCFtools (version 0.1.17; Danecek et al. 2011) to exclude loci with over 50% missing data across individuals. Only biallelic sites were retained, and indels were removed. Individuals with more than 60% missing data were excluded, resulting in a final set of 781 individuals for analysis. Further filters were applied to site and genotype depth (--min-meanDP 4 --max-meanDP 40 --minDP 5 --maxDP 40), and sites with over 70% missing data were removed. Loci spaced less than 100 bp apart were clustered into RAD regions as described by Dittberner et al. (2019). Regions with abnormally high or low coverage were excluded based on specific thresholds: mean coverage greater than twice the overall mean or less than one-third, maximum coverage exceeding twice the mean maximum coverage across all regions, or regions shorter than 150 bp. Sites absent in parental lines and ambiguous bases were also removed.

Finally, I applied a minor allele frequency filter (--maf 0.25) to the dataset. SNPs (single nucleotide polymorphisms) were extracted using VCFtools (version 0.1.17; Danecek et al. 2011) and custom Python scripts, resulting in a final VCF file containing 5,360 SNP markers across 781 individuals.

Linkage Map Construction, Genotype Correction, Segregation Distortion, and Selection Coefficient

The genetic map was constructed using a high-quality dataset of 5360 SNP markers, with the R/qtl (version 1.66; Broman et al. 2003) and ASMap (version 1.0-7; Taylor & Butler 2017) packages in R (version 4.2.3). Detailed methodology and scripts for this process are available in the Appendix repository on GitHub, under Chapter 2, Genetic Map section. I applied filtering procedures to 781 individuals to assess missing data, removing 37 individuals with missing data exceeding 3,500 loci and excluding two additional individuals due to mislabeling. Duplicated

markers were identified and removed, resulting in the discarding of 47 markers. Markers with more than 23% missing data were subsequently filtered out. The analysis of the remaining 2164 markers included examining their distribution across the genome, comparing segregation distortion patterns with allelic proportions and missingness, and excluding outliers based on allelic proportions. I further removed markers with fractions of heterozygotes lower than 25% or higher than 75%. This process resulted in 2,096 remaining markers.

To improve genotype accuracy, particularly for heterozygous loci located in low coverage regions, I developed a Python script to correct miscalled genotypes and impute missing data using a sliding window approach. A window size of 2 Mb with a 0.5 Mb step size provided the most effective correction and imputation. No further markers or individuals were removed after this correction and imputation step. The finalized dataset was then used to construct the genetic map in ASMap, applying the 'Kosambi' mapping function.

Chromosomal orientation was assessed using the constructed genetic map, identifying inversions on chromosomes 3, 4, 6, and 7 due to assembly issues. These regions were adjusted by inverting physical distances on the genetic map. I also used RepeatMasker (version 4.1.6; Smit et al. 2015) on genome annotations to detect and remove markers within repetitive regions. This final analysis produced a genetic map of 2,082 markers distributed across eight chromosomes for 742 individuals. I assessed deviation from Hardy-Weinberg equilibrium (HWE) within each region by applying a test of segregation distortion (profileMark) for each marker with Bonferroni correction using the ASMap package in R. Selection coefficients were then inferred in these regions, with significance tested using the Z-score test (Figure 6) For each SNP, the expected frequency (p=0.5) and observed frequency were used to estimate the selection coefficient (s). The selection coefficient was derived as $s = \Delta p / p(1-p)$, where Δp represents the difference between the observed and expected frequencies. For assessing the significance of coefficients, a Z-score test was performed. The Z-scores were calculated using the standard deviation of selection coefficients across the entire dataset and per chromosome to account for chromosome-specific variations. P-values were obtained from the Z-scores, and SNPs with p<0.05 were classified as significant, indicating potential selection events.

QTL Mapping

QTL analyses were conducted using the R/qtl and QTLtools packages (version 1.66; Broman et al. 2003; version 1.3.1; Delaneau et al. 2017) in R. I performed QTL mapping on the residuals extracted from models that accounted for environmental effects on the phenotypes of 22 traits

listed in Table 3. For efficiency of the process, I wrote a loop to sequentially analyze each of the 22 traits.

For each trait, I used the scantwo function to perform a two-dimensional genome scan with a two-QTL model, applying the Haley–Knott regression algorithm (Haley & Knott 1992). Penalties were calculated from 1,000 permutations of the scantwo function to support the stepwise fitting of multiple QTL models. The stepwiseqtl function was then employed, with a maximum of five QTL, using Haley–Knott regression to search for optimized models. I activated the refine.locations option in stepwiseqtl to improve the localization of QTLs and deactivated the additive.only option to allow for potential interactions between QTLs in the model.

I then looked into the summary output of stepwiseqtl to obtain information on the percent variance explained by each QTL, as well as the peak LOD scores, and the additive (a) and dominance (d) effects for each significant QTL identified in the best stepwise models for each trait. For each identified QTL, I determined the 1.5 LOD confidence interval using the lodint function in R/qtl. Finally, I used the segmentsOnMap function from QTLtools to visualize QTL segments on the genetic map, and ggplot2 (version 3.5.1; Wickham 2016) to plot QTL effect sizes using the LOD scores obtained from the summary output of stepwiseqtl.

Chapter 3: Flowering time QTL fine-mapping

Common Garden Experiment and Phenotyping

For the fine-mapping experiment targeting the largest QTL associated with Days to Flowering (first QTL on chromosome 8), I identified F2 lines that were heterozygous for the QTL of interest and homozygous for other Days to Flowering QTLs, resulting in a total of 15 lines (Table 5). I sowed 90 F3 seeds per line in seedling trays and transferred them to the cold chamber for vernalisation, planting three seeds per pot. After two weeks, I transplanted one seedling into each 7x7 cm pot filled with 'Topferde' (Einheitserde, Sinntal-Altengronau, Germany), resulting in 30 seedlings per line, and pots kept in the greenhouse for six weeks.

Then, plants were transplanted into larger 9x9 cm pots and moved to cold frames in the garden for seven weeks. During this period, leaf material was harvested from each plant, and DNA was extracted from fresh leaves using the NucleoSpin® 8 Plant II protocol. The plants were then transferred to new 11x11 cm pots and placed on tables in the garden under a bird-protected cage.

In total, I phenotyped flowering time, inflorescence height, internode length, number of shoots, plant height, stem leaf density, stem height, and rosette diameter for 483 plants in two successive trials. The first trial began on September 26, 2022, and the second on November 16, 2022.

Primer Design, PCR, and Statistical Analyses

Geneious Prime® (version 2024.0.5) was used to design species-specific primers targeting the QTL region based on the *A. nemorensis* and *A. sagittata* genomes. A total of five pairs of PCR markers were developed, dividing the QTL region into four intervals. PCR was conducted to test these primers on plant DNA from 407 lines, for identifying recombinants and locating their recombination events within the predefined intervals.

Given the observed variation in flowering time among F3 families and the environmental effects of the two trials, I constructed a quantitative model using the glm function from the stats package (version 3.6.2) in R, accounting for both genotypic (family) and environmental effects. This model was used to evaluate the effect of each interval in explaining the flowering time distribution. The same model was then applied to assess the impact of intervals on traits with overlapping QTLs in the same region from the F2 mapping population (Inflorescence Height, Rosette Diameter, and

Stem Height). Parental DNA and Nuclease-Free water used as positive and negative controls, respectively.

3. Results

Chapter 1: Growth variation under nutrient-limiting conditions

A total of 159 plants from 10 different accessions were included in the statistical analyses of the dry root-to-shoot ratio experiment. These plants represented four different populations: Adl-1, Con-1, Lob, and Rhine. Germination and survival rates varied among the accessions, and not all germinated plants survived under nutrient-limiting conditions., with the summarized data presented in Table 1.

Table 1. Overview of samples in the dry root-to-shoot ratio experiment in *Arabis* species. The number of germinated plants varied across accessions.

Accession	Species	Population	Germinated	Survived
10	A. nemorensis	Rhine	20	16
103	A. nemorensis	Rhine	20	17
104	A. nemorensis	Rhine	20	13
105	A. nemorensis	Rhine	20	20
296	A. nemorensis	Con-1	12	11
173	A. sagittata	Adl-1	20	17
261	A. sagittata	Lob	20	20
271	A. sagittata	Lob	20	16
275	A. sagittata	Lob	19	15
381	A. sagittata	Rhine	17	14

The minimum (0.01577) and maximum (0.67494) dry root-to-shoot ratios among the 159 individuals analyzed—77 *Arabis nemorensis* and 82 *A. sagittata*—were detected in *A. nemorensis* (Appendix repository on GitHub, under Chapter 1). The mean ratio was 0.26362, with a median of 0.25272. Contrary to expectations that *A. sagittata* would grow slower under nutrient-limiting conditions and invest more in root formation, statistical analyses indicated no significant effect of species on the dry root-to-shoot ratio (p=0.263; Figure 1B).

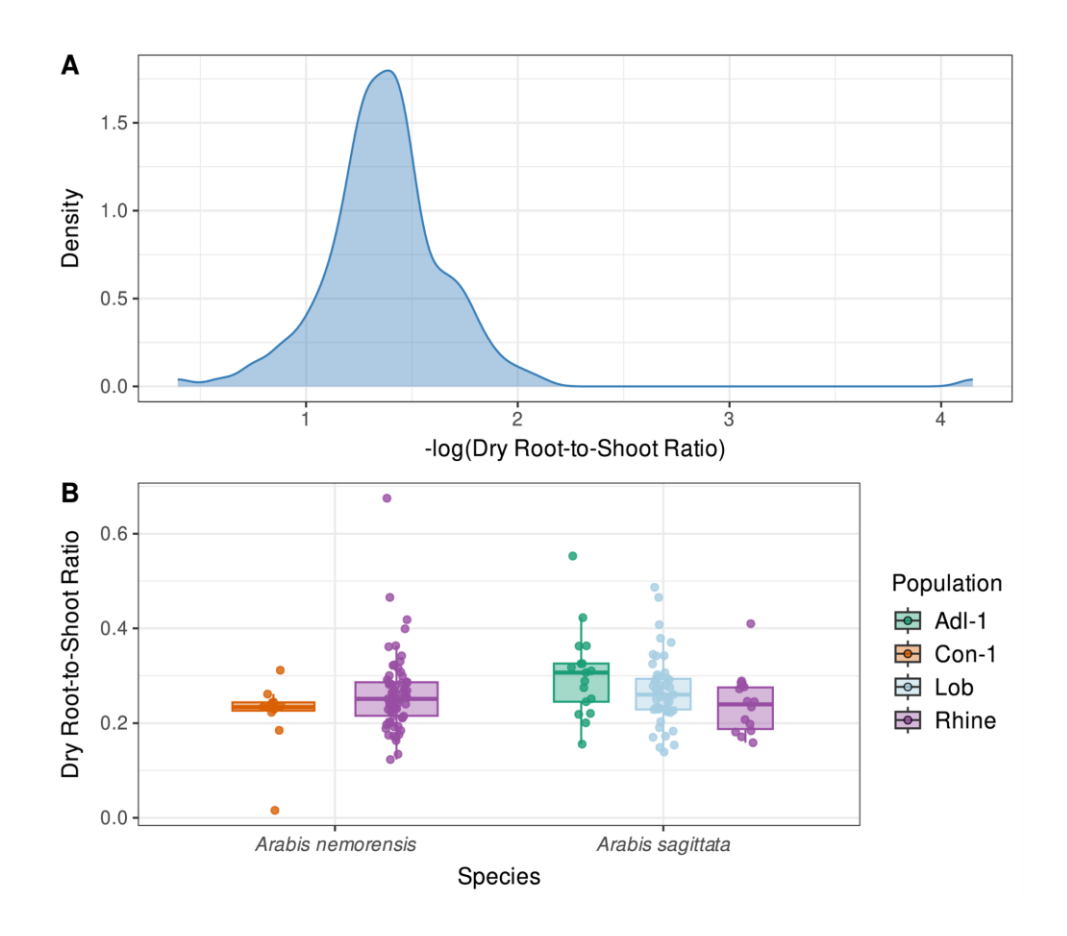


Figure 1. Dry root-to-shoot ratio distribution in *Arabis* species. The distribution of dry root-to-shoot ratios in *A. nemorensis* and *A. sagittata* from different populations is shown. The dry root-to-shoot ratio was measured under nutrient-limiting conditions among 159 plants. (A) Displays the negative logarithm of the dry root-to-shoot ratio across all individuals. (B) Visualizes the variance in dry root-to-shoot ratios between the two species across different populations. Statistical analyses showed no significant difference between species (p=0.263).

In addition to the root-to-shoot ratio, root-to-biomass and shoot-to-biomass ratios were measured, and no significant differences were observed between the species. However, biomass differed significantly between the species. *A. sagittata* had a mean biomass of 0.05627 and a median of 0.05485, while *A. nemorensis* exhibited a significantly larger mean biomass of 0.07005 (p=9.47E-06, Figure 2). Interestingly, this finding was contrary to expectations based on the ecological backgrounds of the species. A detailed summary of these results is provided in Table 2.

Notably, within the Rhine population—the hybridization hotspot—the effect of species on biomass was not significant (*p*=0.0614). However, the estimated effect size of -0.011669 for *A. sagittata* indicates that *A. sagittata* again showed a smaller mean biomass (Figure 3).

Table 2. Statistical analysis of species effects on different traits under nutrient-limiting conditions. Traits represent dry weight measurements. Among the traits analyzed, only total biomass showed a significant difference between the species.

Trait	Estimated Effect A. sagittata	Std. Error	p-value
Biomass	-0.014231	0.003104	9.47E-06
Shoot-to-Biomass	-0.007727	0.006439	0.232
Root-to-Biomass	0.00773	0.006439	0.232
Root-to-Shoot	0.01223	0.01088	0.263

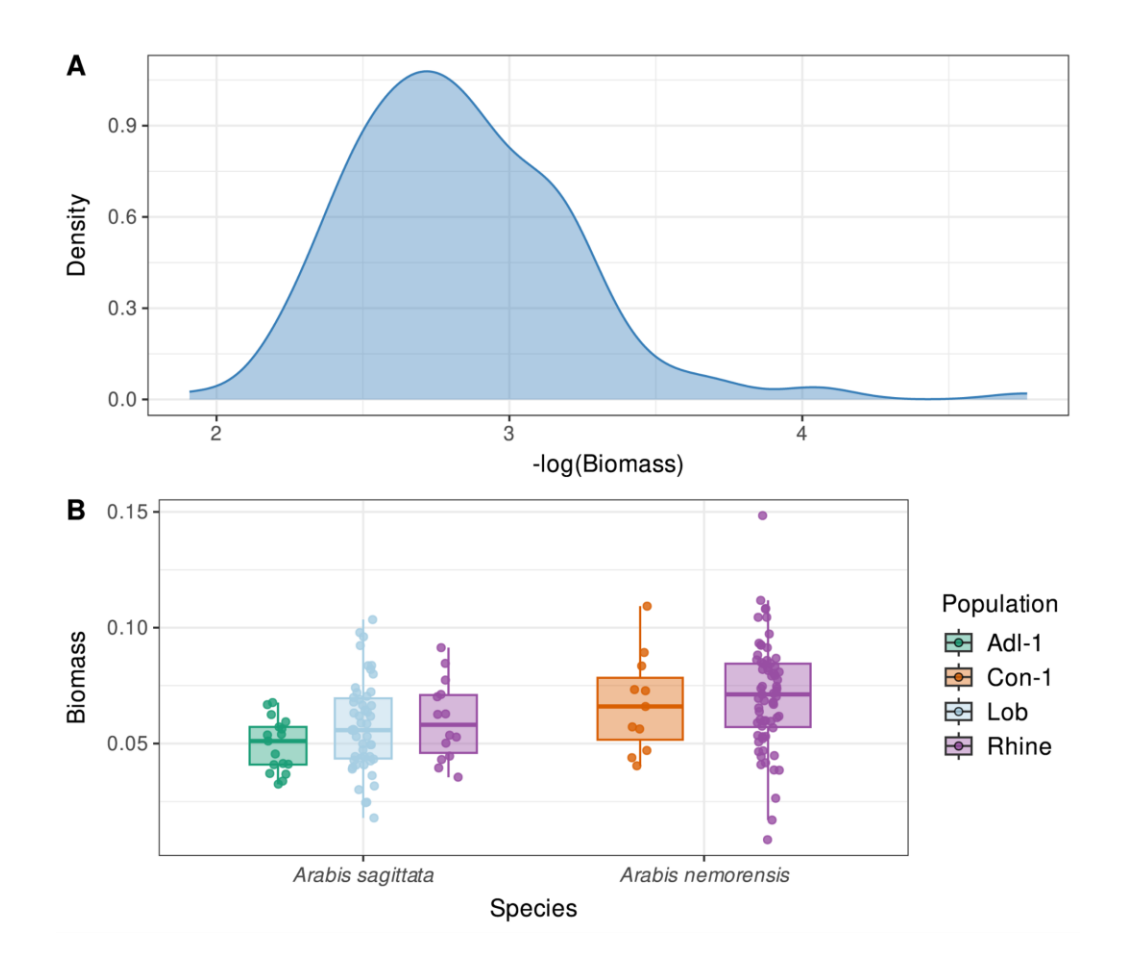


Figure 2. Dry biomass distribution in *Arabis* **species.** The dry biomass of 159 plants from different populations of *A. nemorensis* and *A. sagittata* is depicted. (A) Displays the negative logarithm of the biomass across all individuals. (B) Visualizes the variance in biomass between the two species across different populations. Statistical analysis revealed a significant difference in biomass between species, with *A. nemorensis* exhibiting greater biomass than *A. sagittata* (*p*=9.47E-06).

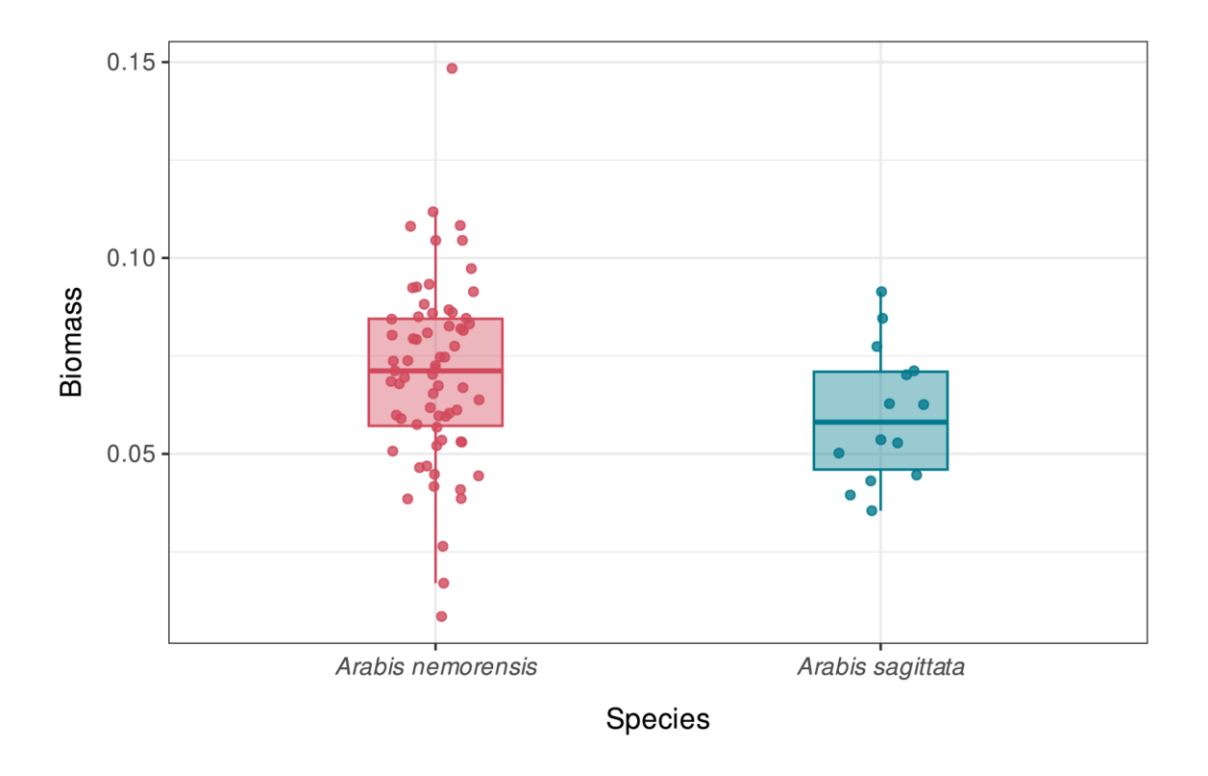


Figure 3. Dry biomass distribution in *Arabis* species of the Rhine population. The variance in dry biomass of 81 different accessions of *A. nemorensis* (67) and *A. sagittata* (14) from the Rhine population is depicted. Statistical analysis revealed no significant difference in biomass between species (p=0.0614).

Chapter 2: Genetic architecture of phenotypic differences between endangered hybridizing *Arabis* floodplain species

Phenotypic Differences of Ecologically Relevant Traits

In total, 1,193 individuals germinated in the greenhouse and were set to grow in a common garden situated at the University of Cologne. A complete list of phenotypes measured in these experiments can be found in Table 3. All replicates of the *A. nemorensis* and *A. sagittata* survived the common garden experiment (35 *A. nemorensis* and 35 *A. sagittata*).

Table 3. Phenotypic traits differences between parents. This table summarizes the phenotypic traits measured in the common garden experiment for F2 hybrids and their parental replicates (A. nemorensis and A. sagittata). Means represent the average value for each trait within parental replicates (35 individuals per species). The "Distance" column shows the absolute difference between the species' means. The p-values indicate the significance of the difference between species based on t-statistics. Significance codes are as follows: *** (p < 0.001), ** (p < 0.01), and * (p < 0.05).

Trait	Mean <i>A. nem</i>	Mean A. sag	Distance	<i>p</i> -value	Significance
Days to Bolting (B.T)	157.2857	169.2857	12	1.302E-19	***
Days to Flowering (F.T)	183.5714	193.4286	9.8571	5.556E-14	***
Fertility Score (W.S)	0.0298	0.0295	0.0004	6.238E-01	
Inflorescence Height (P.H)	35.25	34.5714	0.6786	4.537E-02	*
Lamina Length (Lam)	1.2729	1.4646	0.1916	1.179E-03	**
Lamina L/W (LLW)	1.476	1.7938	0.3178	3.702E-12	***
Leaf Length (L.L)	1.5562	1.7161	0.1599	7.591E-01	
Leaf Width (L.W)	0.8589	0.8213	0.0376	1.667E-02	*
Number of Stem Leaves (N.L)	28.1429	18.1429	10	4.567E-20	***
Petal Length (Pet)	4.0569	5.3579	1.301	1.887E-21	***
Petiole Length (Pti)	0.2833	0.2516	0.0317	1.084E-06	***
Rosette Diameter 1 (RD1)	1.8331	2.2419	0.4087	2.334E-01	
Rosette Diameter 2 (RD2)	3.2946	3.6893	0.3947	4.922E-03	**
Rosette Diameter 3 (RD3)	3.3611	3.4424	0.0813	1.502E-03	**
Rosette Diameter 4 (RD4)	3.8805	3.911	0.0305	7.447E-03	**

Trait	Mean <i>A. nem</i>	Mean <i>A. sag</i>	Distance	p-value	Significance
Side Shoots (Ssh)	2.7857	2.1429	0.6429	2.802E-02	*
Stem Height (S.H)	40.4286	34.4286	6	2.668E-09	***
Stem Leaf Density (SLD)	0.6979	0.5271	0.1707	5.508E-16	***
Stem Leaf Length (SLL)	2.3894	2.7921	0.4028	1.684E-04	***
Stem Leaf Width (SLW)	1.4021	1.2337	0.1684	2.966E-03	**
Petiole L/Lamina L (P.L)	0.2464	0.1886	0.0579	5.248E-07	***
Ground Shoots (Gsh)	0.2143	1.2857	1.0714	1.414E-08	***

Compared to *A. sagittata*, *A. nemorensis* flowered approximately 12 days earlier (p<0.001). Analysis of t-statistics on the residuals indicated that genotype had a significant effect on rosette diameter 1, 2, and 3 (p<0.01). However, the difference between *A. sagittata* and *A. nemorensis* rosette diameter 1, did not reach statistical significance (p=2.334E-01), with *A. nemorensis* still showing a reduction in diameter. Moreover, F2 hybrids display signatures of transgressive segregation, where many hybrids showed extreme trait values compared to their parents (Figure 4). Although there was no significant difference between parents in the seed production (Fertility score or W.S, p=6.238E-01), outbreeding depression was seen for most of F2s (Figure 4). However, there were few individuals that had higher seed production compared to their parents. *A. nemorensis* individuals displayed a markedly higher number of stem leaves than *A. sagittata* (Mean difference = 10 leaves, p<0.001).

Among the subset of 214 plants that were subjected to four weeks of flooding, there was no significant difference between the survival to flooding in these two species ($\chi^2(1,N=14)=0.43$, p=0.5116).

The reciprocal cross effect analysis revealed significant impacts of cross direction on few traits, suggesting maternal influence and potential cytoplasmic effects (Table 4). Traits such as Stem Leaf Length (SLL, p=0.00003), Rosette Diameter at early stages (RD1, p=0.00008), and Petiole Length (Pti, p=0.00591) exhibited strong associations with the direction of the cross. Additionally, Petiole Length-to-Lamina Length Ratio (P.L, p=0.01190), Rosette Diameter 2 (RD2, p=0.01358), and Rosette Diameter 3 (RD3, p=0.03091) also displayed significant maternal effects, highlighting the potential contributions of maternal inheritance to these traits.

In contrast, most of traits, including Days to Bolting (B.T), Days to Flowering (F.T), Fertility Score (Seed Production or W.S), and structural traits like Inflorescence Height (P.H) and Number of Stem Leaves (N.L), showed no significant effects (p>0.05), indicating limited or negligible maternal influence.

These results identify specific traits that are maternally influenced, providing valuable insights into the role of cytoplasmic inheritance and maternal effects in shaping the phenotype of the F2 population.

Table 4. Results of reciprocal cross effect analysis on phenotypic traits. The table summarizes the *p*-values from the analysis of cross direction and maternal influence on phenotypic traits in the F2 population. Significant *p*-values are bolded for emphasis.

Trait	Estimated Effect A. sagitatta Female	p-value
Days to Bolting (B.T)	0.0073489	0.5911
Days to Flowering (F.T)	0.008801	0.45541
Fertility Score (W.S)	0.04619	0.8541
Inflorescence Height (P.H)	0.007968	0.91211
Lamina Length (Lam)	-0.12019	0.16244
Lamina L/W (LLW)	0.01550	0.75859
Leaf Length (L.L)	-0.04371	0.60346
Leaf Width (L.W)	-0.12873	0.09654
Number of Stem Leaves (N.L)	-0.054995	0.46388
Petal Length (Pet)	0.01575	0.675
Petiole Length (Pti)	0.68109	0.00591
Rosette Diameter 1 (RD1)	-0.32351	0.00008
Rosette Diameter 2 (RD2)	-0.20741	0.01358
Rosette Diameter 3 (RD3)	-0.193682	0.03091
Rosette Diameter 4 (RD4)	-0.0003114	0.9968
Side Shoots (Ssh)	-0.322387	0.05804
Stem Height (S.H)	-0.0051278	0.93638
Stem Leaf Density (SLD)	-0.0230448	0.7342
Stem Leaf Length (SLL)	0.21512	0.00003
Stem Leaf Width (SLW)	0.066639	0.2715
Petiole L/Lamina L (P.L)	0.69893	0.0119
Ground Shoots (Gsh)	-0.22314	0.4783

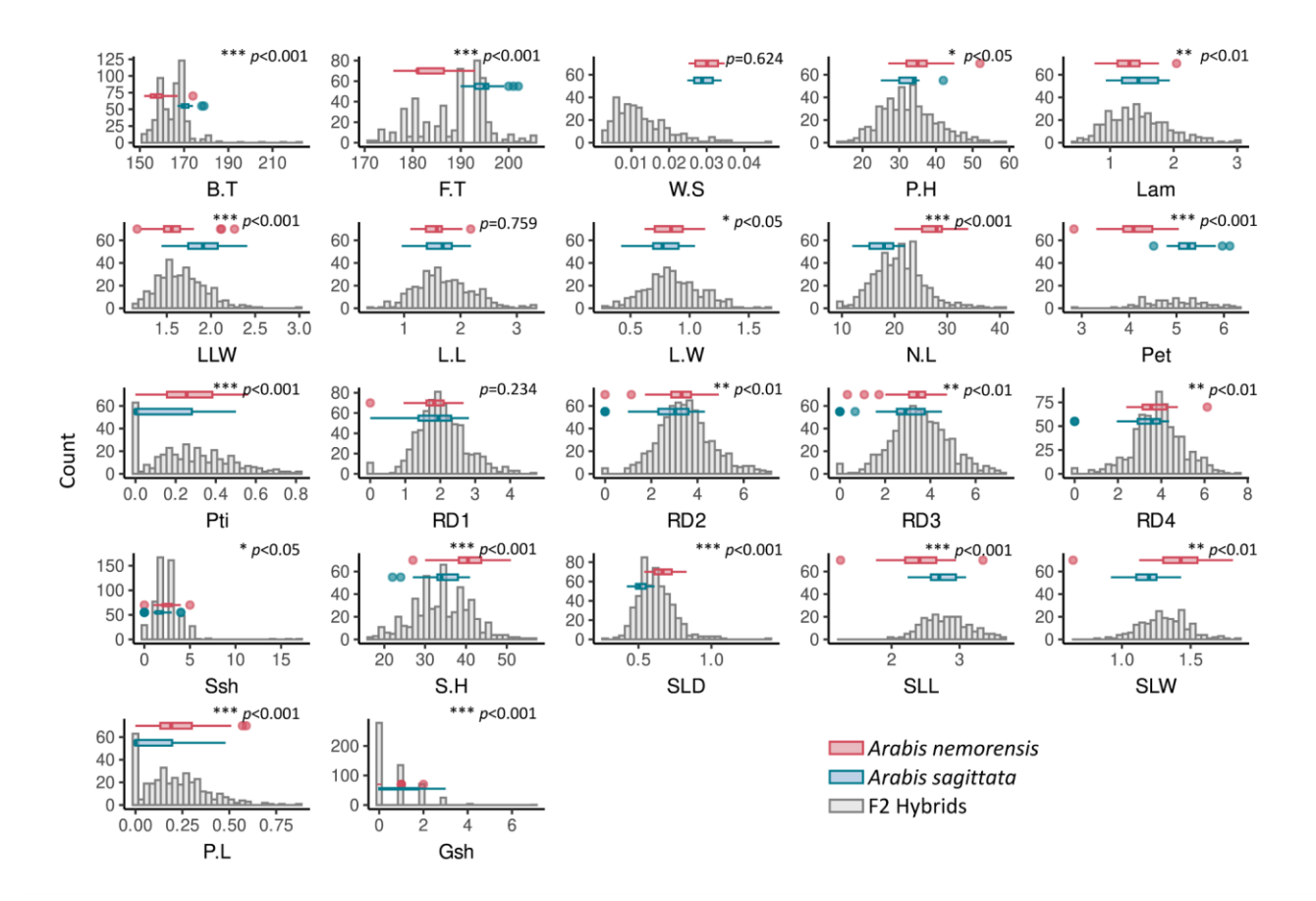


Figure 4. Phenotypes distribution of the mapping population. The distribution of traits in the F2 progeny and their parental lines is shown. Phenotypes were measured in a common garden experiment involving replicates of two parental lines and their F2 hybrid offspring (1,193 plants). Histograms illustrate the distribution of traits in the F2 generation, while boxplots highlight trait variations between the two parental lines. Evidence of transgressive segregation was observed in most traits in the F2 hybrids. The *p*-values from t-statistics analyses on parental replicates demonstrate the significant influence of genotype on each trait. The measured phenotypes include: B.T (Days to Bolting), F.T (Days to Flowering), W.S (Fertility Score - Seed Production), P.H (Inflorescence Height), Lam (Lamina Length), LLW (Lamina Length-to-Width Ratio), L.L (Leaf Length), L.W (Leaf Width), N.L (Number of Stem Leaves), Pet (Petal Length), Pti (Petiole Length), RD1-4 (Rosette Diameter at Four Time Points), Ssh (Side Shoots), S.H (Stem Height), SLD (Stem Leaf Density), SLL (Stem Leaf Length), SLW (Stem Leaf Width), P.L (Petiole Length-to-Lamina Length Ratio), and Gsh (Ground Shoots). For all traits, except W.S (fertility score), L.L (leaf length), and RD1 (first rosette diameter measurement), the differences between *A. nemorensis* and *A. sagittata* were significant. Additionally, hybrid depression was observed in the F2 progeny compared to their parental lines.

Spearman correlation analysis of 22 traits in the F2 population revealed both positive and negative relationships among ecologically relevant traits (Figures 5 and 6). Traits associated with leaf shape, such as Lamina Length (Lam) and Leaf Width (L.W), exhibited strong positive correlations (r > 0.8), indicating synchronized growth patterns during leaf expansion. Similarly, Rosette Diameter (RD1–RD4) measured at different time points showed strong positive correlations (r > 0.7), suggesting consistent growth across developmental stages.

Developmental traits, such as Days to Bolting (B.T) and Days to Flowering (F.T), showed moderate correlations with vertical growth traits, including Stem Height (S.H) and Inflorescence Height (P.H). For instance, Inflorescence Height was positively correlated with Days to Flowering (r = 0.535), suggesting that later-flowering individuals allocate more resources to vertical growth. In contrast, Fertility Score (Seed Production or W.S), a component of fitness, exhibited weaker and often non-significant correlations with other traits, indicating potential independence from vegetative and structural phenotypes.

Petiole traits, including Petiole Length (Pti) and its ratio to Lamina Length (P.L), which are often associated with shade avoidance strategies, were moderately correlated with rosette size and leaf shape traits such as Leaf Width (L.W). Overall, these findings highlight the interdependencies among structural traits (e.g., plant size, leaf shape), developmental traits (e.g., flowering time, rosette size over time), and fitness components in *Arabis* F2 hybrids. The statistical analyses of ecologically relevant traits in the common garden experiment provide valuable insights into phenotypic integration and resource allocation strategies in the F2 hybrid population.

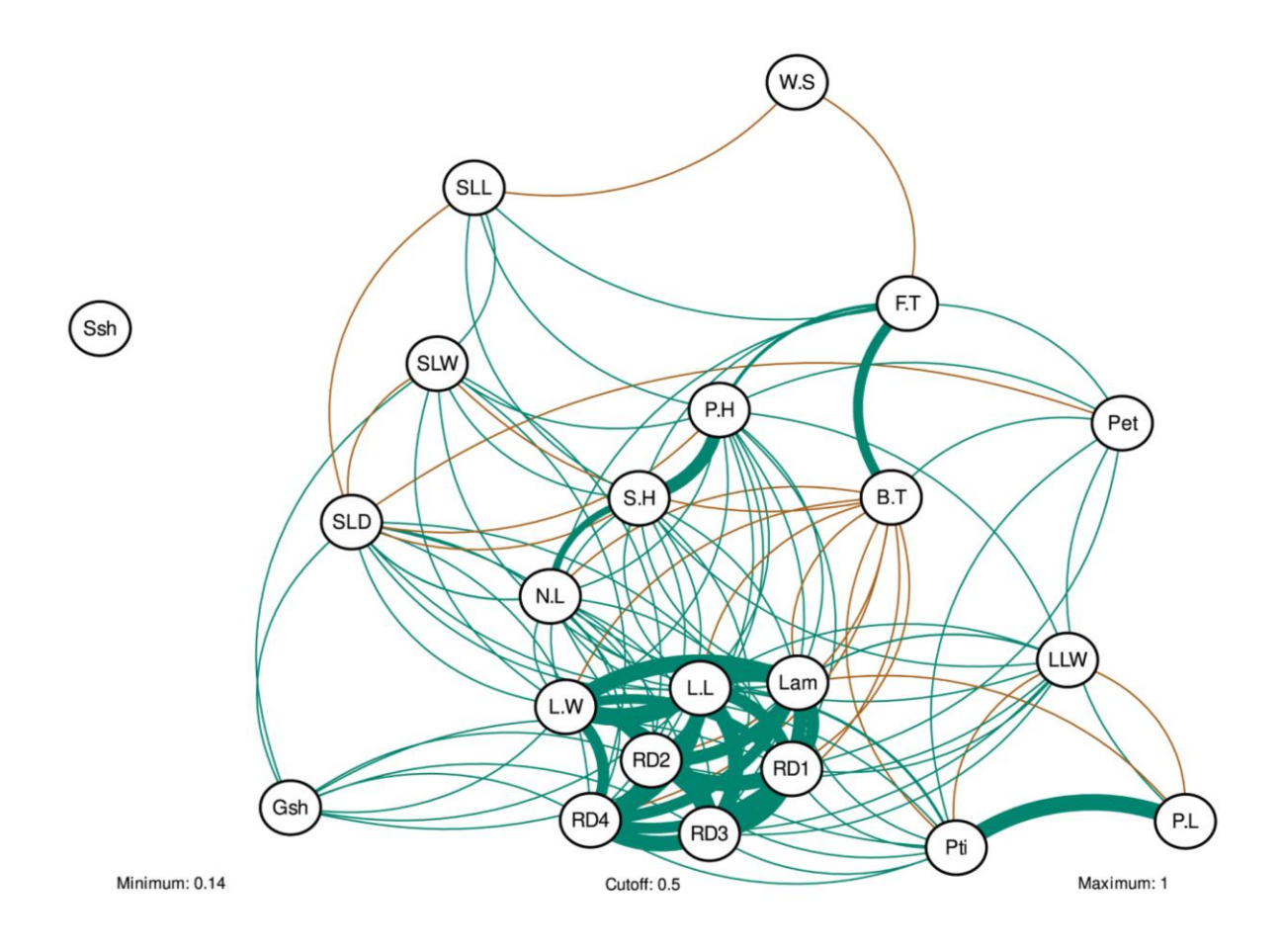


Figure 5. Correlation network of phenotypic traits. The figure above illustrates the relationships among phenotypic traits measured in the common garden experiment. Spearman's rank correlation coefficients were conducted in R to quantify pairwise relationships between traits, with residuals from quasi-Poisson models accounting for variation due to experimental blocks and cross direction. Pairwise correlations were calculated with pairwise deletion for missing data. Edges visualize significant correlations (α = 0.05), adjusted using Bonferroni correction. Edge thickness represents the strength of correlations (cut-off: $|r| \ge 0.5$), with positive correlations shown in green and negative correlations in brown, using a colorblind-friendly palette. The measured phenotypes: B.T (Days to Bolting), F.T (Days to Flowering), W.S (Fertility Score - Seed Production), P.H (Inflorescence Height), Lam (Lamina Length), LLW (Lamina Length-to-Width Ratio), L.L (Leaf Length), L.W (Leaf Width), N.L (Number of Stem Leaves), Pet (Petal Length), Pti (Petiole Length), RD1-4 (Rosette Diameter at Four Time Points), Ssh (Side Shoots), S.H (Stem Height), SLD (Stem Leaf Density), SLL (Stem Leaf Length), SLW (Stem Leaf Width), P.L (Petiole Length-to-Lamina Length Ratio), and Gsh (Ground Shoots).



Figure 6. Correlation heatmap of phenotypic traits. This heatmap provides a complementary visualization of the full correlation matrix using Spearman's rank correlation coefficients. The heatmap was organized hierarchically and displayed significant correlations with corresponding labels. A color gradient was applied to distinguish correlation strengths. Both visualizations provided complementary insights into the complex association patterns among traits, helping to interpret phenotypic relationships in F2 plants within the common garden experiment. The measured phenotypes: B.T (Days to Bolting), F.T (Days to Flowering), W.S (Fertility Score - Seed Production), P.H (Inflorescence Height), Lam (Lamina Length), LLW (Lamina Length-to-Width Ratio), L.L (Leaf Length), L.W (Leaf Width), N.L (Number of Stem Leaves), Pet (Petal Length), Pti (Petiole Length), RD1-4 (Rosette Diameter at Four Time Points), Ssh (Side Shoots), S.H (Stem Height), SLD (Stem Leaf Density), SLL (Stem Leaf Length), SLW (Stem Leaf Width), P.L (Petiole Length-to-Lamina Length Ratio), and Gsh (Ground Shoots).

Genome Assembly

Hifiasm analyses, incorporating a k-mer size of 21 and high-quality reads (*A. nemorensis*: 2.18 million reads; *A. sagittata*: 1.98 million reads), performed by Dr. T. Ali, yielded genome sizes of 245 Mb for *A. nemorensis* and 249 Mb for *A. sagittata* (Table 5). The primary assembly for *A. nemorensis* contained 3,084 contigs, while *A. sagittata* contained 2,361 contigs. The N50 length was 17.4 Mb for *A. nemorensis* and 27.6 Mb for *A. sagittata*.

Table 5. Assembly statistics of Arabis genomes.

	A. nemorensis	A. sagittata			
Number of HiFi reads (million reads)	2.18	1.98			
Primary assembly	using hifiasm				
Number of contigs	3084	2361			
N50 (Mb)	17.4	27.6			
Number of longest contigs	14	9			
Final RagTag-generated assembly using A. alpina genome					
Number of contigs	3059	2344			
N50 (Mb)	26.6	28.4			
Number of scaffolds	8	8			
Complete BUSCOs (%)	99.3	99.4			
Genome total size (Mb)	245	249			
GC content (%)	36.3	36.7			
AT content (%)	63.7	63.3			

After scaffolding with the *A. alpina* genome using RagTag, the N50 length increased to 26.6 Mb for *A. nemorensis* and 28.4 Mb for *A. sagittata*. Complete BUSCO scores were 99.3% for *A. nemorensis* and 99.4% for *A. sagittata*, confirming high genome completeness. The final number of scaffolds for both species was reduced to eight, corresponding to the expected chromosome number.

Comparative analyses of the genomes revealed potential inversions at several locations on chromosomes 3, 4, 5, 6, and 7 (Figure 7). To determine whether these represent biological structural inversions or assembly-related artifacts, these positions can be cross-referenced with the genetic map (Figure 8).

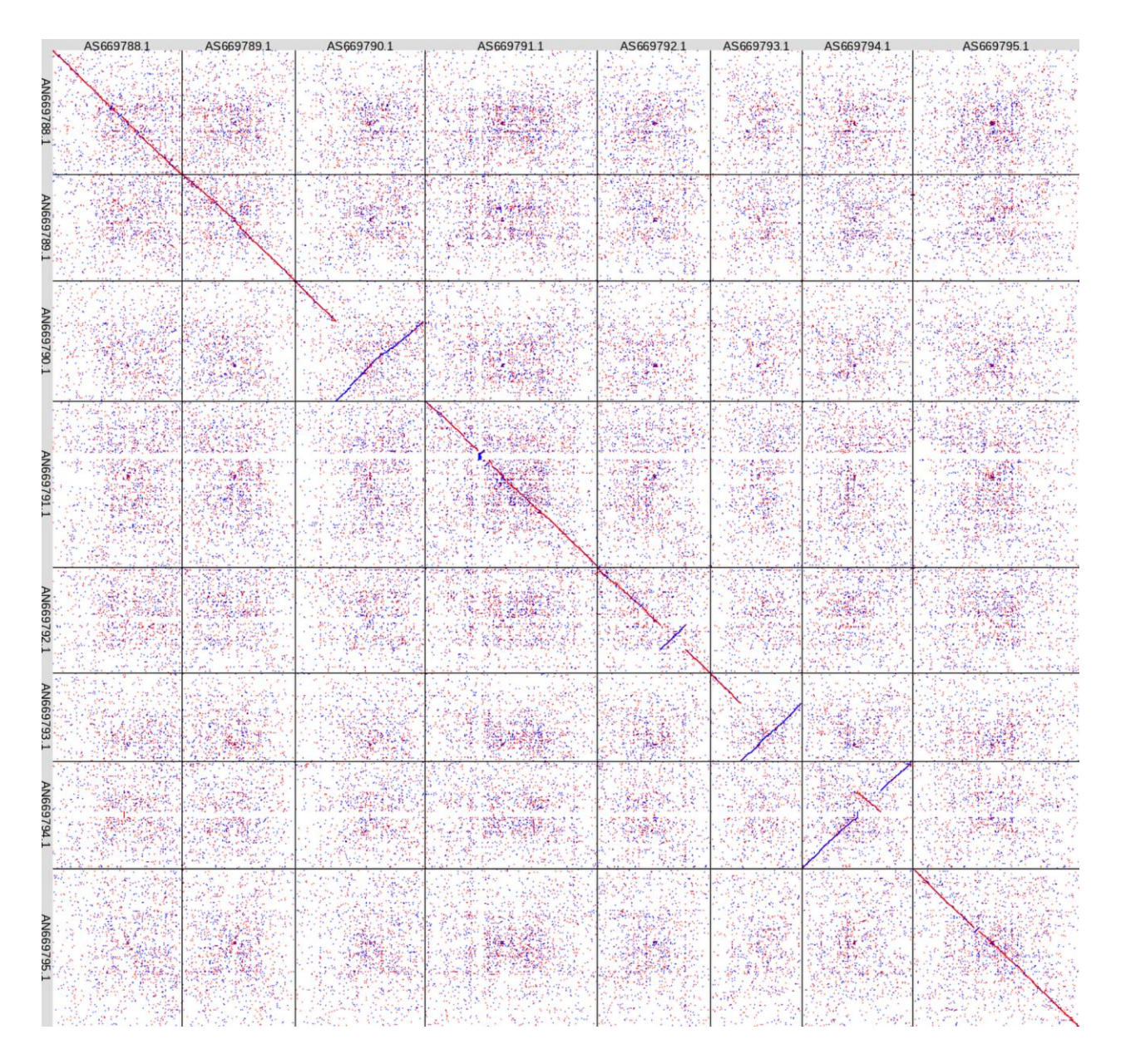


Figure 7. Synteny and rearrangement plot between *A. nemorensis* and *A. sagittata* genomes. The dot plot illustrates synteny and the localization of genomic rearrangements between the final RagTaggenerated assemblies of *A. nemorensis* and *A. sagittata*. The x-axis represents scaffolds (1 to 8) of *A. sagittata* (from left to right), while the y-axis represents scaffolds (1 to 8) of *A. nemorensis* (from top to bottom). Potential inversions are observed on chromosomes 3, 4, 5, 6, and 7.

Genetic Map and Segregation Distortion

To investigate the genetic architecture underlying trait variation, I constructed a genetic map. The map consisted of eight linkage groups (LGs) based on 742 F2 individuals genotyped at 2,082 reliable SNP markers. For an overview of the number of SNPs per chromosome, as well as their physical and genetic lengths, refer to Table 6. The linkage map spanned a total length of 240 cM.

The highest number of markers (369) was found on linkage group 4 (LG4), which corresponds to the longest chromosome (41 Mb). In contrast, the lowest number of markers (160) was located on LG6, with a physical length of 22 Mb. A correlation between the genetic and physical distances of SNPs was observed across the genome, indicating an approximately uniform recombination probability (Figure 8). However, some decrease in recombination rates was visible around centromeric regions.

Table 6. Genetic map overview. This table summarizes the physical and genetic lengths of each chromosome, along with the number of SNP markers. The total number of SNPs included in the map is 2,082.

Chromosome	Physical Length (Mb)	Genetic Length (cM)	Number of SNPs
1	32	185	304
2	26	130	232
3	30	208	244
4	41	186	369
5	27	140	202
6	22	138	160
7	21	115	220
8	38	240	351

To have a better understanding of recombination breakpoints in the mapping population, I plotted the genotypes across the population (Figure 9). This visualization allowed me to identify, for each individual, the approximate locations on each chromosome where recombination occurred, and

the genotype shifted. Additionally, it provided an overview of genotype distribution along the chromosomes. Chromosomes 4 and 7 displayed a higher proportion of green, indicating a greater frequency of *A. sagittata* homozygous genotypes (SS) compared to other chromosomes.

The overall genotype distribution in the mapping population was as follows: NN (homozygous *A. nemorensis*) accounted for 19.5%, NS (heterozygous) for 48.7%, and SS (homozygous *A. sagittata*) for 31.8%. This analysis covered 99.7% of all genotyped markers.

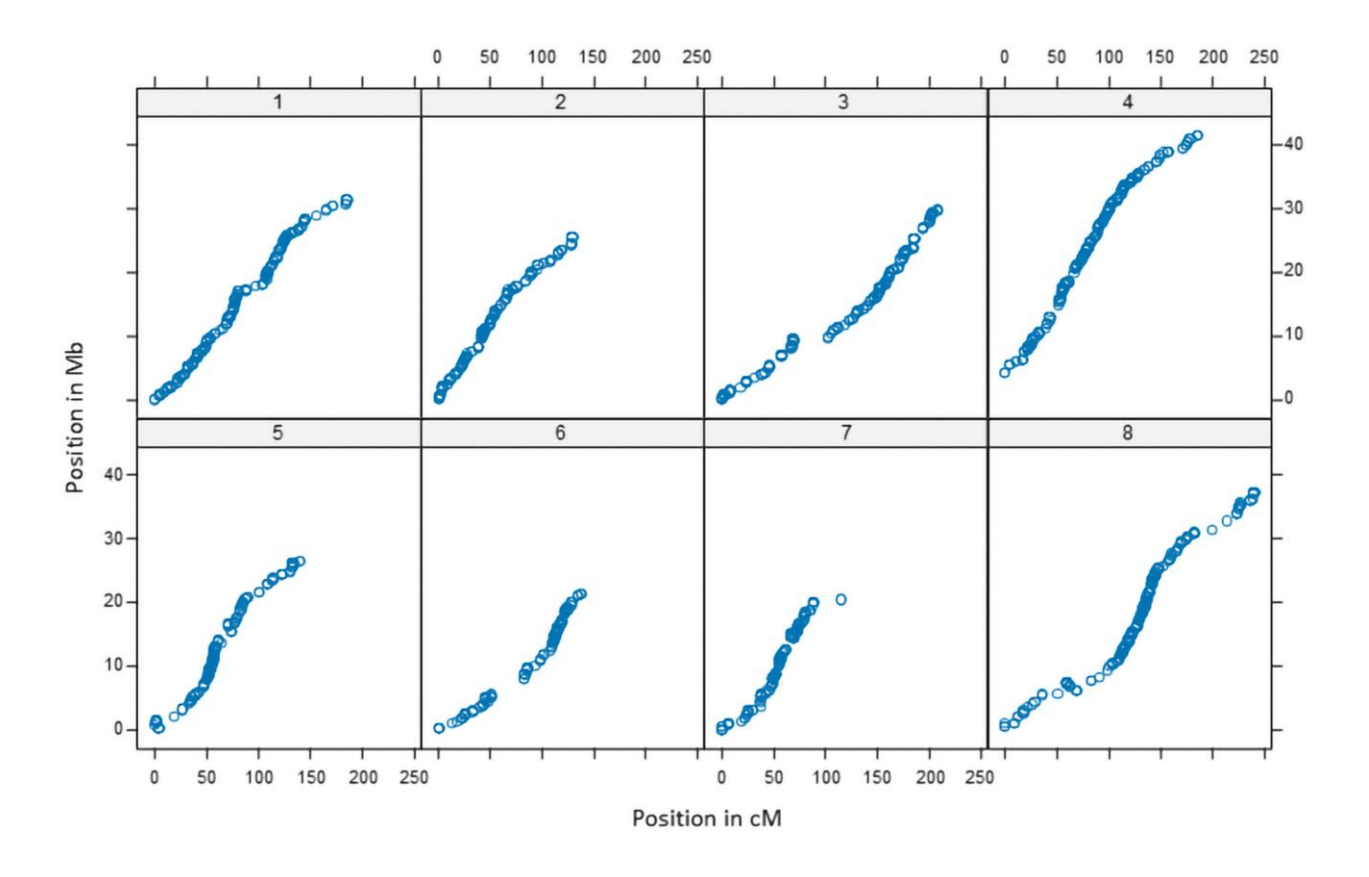


Figure 8. Correlation between SNPs genetic and physical distance. The relationship between genetic and physical distances is shown across the eight linkage groups constructed from 742 F2 individuals genotyped at 2,082 reliable SNP markers. The x-axis represents the genetic distance (cM), while the y-axis shows the physical distance (Mb) of markers along the chromosomes.

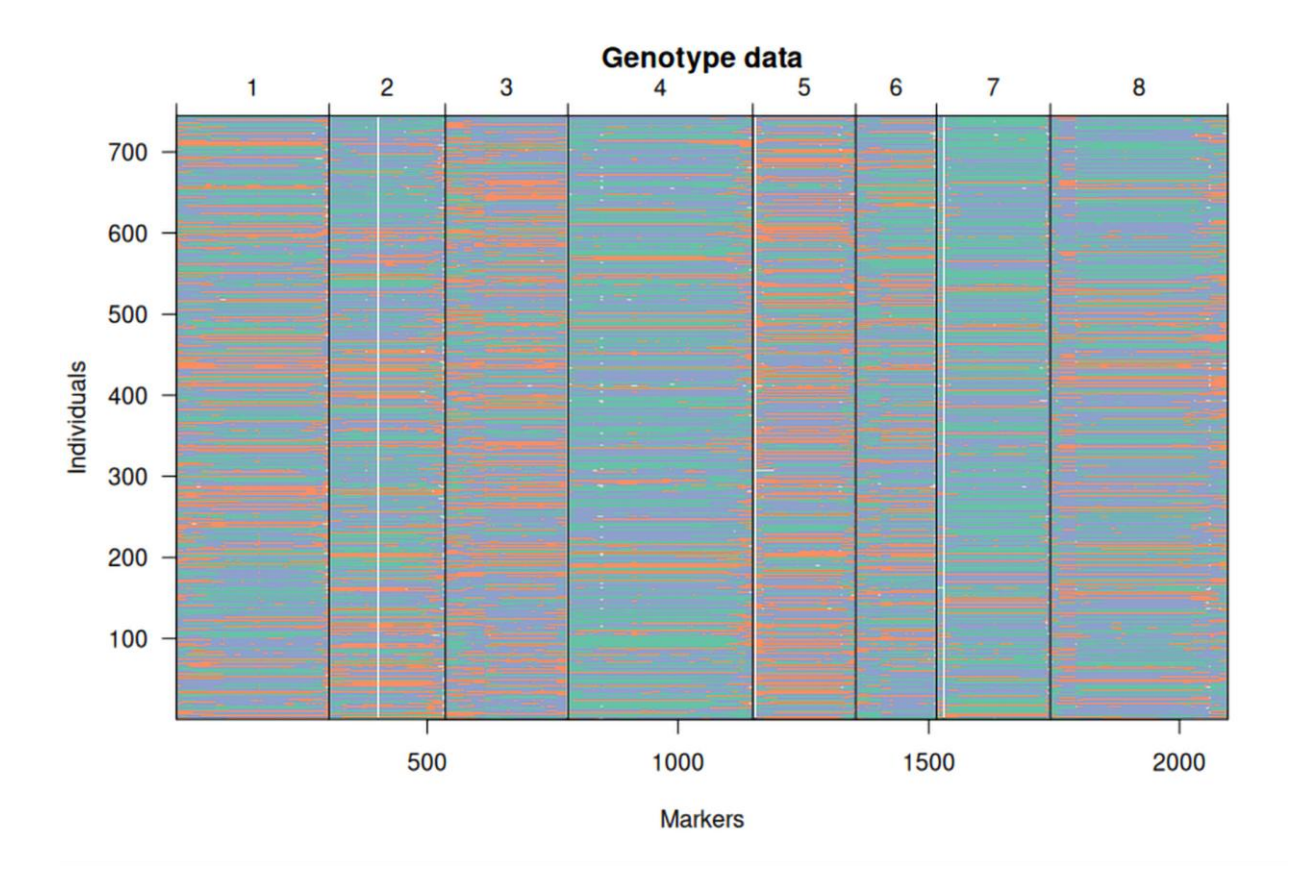


Figure 9. Mosaic plot of SNP distribution along the genome in the *Arabis* mapping population. The plot depicts the distribution of 2,082 SNP markers across the genome for each of the 742 individuals in the mapping population. Different colors represent the genotypes observed at each marker: orange = NN, purple = NS, green = SS, and grey = missing data (N: *A. nemorensis* allele; S: *A. sagittata* allele). The y-axis represents individuals, while the x-axis shows the SNP markers distributed across 8 chromosomes. This visualization highlights the recombination breakpoints within the chromosomes of each individual.

Using frequency of allele N, most SNPs on chromosome 4 and all SNPs on chromosome 7 were significantly distorted from Hardy-Weinberg equilibrium (HWE; Figure 10A). To estimate the strength of selection in these distorted regions across the genome, I calculated deviations from expected allele frequencies in the F2 population (Figure 10B). This analysis identified potential selection acting on several genomic regions. In addition to chromosomes 4 and 7, which showed the strongest distortion, chromosomes 5 and 6, as well as a few markers on other chromosomes, were significantly influenced by selection.

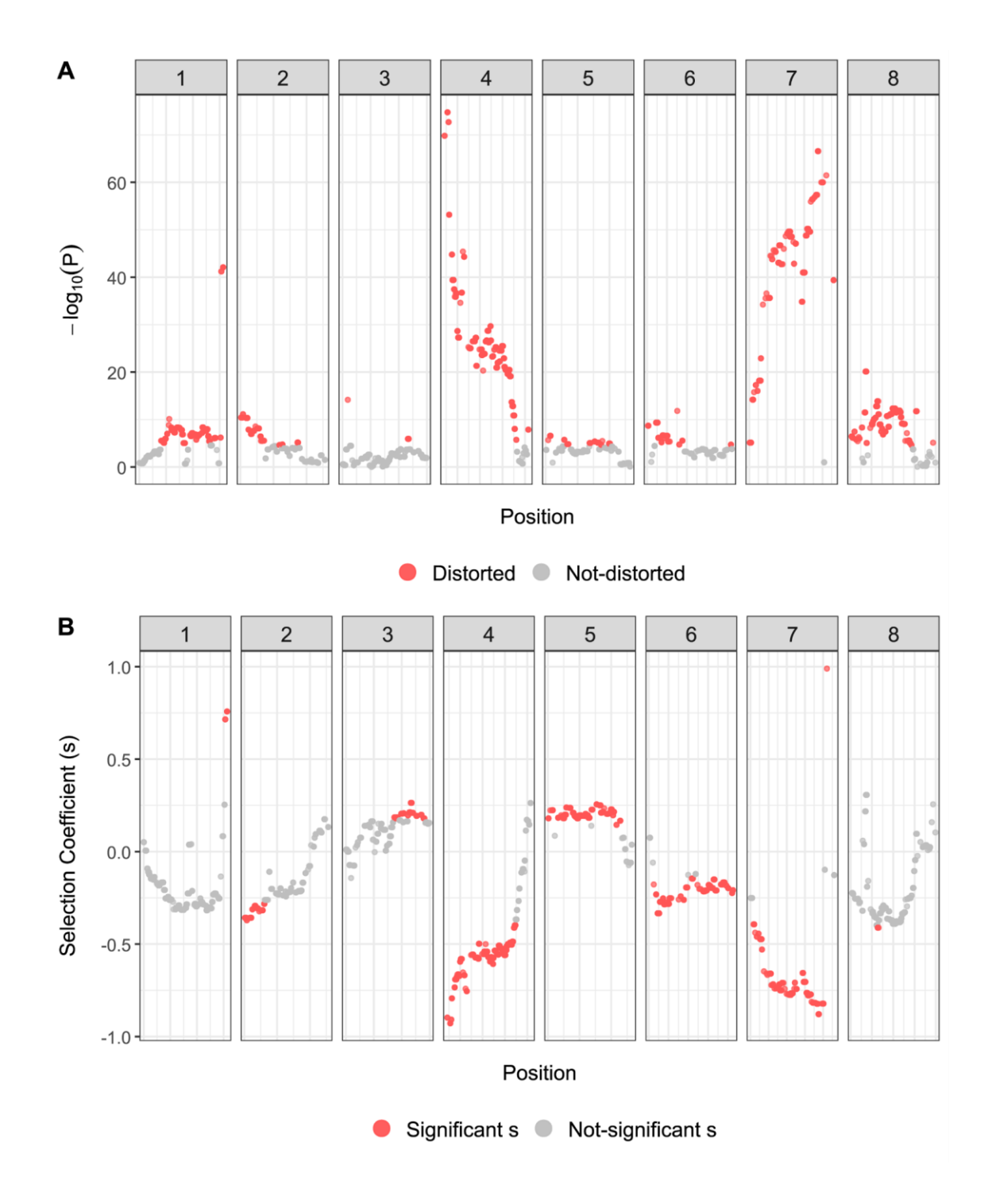


Figure 10. Segregation distortion and strength of selection along the genome. This figure illustrates segregation distortion and the strength of selection across the genome in the F2 population. (A) SNPs significantly deviating from Hardy-Weinberg equilibrium (HWE) are highlighted, particularly on chromosomes 4 and 7. (B) Selection coefficients (s) were calculated based on deviations from expected allele frequencies, with significant SNPs (p<0.05) indicating potential selection hotspots across chromosomes 4, 5, 6, 7, and others.

Genetic Architecture of Ecologically Relevant Traits

I detected significant QTLs for 20 traits. The number of QTLs per trait ranged from 1 (Lamina Length) to 5 (Days to Flowering). The most significant QTL (LOD score > 40) was identified on chromosome 8, accounting for more than 20% of variation in flowering time. In contrast, the lowest LOD score (3.027) was observed in one of the Leaf Width QTLs. In total, 58 QTLs were identified along the genome. We observed overlapping QTLs for multiple traits, including 9 on chromosome 1, 3 on chromosome 2, 11 on chromosome 3, 4 on chromosome 4, 3 on chromosome 5, 2 on chromosome 6, 6 on chromosome 7, and 20 on chromosome 8 (Figure 11). Notably, one QTL associated with Fertility Score on chromosome 6 did not overlap with any other QTLs. The data has been summarized in Figure 11 and Table 7.

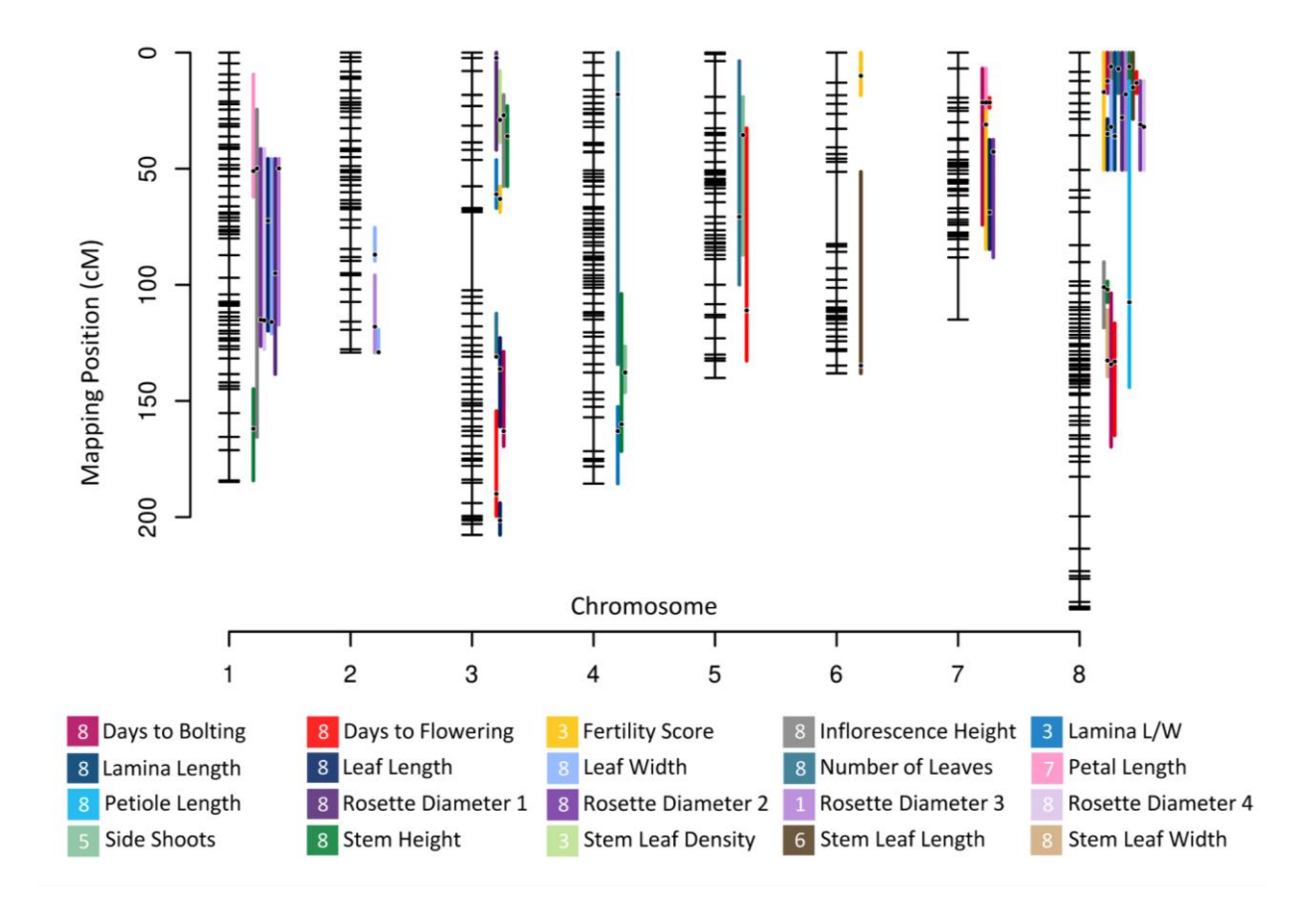


Figure 11. Genetic map with QTLs for ecologically relevant traits. The plot above illustrates significant detected QTLs and their location on the genetic map. Horizontal bars represent mapped SNP markers. Gaps between bars stand for the genetic distance between SNP markers in cM. Traits are listed in alphabetical order. The chromosome containing the strongest QTL of each trait is written in the square.

The strongest QTLs for traits such as Days to Bolting, Days to Flowering, Inflorescence Height, Leaf Length and Width, Number of Stem Leaves, and Rosette Diameters 1, 2, and 4, as well as Stem Height and Stem Leaf Width, were all located on chromosome 8. Additionally, strongest QTLs for Petal Length, Rosette Diameter 3, Side Shoots, Stem Leaf Density, and Stem Leaf Length were identified on chromosomes 7, 1, 5, 3, and 6, respectively. A complete overview can be found in Table 7.

QTLs with LOD scores higher than 10 were detected for traits such as Days to Bolting and Flowering, Inflorescence Height, Lamina Length-to-Width ratio, Number of Stem Leaves, Stem Height, and Stem Leaf Width (Figure 12). However, most QTLs had smaller effect sizes.

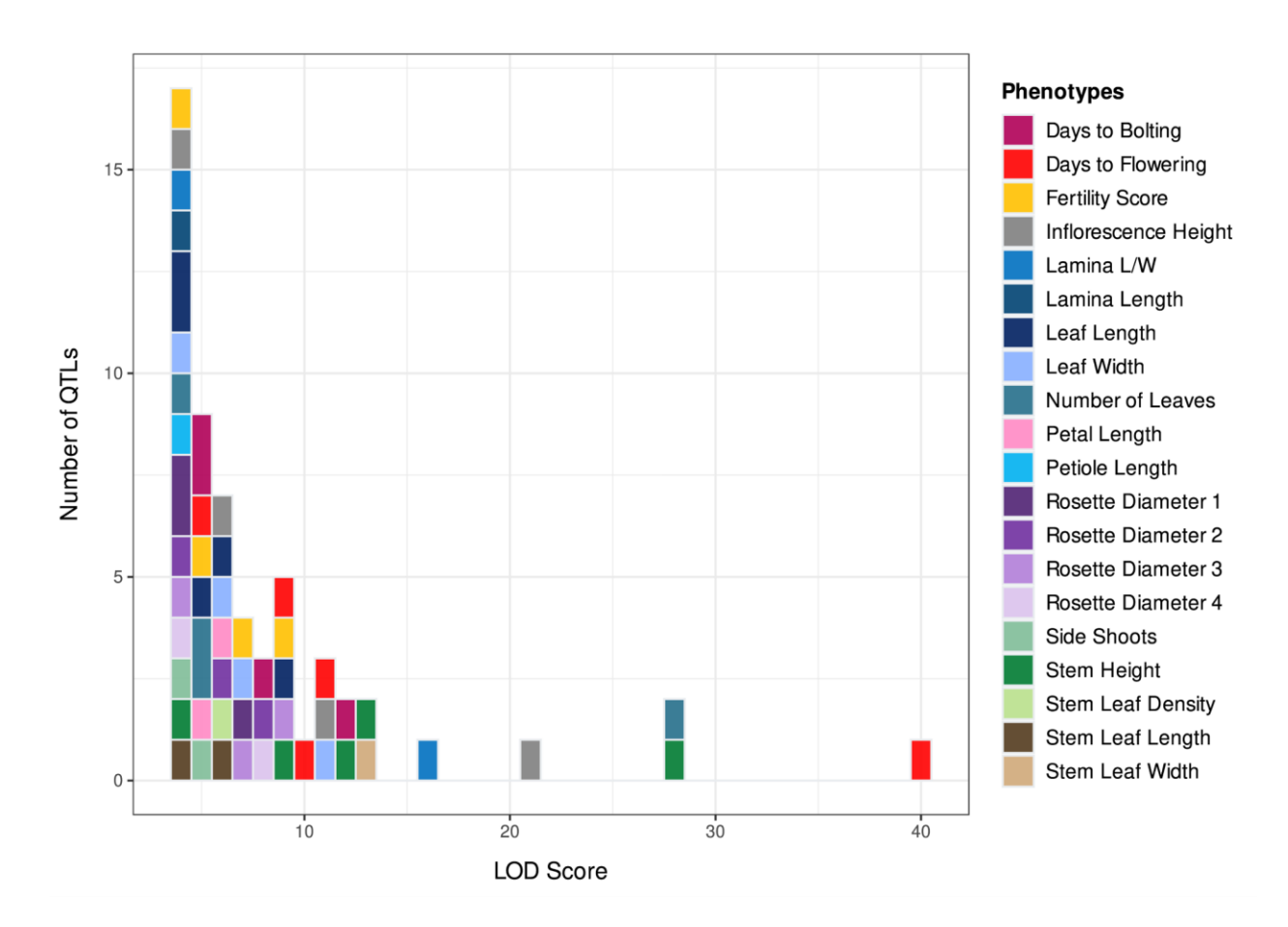


Figure 12. QTLs LOD score distribution. The figure above shows the distribution of ecological relevant traits QTLs detected in the F2 population LOD scores. Each block represents one QTL and color phenotypes.

The genetic architecture of fertility score appeared fairly simple: a large effect QTL (LOD = 8.774) was detected on chromosome 3 (Figure 13), which explained more than 30% of the phenotypic variation and involved inter-allelic incompatibility at position 8362080 bp on chromosome 3. Individuals with the NS heterozygous genotype at this marker displayed markedly lower fertility. In addition, three smaller QTLs explaining 2.683%, 4.641% and 3.507% of the variation were found on chromosome 6, 7 and 8, respectively. It can be concluded that the genetic basis of outbreeding depression is relatively simple in this population.

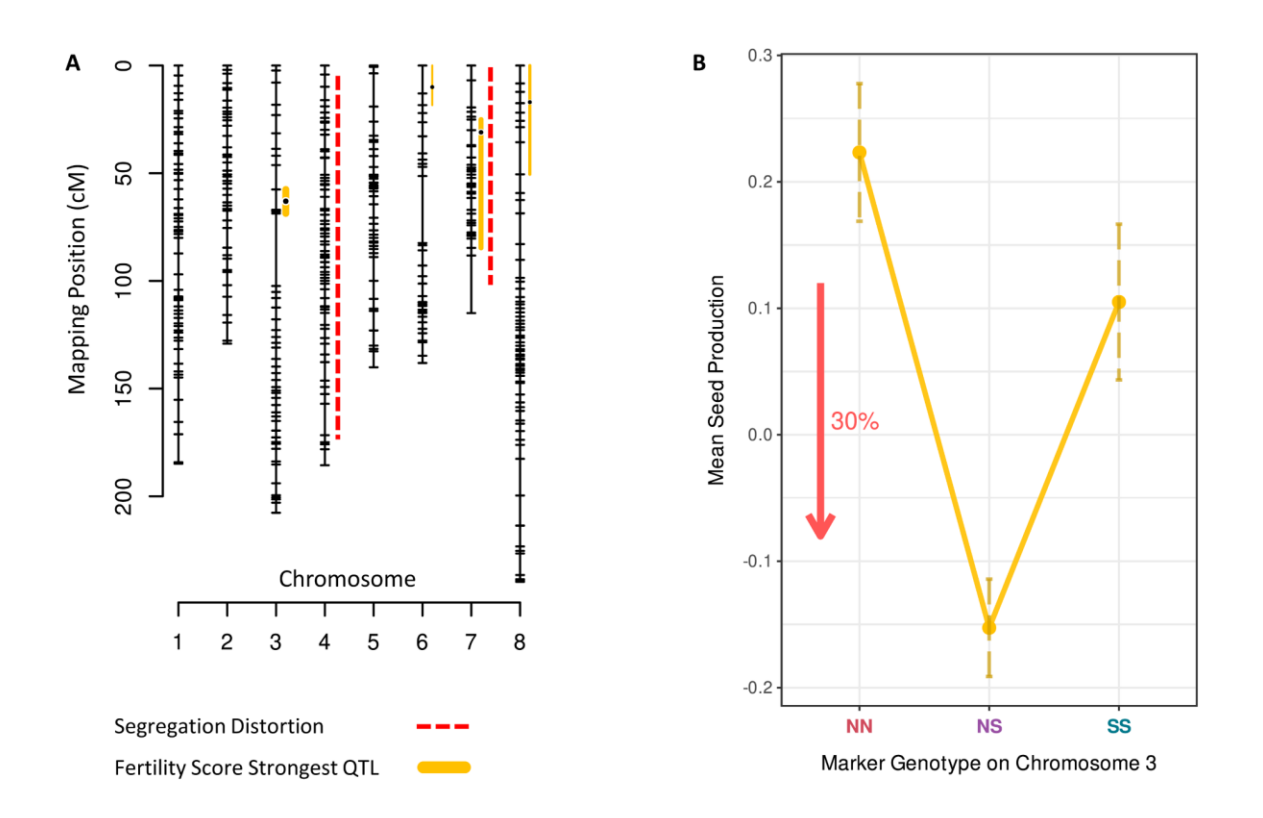


Figure 13. Genetic architecture of fertility score. (A) The genetic architecture of Fertility Score and segregation distortion are displayed. The width of the bars represents the strength of the LOD score for each QTL. (B) The effect of the strongest Fertility Score QTL located on chromosome 3 is shown, highlighting its inter-allelic incompatibility.

Of the 22 traits scored, Ground Shoots (Gsh), Petiole Length-to-Lamina Length ratio (P.L), and Survival to Flooding revealed no significant QTL. For two of these three traits (Ground Shoots, Petiole Length-to-Lamina Length ratio), significant differences between species were observed. The absence of QTLs for these traits suggests they may have a polygenic genetic basis, with the effect of individual variants too small to be individually detected.

Table 7. QTLs of ecologically relevant traits in the *Arabis* mapping population. This table summarizes the number, positions, LOD scores, percentage of phenotypic variance explained, and estimated additive and dominance effects of each QTL. The number of observations per trait in the F2 population is indicated. Significance differences between parental lines are denoted as follows: **** (p < 0.001), ** (0.001 < p < 0.01), * (0.01 < p < 0.05), and . (0.05 < p < 0.1).

Trait	Number of Observation	Sig Parental Difference	Chr@ Position (cM)	LOD	%Variance Explained	est a	est d
	631	***	3@163.0	5.146	3.13	0.0059139	-0.0127649
Days to Bolting			7@21.5	5.359	3.263	0.0109895	0.0026476
(B.T)			8@12.2	7.786	4.783	-0.0119891	0.0004472
			8@134.2	12.396	7.746	0.0162444	-0.0036196
		l.	3@190.0	10.003	4.952	0.012242	-0.001815
		***	5@111.0	4.69	2.273	-0.007092	0.003427
Days to Flowering (F.T)	578		7@21.5	11.23	5.587	0.011243	-0.001854
			8@13.0	40.452	22.701	-0.021252	0.00832
			8@133.0	8.913	4.393	0.009159	-0.005437
	552		3@63.0	8.774	6.165	-0.05627	-0.36635
Fertility Score (W.S)			6@10.0	3.897	2.683	0.17239	-0.05558
			7@31.0	6.663	4.641	0.20569	-0.05308
			8@17.0	5.07	3.507	0.17808	-0.02882
Inflorescence Height (P.H)	578		1@49.9	4.166	2.385	-0.012682	0.062053
			3@27.0	11.394	6.714	0.078301	0.016361
			8@6.0	20.789	12.728	-0.094477	0.076771
			8@101.0	6.383	3.686	-0.062798	-0.038649
Lamina Length (Lam)	436	*	8@36.0	4.334081	4.474593	-0.07559	0.04225
Lamina L/W (LLW)	436	***	3@61.0	15.635	14.89	0.089464	-0.031374
Laiiiiia L/VV (LLVV)			4@163.0	4.045	3.62	0.041307	0.028487

Trait	Number of Observation	Sig Parental Difference	Chr@ Position (cM)	LOD	%Variance Explained	est a	est d
	436		1@72.4	4.458	3.766	0.071867	-0.012244
			3@136.2	5.214	4.423	-0.007829	0.118366
Leaf Length (L.L)			3@201.4	5.617	4.775	0.066584	-0.094772
			7@68.8	4.284	3.615	-0.020747	0.086727
			8@35.0	9.433	8.183	-0.104748	0.036218
			1@116.0	4.313	3.893	0.06977	0.04546
Leaf Width (L.W)	436		2@87.0	3.027	2.713	-0.04395	0.056
Lear Width (L.W)	430		2@129.0	5.987	5.452	0.09125	0.0124
			8@32.0	6.705	6.129	-0.08197	0.03677
	625	***	3@130.9	4.581	2.557	0.025147	0.059693
Number of Stem			4@18.0	4.001	2.228	0.056356	0.010451
Leaves (N.L)			5@70.7	5.384	3.014	-0.055649	0.00469
			8@7.0	28.109	17.139	-0.119377	0.052082
Petal Length (Pet)	106	***	1@51.0	4.863	15.82	0.06491	0.03908
. ota: 2011 9 (1 01)	100		7@21.5	5.689	18.85	0.07916	0.01348
Petiole Length (Pti)	361	**	8@107.5	3.813672	4.748544	-0.1532	-0.03513
Rosette Diameter 1 (RD1)	695		1@95.0	4.498	2.747	1@95.0a	-0.02059
			3@2.3	3.632	2.212	3@2.3a	0.0231
			8@28.0	6.942	4.275	8@28.0a	0.03299
Rosette Diameter 2 (RD2)	700		1@115.0	6.158	3.703	1@115.0a	1@115.0d
			7@42.7	3.839	2.291	7@42.7a	7@42.7d
			8@31.0	7.822	4.729	8@31.0a	8@31.0d
Rosette Diameter	696		1@49.9	9.389	5.683	0.10271	-0.005208
3 (RD3)			2@118.0	4.024	2.392	0.043216	0.071859

Trait	Number of Observation	Sig Parental Difference	Chr@ Position (cM)	LOD	%Variance Explained	est a	est d
			8@18.0	7.209	4.332	-0.087105	0.022622
Rosette Diameter 4 (RD4)	701	*	1@115.3	4.33	2.678	0.061815	0.014845
	701		8@32.0	7.814	4.888	-0.078677	0.035138
Sida Shaata (Ssh)	595	*	4@137.7	3.859	2.842	-0.11993	-0.03855
Side Shoots (Ssh)	595		5@35.5	4.875	3.605	0.12658	0.03145
	625	***	1@162.0	3.594	1.778	-0.029247	0.036282
Stem Height (S.H)			3@36.0	13.598	6.984	0.074366	0.005981
			4@160.0	4.386	2.177	0.042699	-0.004189
			8@6.0	26.851	14.5	-0.091994	0.070533
			8@102.0	7.858	3.951	-0.059677	-0.004408
Stem Leaf Density (SLD)	624	***	3@29.0	5.759854	4.161738	-0.0524259	-0.0180808
Stem Leaf Length (SLL)	259	**	6@134.8	5.918	9.356	0.046349	0.011155
			8@15.0	3.967	6.163	-0.03538	0.01124
Stem Leaf Width (SLW)	259	***	8@132.5	13.22767	20.95838	-0.084603	0.017725

Chapter 3: Flowering time QTL fine-mapping

Flowering Time Responsible Genes

The largest QTL detected in this study impacts the timing of flowering and is located on chromosome 8, where two candidate flowering time genes are located: *FLC*, a regulator involved in the vernalization pathway, and *CONSTANS*, a regulator involved in the photoperiod pathway (Andrés & Coupland 2012). *FLC* has been shown to be a key variant shaping flowering time in many Brassicaceae species, including the congeneric species *Arabis alpina* (Soppe et al. 2021). The gene *CONSTANS* is also located within the boundaries of this largest QTL. In order to test whether one of these candidate genes was responsible for the variation, I selected 15 F2 individuals that were heterozygous in the chromosome 8 QTL and homozygous on the other QTLs and grew 30 of their seeds. Total of 410 plants were assessed for flowering time in 15 F3 families and two trials, one planted in September and the other one in November. Both trials and families differed time to flowering (Figure 14, Table 8, Appendix repository on GitHub, under Chapter 3).

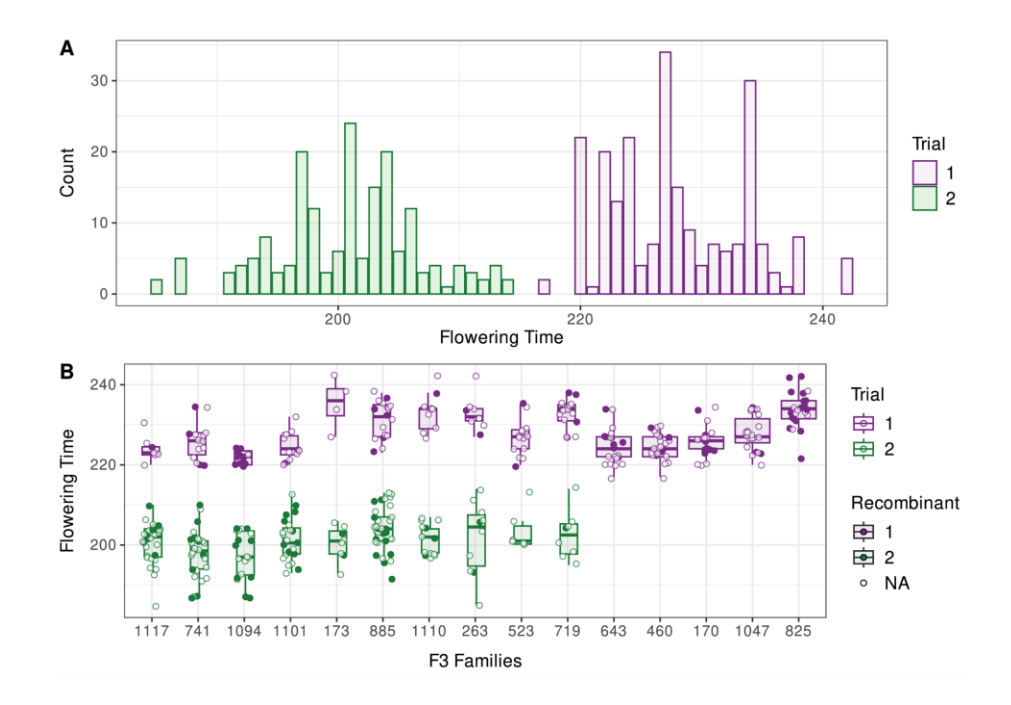


Figure 14. Distribution of flowering time in *Arabis* **F3 hybrids.** The figure represents the distribution of flowering time among 410 F3 plants across two trials. These plants belong to 15 different genotypic classes (derived from 15 distinct F2 lines). Individuals displaying recombination are shown in dark color, while non-recombinant lines are depicted with transparency.

In Trial 1, Family 825, with most replicates, displayed the latest mean flowering time at 233 days (n=23, SD=4.50). Conversely, Family 1094 flowered earliest with the lowest variation, averaging 222 days (n=15, SD=1.62). In the second trial, plants generally showed earlier flowering than the first trial (Table 8). This may be due to differences in environmental conditions such as temperature, or light intensity, despite efforts to maintain consistent settings in both common garden experiments. Family 1094 was again the earliest to flower with a mean of 198 days (n=19, SD=5.86), while Family 885 had the latest mean flowering time at 204 days (n=34, SD=5.43). The lowest variation was observed in Family 173, while the highest variation was seen in Family 263.

Table 8. Overview of *Arabis* **F3 families' mean flowering time.** This table provides the mean flowering time for each F3 family across the two trials of the fine-mapping experiment. Trial 2 did not include all 15 families.

F3 Family	Mean Flowering Time in Trial 1	Mean Flowering Time in Trial 2
170	226	NA
173	235	200
263	233	202
460	225	NA
523	227	204
643	224	NA
719	233	202
741	226	198
825	234	NA
885	231	204
1047	228	NA
1094	222	198
1101	225	201
1110	233	201
1117	224	201

With 410 plants and a QTL region that was ~17 cM, I expected 80 recombinants. Interestingly, I identified 138 recombinants, suggesting that the recombination rate had been slightly

underestimated in the F2 population. I compared four models to identify the chromosomal fragments that best explained flowering time variation, after accounting for all other factors of the experimental design. Using Akaike's criterion and comparing p-values, I identified fragment 2 as the most likely to explain flowering time variation (Figure 15, p=0.0118). This segment ranges from position 1,831,324 bp to position 2,125,083 bp at the beginning of Chromosome 8. This ~300 kb region contains 64 genes, 31 of which have a known orthologs in *Arabidopsis thaliana*. Only one of these, TFL1, is known to regulate flowering time in *A. thaliana* (Cerise et al. 2023). A loss-of-function mutation in *TFL1* induces earlier flowering in *A. thaliana* and belongs to the autonomous pathway. The fine mapping allowed to exclude the role of flowering loci such as *FLC* or *CO* within the QTL region.

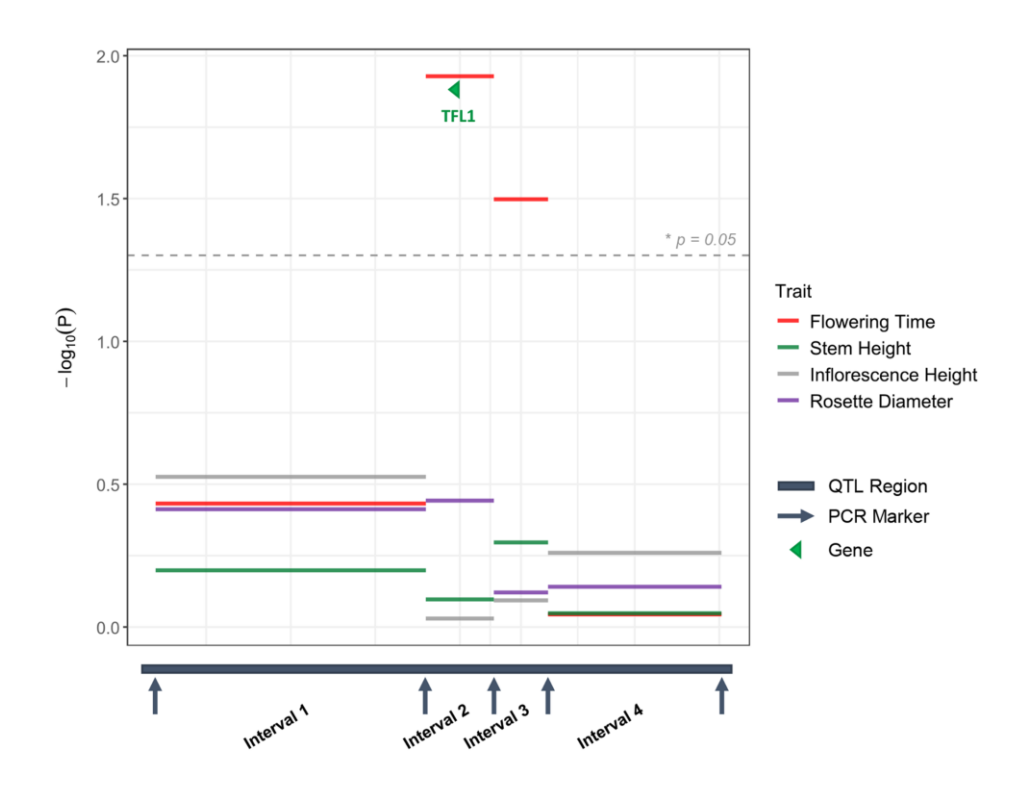


Figure 15. Fine-mapping of flowering time QTL #1, which explains 22.7% of flowering time variation.

The figure illustrates the effect of genomic intervals within the QTL region in explaining the variation in Flowering Time, Inflorescence Height, Rosette Diameter, and Stem Height. The x-axis represents the strongest flowering time QTL region, divided into intervals defined by species-specific primers with adjusted lengths for fine mapping. The dashed line indicates the significance threshold. Different bar colors represent different traits. The TFL1 gene was detected in interval 2, which shows the strongest effect on flowering time.

Although there were QTLs for Inflorescence Height, Rosette Diameter, and Stem Height, on chromosome 8 in F2s, the chromosomal region that was fine mapped did not explaining the variation of these traits in F3s (Figure 16 to 19). Inflorescence Height, Rosette Diameter and Stem Height are thus controlled by a QTL independent of the flowering time QTL in the TFL1-containing fragment, with the S allele advancing flowering.

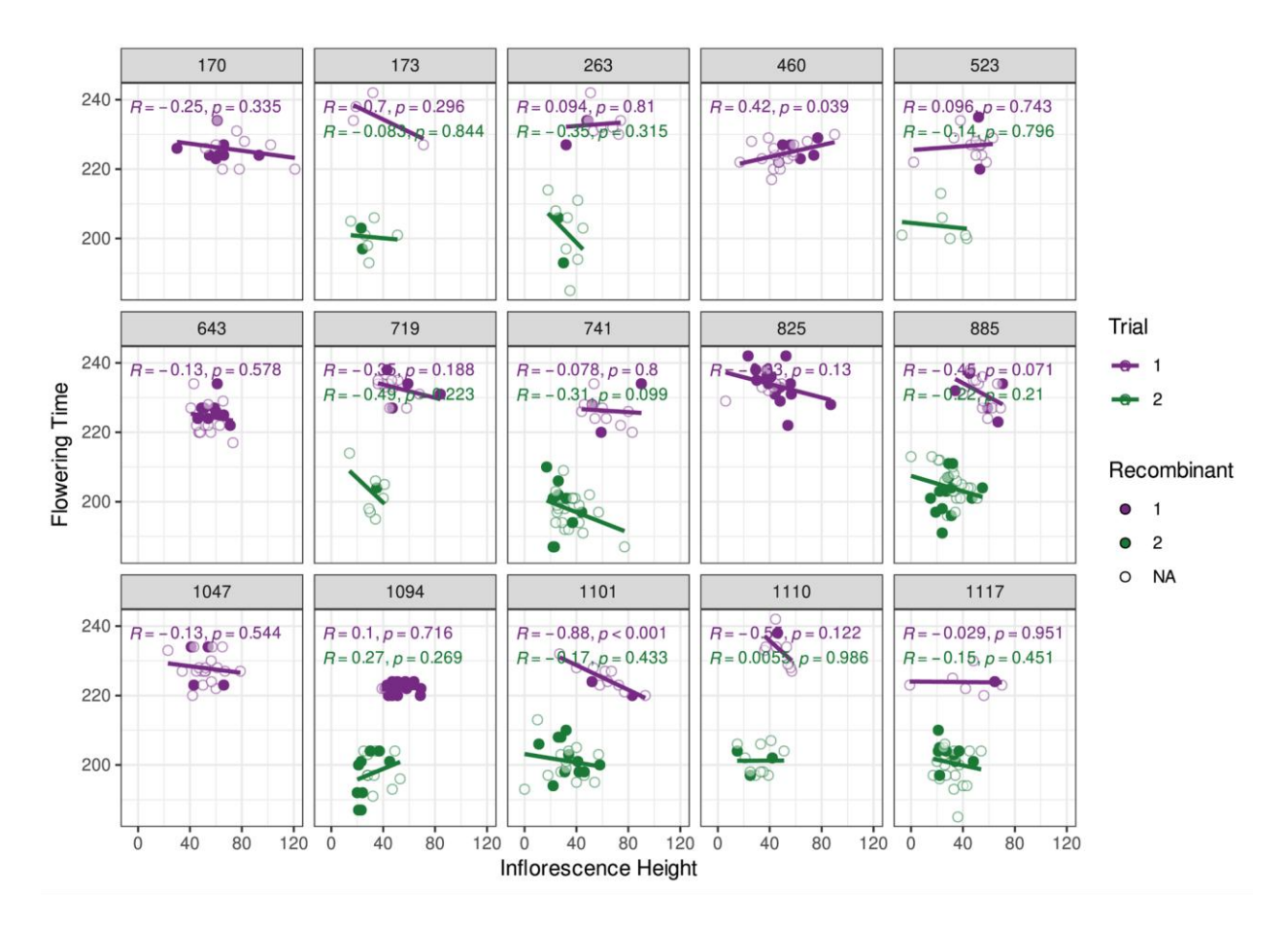


Figure 16. Phenotypic correlations between Inflorescence Height and Flowering Time in *Arabis* F3 plants. This figure illustrates the correlation between Inflorescence Height and Flowering Time, highlighting the significant influence of Inflorescence Height on variation in Flowering Time. Data is shown for each genotype class across both trials. Individuals with recombination events are depicted in dark colors, while non-recombinant lines are shown with transparency.

Linear mixed model results show there is no significant influence of Plant Height, Internode Length, and Stem Leaf Density on differences in flowering time. However, I detected significant effects of Inflorescence Height, Rosette Diameter, Shoot Number, and Stem Height on flowering time. Therefore, I further looked into the interaction of those traits and genotype class on

explaining the variation of flowering time. Further details on the correlation of phenotypes within each family can be found in Figure 16 to 19.

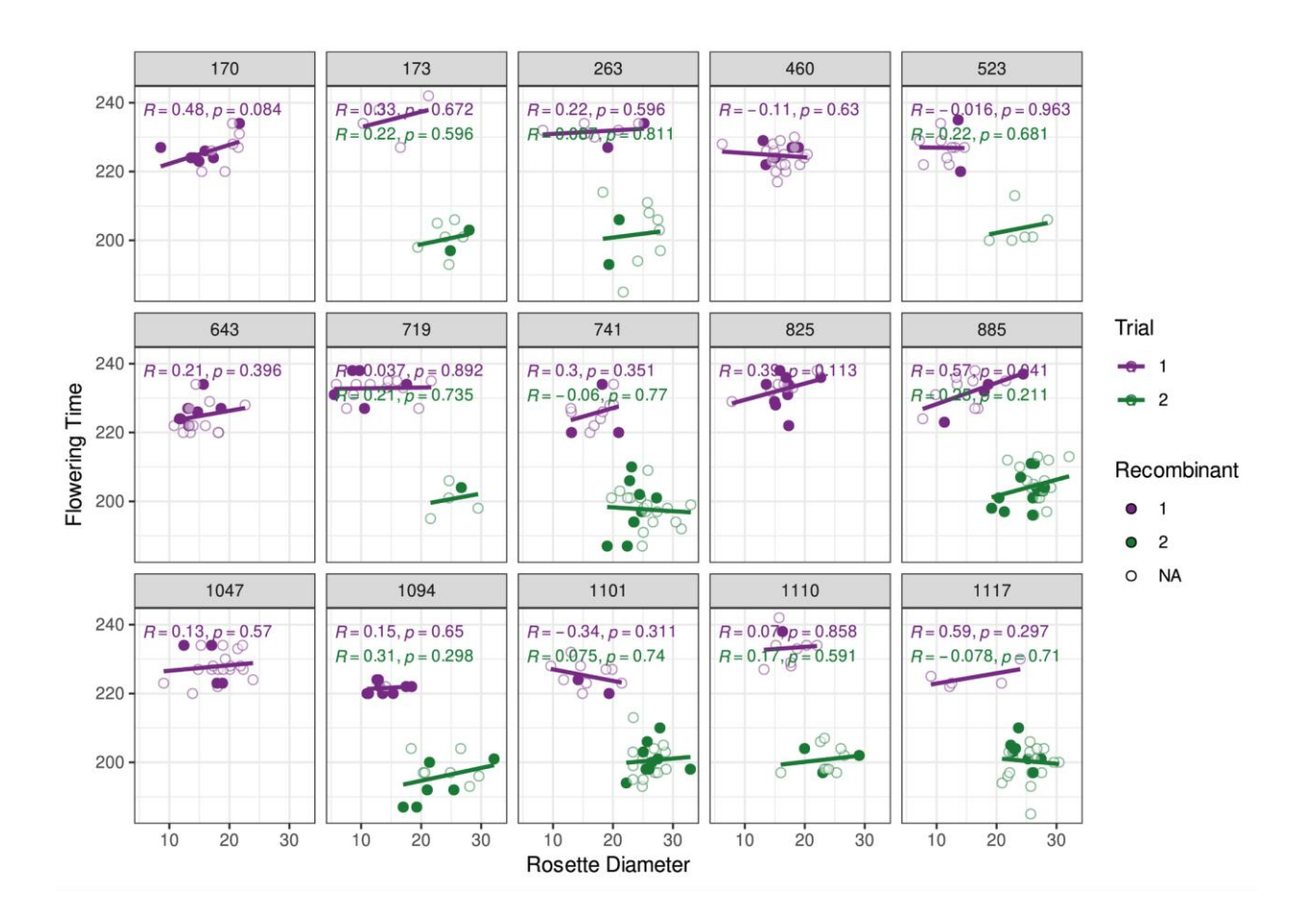


Figure 17. Phenotypic correlations between Rosette Diameter and Flowering Time in *Arabis* F3 plants. This figure illustrates the correlation between Rosette Diameter and Flowering Time, highlighting the significant influence of Rosette Diameter on variation in Flowering Time. Data is shown for each genotype class across both trials. Individuals with recombination events are depicted in dark colors, while non-recombinant lines are shown with transparency.

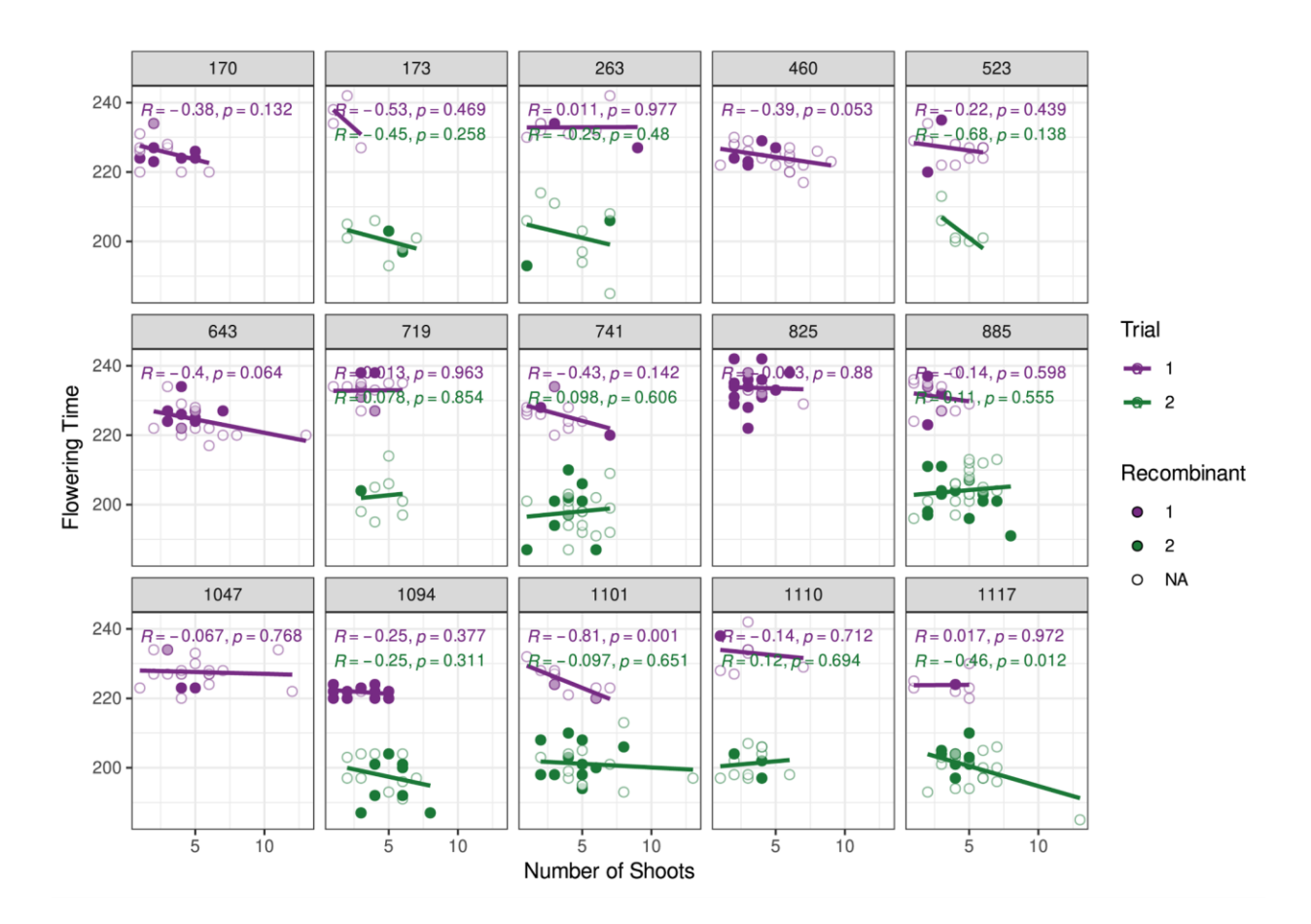


Figure 18. Phenotypic correlations between Number of Shoots and Flowering Time in *Arabis* F3 plants. This figure illustrates the correlation between Number of Shoots and Flowering Time, highlighting the significant influence of Number of Shoots on variation in Flowering Time. Data is shown for each genotype class across both trials. Individuals with recombination events are depicted in dark colors, while non-recombinant lines are shown with transparency.

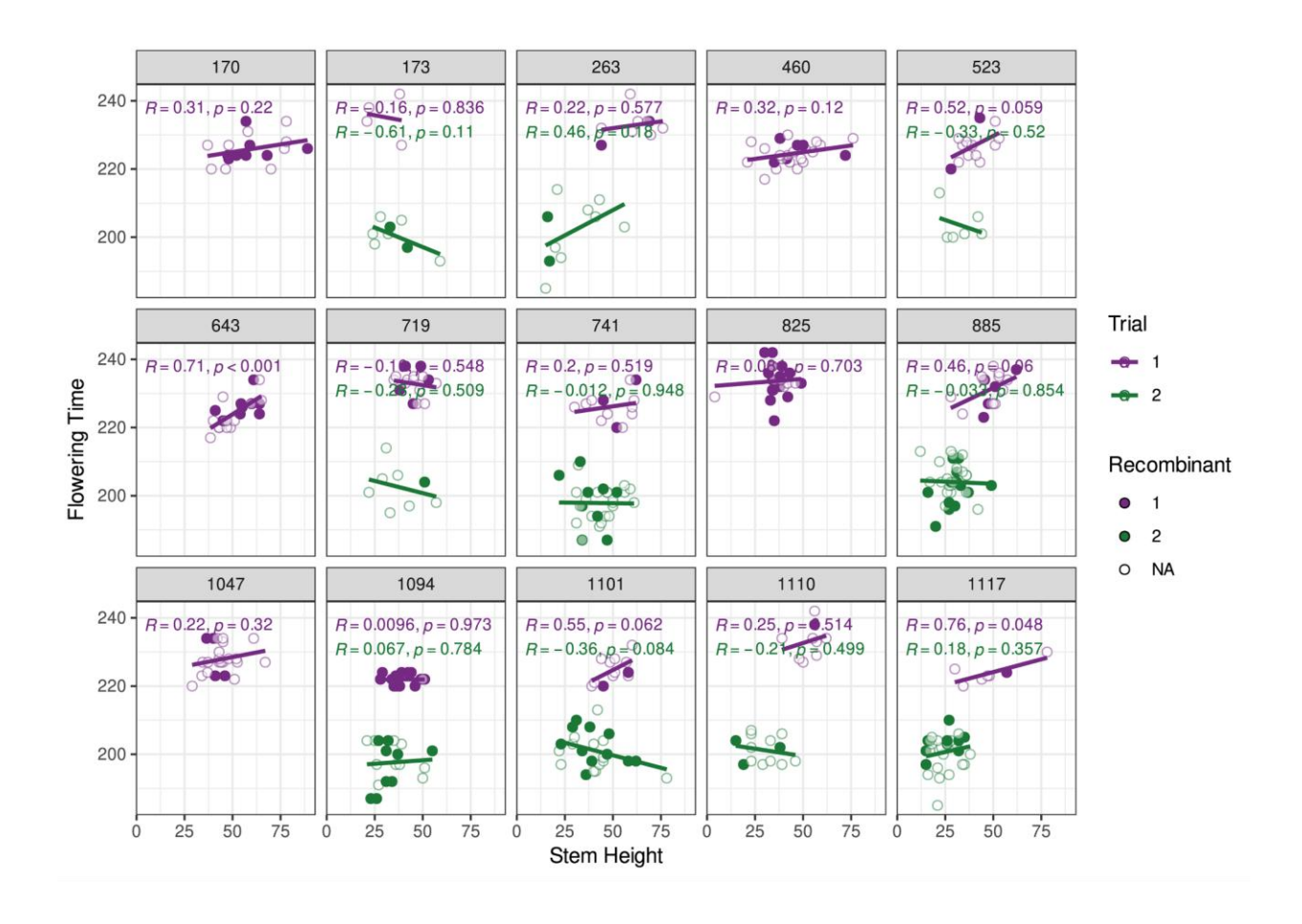


Figure 19. Phenotypic correlations between Stem Height and Flowering Time in *Arabis* F3 plants. This figure illustrates the correlation between Stem Height and Flowering Time, highlighting the significant

influence of Stem Height on variation in Flowering Time. Data is shown for each genotype class across both trials. Individuals with recombination events are depicted in dark colors, while non-recombinant lines are shown with transparency.

4. Discussion

Chapter 1: Growth variation under nutrient-limiting conditions

How do plants respond to different soil compositions? How do they perform under nutrient-limiting conditions? Which traits provide the most insight into the effects of soil conditions on plants? These questions, among others, can often be addressed by examining plant roots. Roots serve as the pioneering frontier of plants, extending into the soil and playing a critical role in the uptake of water and nutrients (Lynch 1995; Hermans et al. 2006; Ober et al. 2021; Schneider & Lynch 2024).

Various studies have investigated root trait variation in *Arabidopsis thaliana* (Lefebvre et al. 2009; Rosas et al. 2013; Ferguson et al. 2015; Dong et al. 2020). Many of these studies have focused on root growth responses or comparisons between below- and above-ground traits, particularly under nutrient-limiting conditions (Lefebvre et al. 2009; Jalal et al. 2023). Nutrient-deficient soils significantly influence plant development and physiological processes, which have long been a critical factor in plant evolution under natural selection pressures (Lefebvre et al. 2009; Anneberg & Segraves 2020; Karthika et al. 2020).

Nutrient deficiencies affect plants in various ways. For example, nitrogen (N) deficiency leads to shorter vegetative growth, yellowing of older leaves, reduced plant size, and earlier flowering and fruiting. Phosphorus (P) deficiency slows both shoot and root growth but typically does not alter leaf color. Potassium (K) deficiency weakens root structure and increases glucosinolate levels in roots to mitigate stress. Sulfur (S) deficiency results in shorter, thinner stems, chlorosis (yellowing) of young leaves, and altered stress responses. Iron (Fe) deficiency causes iron chlorosis and modified root growth, while molybdenum (Mo) deficiency impacts the uptake of carbon (C), nitrogen (N), and sulfur (S) (Tejada-Jiménez et al. 2007; Jung et al. 2009; Anjum et al. 2012; Singh et al. 2018; Lynch 2019; Karthika et al. 2020).

A previous study by M. Casado in 2020 (bachelor's thesis) identified significant differences in below- and above-ground resource allocation between *Arabis nemorensis* and *A. sagittata* when grown in nutrient-poor soil. To verify these findings on a larger scale and investigate whether the two species exhibit significant differences in root-to-shoot allocation under nutrient-poor conditions, I conducted growth experiments using a single nutrient-limiting scenario: soil composed of 95% quartz sand and measured the root-to-shoot ratio of plants.

Contrary to my expectations, the results showed no significant difference between the two species in their root-to-shoot investment ratio under nutrient-limited conditions. This experiment, conducted with a single soil type, did not account for the potential influence of local edaphic conditions, which may play a critical role in root trait variation. This limitation contrasts with the findings of Ferguson et al. (2015), who demonstrated that local edaphic conditions significantly influence variation in both root and shoot traits in *A. thaliana*. Similarly, studies on wheat have shown that environmental factors such as drought and moisture concentration in upper soil layers drive root growth deeper to access water and nutrients (Rich et al. 2015; Ober et al. 2021). Interestingly, the total biomass was significantly affected by species, with *A. nemorensis* exhibiting greater biomass—contrary to expectations. However, when examining the Rhine population specifically, biomass differences between the two species were not significant.

Given the ecological differences between these two species (*A. nemorensis*, a meadow-endemic species that does not require longer roots, and *A. sagittata*, commonly found in dry calcareous lands) and the phenotypic differences characterized in Chapter 2, it is premature to conclude that the two species do not differ in their patterns of resource allocation to shoots versus roots. Future experiments should incorporate soil nutrient compositions reflective of natural field locations where these species co-occur. Recent findings by Y. Özoglan (personal communication) regarding molybdenum (Mo) deficiency in natural fields further emphasizes the importance of replicating field conditions in controlled greenhouse experiments. Such studies should test a range of soil types, from nutrient-poor to nutrient-rich, to provide a more comprehensive understanding of root-to-shoot ratios and biomass measurements.

These experiments are essential to determine the extent to which root structure varies between these species and how their ecological differentiation relates to nutrient availability and local adaptation. This broader perspective is crucial to assess whether the lack of observed differences is due to the absence of genetic differences between the species.

Future studies should try to answer the following questions:

- 1. What genetic or environmental factors contribute to the larger biomass observed in *A. nemorensis*?
- 2. How does the lack of significant biomass differences in the Rhine population relate to hybridization dynamics?
- 3. How do soil nutrient compositions in natural habitats influence root and shoot trait variation in these species?

- 4. To what extent do edaphic conditions drive local adaptation in *A. nemorensis* and *A. sagittata*?
- 5. Exploring the drought responses of these species through drought-tolerance experiments in a mapping population, coupled with QTL mapping.

The answer of these questions and the outcomes of these experiments, would provide deeper insights into the genetic and ecological mechanisms underlying growth and adaptation in *Arabis* species under nutrient-limited conditions.

Chapter 2: Genetic architecture of phenotypic differences between endangered hybridizing *Arabis* floodplain species

Our study provides insights into the impacts of hybridization between two endangered plant species, emphasizing the importance of identifying hybridization hotspots in nature and understanding the conditions under which hybridization occurs. I aimed to explore the phenotypic differences between the closely related hybridizing species *Arabis nemorensis* and *A. sagittata*, uncover the genetic basis of their divergence, and evaluate the potential for the emergence of novel genetic combinations with higher fitness and adaptability in the hybridization hotspot.

The analysis of ecologically relevant traits from the common-garden experiment and association analyses confirmed phenotypic and genetic differences between the two species, highlighting the complex outcomes of introgression. Most notably, the majority of traits exhibited transgressive segregation, where hybrid phenotypes extend beyond the range of their parents. This phenomenon, often associated with novel allelic combinations, may confer adaptive advantages. However, in the case of seed production, hybrids displayed significantly lower yields compared to their parents, likely due to hybrid depression caused by underlying genetic incompatibilities.

These incompatibilities are one of the main obstacles in the evolution of hybrids, a concept described as Dobzhansky–Muller model of hybrid incompatibility which means some allelic combination drive from diverging species may be incompatible and therefore reduce the fitness of hybrids (Dobzhansky 1936; Muller 1942). Genetic incompatibilities have been extensively studied across taxa (Bomblies & Weigel 2007; Masly & Presgraves 2007; White et al. 2011; Schumer et al. 2014; Zuellig & Sweigart 2018; Coughlan & Matute 2020).

Interestingly, population genetic analyses suggest that selection against incompatibilities can create the illusion of rapid fixation of introgressed fragments near these loci (Li et al. 2022). Introgression tends to occur more frequently in genomic regions with higher recombination rates, as recombination reduces linkage disequilibrium, separating incompatible alleles from introgressed haplotypes more effectively (Brandvain et al. 2014; Schumer et al. 2018; Owens et al. 2021). This recombination-driven purging of incompatible alleles can further contribute to the illusional rapid rise of introgressed regions (Schumer et al. 2018; Li et al. 2022). Consequently, this phenomenon complicates disentanglement of positive and negative selection along the genome.

In addition, I observed regions of segregation distortion in the genome, particularly on chromosomes 4 and 7. Segregation distortion refers to deviations in allele frequencies from Mendelian expectations in offspring. This phenomenon is well-documented in various plant species, including *Zea* (maize; Lu et al. 2002) and *Solanum* (potato; Manrique-Carpintero et al. 2016). Segregation distortion can arise from selection against one parental allele at different developmental stages (Lyttle 1993). One potential mechanism is meiotic drive, a "selfish" behavior where certain chromosomes or genetic elements manipulate meiosis to increase their transmission frequency, often at the expense of homologous counterparts (Lyttle 1993; Malik 2005; Coulton et al. 2020). This results in the driving element being transmitted at a higher frequency than expected under normal segregation (Malik 2005; Fishman & Saunders 2008; Talbert & Henikoff 2020).

Studies suggest that meiotic drive-induced segregation distortion can negatively impact fitness. For example, in *Mimulus* (monkeyflower), Fishman & Saunders (2008) demonstrated that individuals homozygous for the driving D allele suffered from reduced pollen viability, despite the allele's transmission advantage through female meiosis. Such trade-offs highlight how the selfish behavior of meiotic drive elements can undermine overall reproductive success (Malik 2005; Fishman & Saunders 2008).

In our system, I measured the deviation of observed allele frequencies from expected Mendelian ratios (1:2:1 for genotypes NN, NS, SS) in the F2 population using N allele. Significant deviations were observed; however, a thorough analysis of both genotypic distributions and allele frequencies is necessary to conclusively determine whether meiotic drive is responsible for these deviations.

Our results indicate that incompatibilities complicate the potential for hybrids to achieve stable and advantageous genetic combinations, as they reduce seed production. However, the genetic basis of these incompatibilities, along with observed segregation distortion, appears relatively simple, with only a few loci responsible. Interestingly, about 30% of the traits examined were independent of these incompatibilities. This suggests that by overcoming inter-allelic fertility barriers through backcrossing, progeny could achieve higher fitness relative to their parents in terms of seed production. Thus, hybrid plants could bypass reproductive barriers and contribute to population viability. Furthermore, the presence of traits independent of genetic incompatibilities raises the possibility that some hybrids could adapt to new environments, potentially leading to the emergence of a "super-genotype."

Future directions and open questions:

Our findings emphasize the need for further research to disentangle the genetic and environmental factors shaping hybrid fitness and adaptability. Future studies should include:

- 1. Could this study represent a scenario by which hybrids adapt to survive in natural environments?
- 2. Under what conditions might hybrids overcome genetic incompatibilities and achieve higher fitness?
- 3. What characteristics and trait combinations would convert hybrids into adaptive supergenotypes?
- 4. How do environmental factors, such as flooding and drought, interact with genetic incompatibilities to influence hybrid survival?
- 5. How does competition with other species affect hybrid fitness in the natural field?
- 6. What role do recombination rates play in separating incompatible alleles from introgressed haplotypes?
- 7. Is meiotic drive responsible for the segregation distortion observed on chromosomes 4 and 7, or are other mechanisms at play?
- 8. This could be achieved by backcrossing selected F3 lines to one of the parental species (*A. nemorensis* or *A. sagittata*), particularly species showing an excess of allele in the F2 population.
- 9. Explore the genetic basis of drought tolerance in hybrids, a crucial factor for survival given the increasing temperatures and droughts in the hybrids' habitat over the past few years, focusing on root traits.

Future studies can provide broader understanding of the genetic and evolutionary dynamics of *Arabis* hybridization, offering a better overview of how hybrid genotypes may drive adaptation and survival in rapidly changing environments.

Chapter 3: Flowering time QTL fine-mapping

One of the most remarkable examples of contemporary evolution in plants is the alteration of flowering time in response to environmental changes driven by global climate change (Cho et al. 2017; Bennett & Dixon 2021; Tun et al. 2021). Many plants adjust their flowering time as a strategy to escape rising temperatures. Examples include *Boechera stricta* (Anderson et al. 2012), *Oryza nivara* (Cai et al. 2019), and species such as *Syringa vulgaris* L., *Sambucus nigra* L., *Crataegus monogyna*, and *Prunus spinosa* L. (Siegmund et al. 2016).

Numerous studies have also investigated the genetic and molecular basis of flowering time in *Arabidopsis thaliana* as a model plant. In our study, I found that changes in flowering time in *Arabis nemorensis* and *A. sagittata* hybrids are not linked to major known flowering time genes such as *FLOWERING LOCUS T (FT)*, *FLOWERING LOCUS C (FLC)*, *FRIGIDA (FRI)*, or *CONSTANS (CO)*. Instead, the results suggest that *TERMINAL FLOWER 1 (TFL1)* is a key regulator, pointing to other genetic factors as drivers of flowering time variation in these species.

TERMINAL FLOWER 1 (TFL1), a member of the phosphatidylethanolamine-binding protein (PEBP) gene family, plays a crucial role in regulating flowering time and plant architecture, particularly in the model plant A. thaliana (Hanano & Goto 2011; Benlloch et al. 2015; Serrano-Mislata et al. 2016; Goretti et al. 2020; Cerise et al. 2023). The PEBP gene family is divided into three major clades: MOTHER OF FT (MFT)-like, FLOWERING LOCUS T (FT)-like, and TERMINAL FLOWER 1 (TFL1)-like (Goretti et al. 2020).

While FT and TFL1 share high sequence similarity in A. thaliana, their functions are antagonistic: FT and its closest homolog TWIN SISTER OF FT (TSF) promote flowering, whereas TFL1 represses flowering and delays the transition to reproductive development (Ratcliffe et al. 1998; Ho Ho & Weigel 2014; Leijten et al. 2018; Bennett & Dixon 2021; Wang et al. 2022). This functional antagonism is also evident in tomato (Solanum lycopersicum), where TFL1 orthologs suppress flowering by opposing the activity of the FT ortholog SINGLE FLOWER TRUSS (SFT) (Shalit et al. 2009). Similarly, in Arabis alpina, the TFL1 ortholog (AaTFL1) regulates delayed flowering transitions (Wang et al. 2011).

Beyond flowering time regulation, *TFL1* is essential for maintaining the indeterminate growth of the shoot apical meristem (SAM), allowing plants to continuously produce flowers on lateral branches (Hanano & Goto 2011; Ho Ho & Weigel 2014; Benlloch et al. 2015; Cerise et al. 2023).

In *tfl1* mutants, SAM growth becomes determinate, converting the shoot meristem into a floral meristem. This premature transition leads to earlier flowering and reduced branching, ultimately decreasing the number of flowers (Serrano-Mislata et al. 2016; Cerise et al. 2023).

In *A. thaliana*, *TFL1* employs its regulatory effect by repressing key floral meristem identity genes, *LEAFY* (*LFY*) and *APETALA1* (*AP1*), within the inflorescence meristem. By inhibiting these genes, *TFL1* ensures the inflorescence meristem retains its indeterminate state. Conversely, in floral meristems, *LFY* and *AP1* repress *TFL1* expression, thereby enabling floral development (Benlloch et al. 2015; Goretti et al. 2020).

Studies by Andrés and Coupland (2012), Wang et al. (2009), and Wang et al. (2011) examined the expression patterns of genes regulating perennial flowering in *A. alpina*. Prior to vernalization, two key genes, *PERPETUAL FLOWERING 1* (*PEP1*) and *TFL1*, are expressed in the shoot apical meristem (SAM) of both flowering-competent adult plants and non-competent young plants (Figure 20).

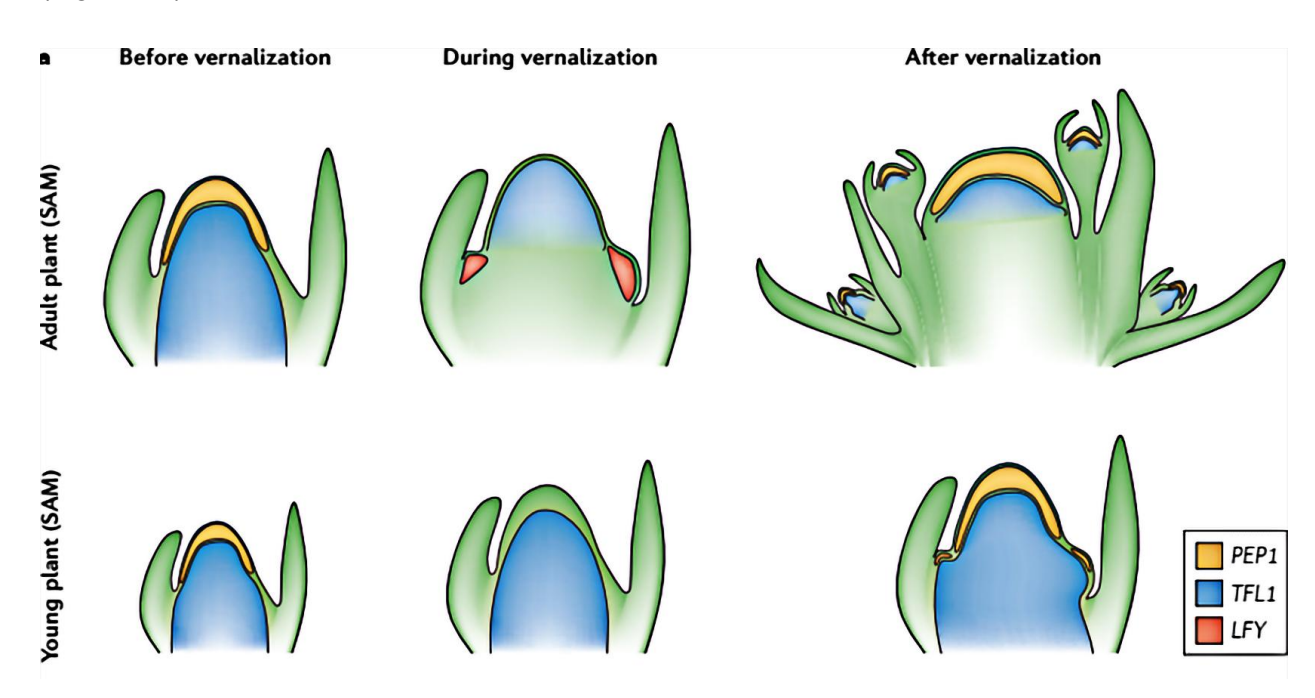


Figure 20. Expression patterns of *PEP1*, *TFL1*, and *LFY* in response to seasonal changes in young and old *A. alpina* plants. Figure adapted from Andrés and Coupland (2012); the quality has been improved for clarity.

In adult plants, vernalization reduces *PEP1* mRNA levels, while *TFL1* expression becomes restricted to the center of the inflorescence meristem. This localized expression of *TFL1* coincides

with the induction of *LFY* mRNA at the flanks of the SAM, promoting the development of floral primordia. Following vernalization, *PEP1* expression reactivates in vegetative axillary meristems, preventing further flowering until the next year.

In young plants, vernalization also reduces *PEP1* mRNA levels; however, *TFL1* expression persists, inhibiting *LFY* activation and blocking the floral transition. After vernalization, *PEP1* mRNA levels increase again in the SAM and axillary meristems, reinforcing the delay in flowering until the following year.

A previous study by Dittberner (2019) demonstrated a significant difference in the number of siliques between *A. nemorensis* and *A. sagittata*, with *A. nemorensis* producing more siliques (Figure 21). Also, in the results presented in Chapter 2, phenotypic analysis from the interspecific F2 common garden experiment revealed that *A. nemorensis* flowers earlier. Additionally, the findings from Chapter 3, which involved the F3 flowering time fine-mapping experiment, characterized differences in the number of shoots within the population. These results suggest that future studies should record variation in the number of siliques as a measurement of branching in these species. This could potentially lead to the identification of *TFL1* again. It is also possible that *TFL1* influences flowering time indirectly by affecting branching and the determinacy of the inflorescence.

Despite the insights gained from this study, the specific genes and quantitative trait loci (QTLs) that influence survival under natural conditions, particularly during extreme environmental events such as flooding and drought, remain unidentified. As demonstrated by Wilczek et al. (2009), variations in flowering time can differ significantly among genotypes depending on germination timing. Since the plants used in the fine-mapping experiment germinated in the fall, it becomes crucial to conduct future research that quantifies the genetic basis of flowering time variation under a broader range of germination timings and environmental conditions. This will provide a clearer understanding of how flowering time, influenced by a complex network of genes, impacts survival and fitness in natural environments.

Future research can address several key questions:

1. Beyond *TFL1*, what other genetic factors contribute to flowering time variation in *A. nemorensis* and *A. sagittata*, and how do they interact within the regulatory network?

- 2. How do extreme environmental conditions, such as flooding or drought, influence flowering time and branching patterns, and what survival strategies might be linked to *TFL1* in these scenarios?
- 3. Given that branching patterns directly influence silique production, how does variation in TFL1 expression correlate with reproductive success and overall fitness in these species? Could TFL1 be identified again if we fine-map the fertility QTLs detected in Chapter 2 on chromosome 8, particularly in the same genomic region?
- 4. *TFL1* was identified as a key flowering regulator in a common garden setting. Will the same association hold in natural field conditions, and what other QTLs might influence flowering time under these variable environments?
- 5. How does the timing of germination or the developmental stage at the onset of vernalization affect *TFL1* expression and subsequent flowering behavior in these species?

Answering these questions can elucidate the genetic and environmental mechanisms controlling flowering time, providing insights into how these species survive and adapt to rapidly changing environments.

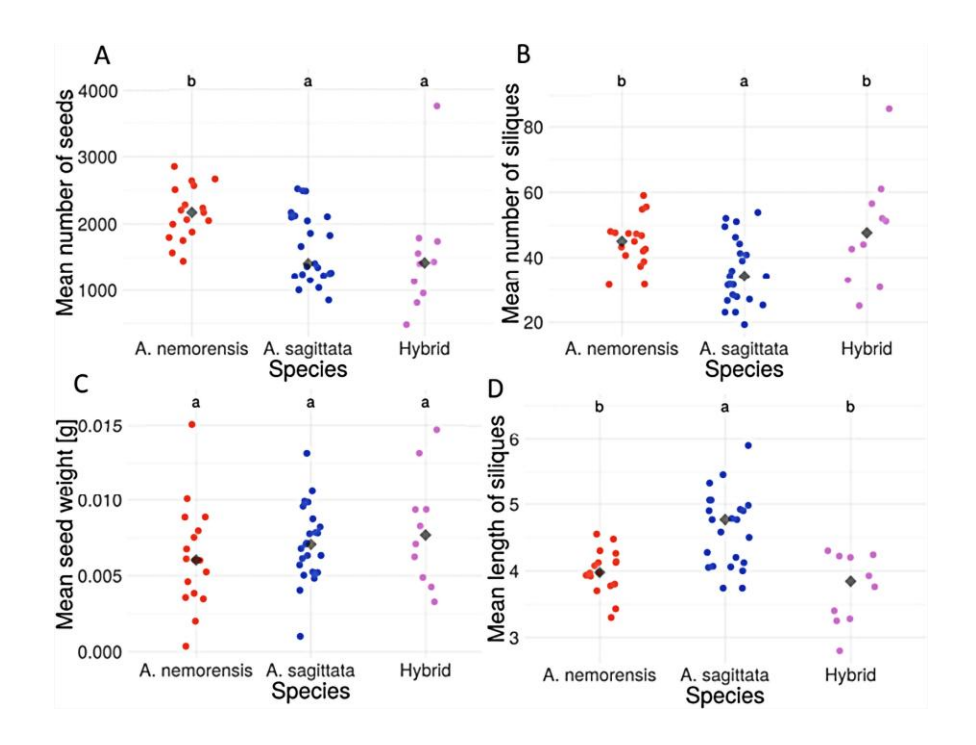


Figure 21. Phenotypic variation in fitness-related traits in *Arabis*. Each point represents the mean value per accession, while diamonds indicate the median. Letters above denote significant differences between groups (p<0.05). Figure taken from Dittberner (2019); the quality has been improved for clarity.

5. Conclusion

This thesis gives a comprehensive exploration of the ecological, genetic, and phenotypic dynamics underlying growth, adaptation, and reproduction in *Arabis nemorensis* and *A. sagittata*, two endangered floodplain species that hybridize. By examining these species under nutrient-limiting conditions, in a common garden of interspecific population, and through the fine-mapping of flowering time QTL, this work highlights the interactions between environmental factors, genetic architecture, and plant performance.

In **Chapter 1**, I examined the response of plants to nutrient-limiting conditions, focusing on root-to-shoot allocation and biomass variation. The results showed no significant differences in root-to-shoot ratios between the species under the nutrient-poor condition, highlighting the need for further studies to incorporate a wider range of soil types reflective of natural habitats. These findings underlie the importance of local edaphic conditions and species-specific ecological strategies in shaping plant growth and resource allocation. Moreover, the larger biomass observed in *A. nemorensis* gives rise to important questions about the genetic and environmental factors contributing to this unexpected variation, which future studies must address.

In **Chapter 2**, I investigated the genetic architecture of phenotypic differences between the two species, with a particular emphasis on hybridization and its consequences. The observed transgressive segregation in hybrids indicates the potential for novel trait combinations, although reduced hybrid seed production, likely caused by genetic incompatibilities, creates a significant challenge. Segregation distortion in specific genomic regions, potentially linked to meiotic drive, adds more complexity to the evolutionary dynamics of hybridization.

This chapter shows clearly how hybridization can simultaneously limit and expand evolutionary potential. However, the relatively simple genetic basis of fertility QTLs, incompatibilities, and segregation distortion, combined with the number of ecologically relevant traits independent of these barriers, suggests that overcoming inter-allelic fertility obstacles through backcrossing could enable progeny to achieve higher fitness compared to their parents in terms of seed production. This ability to bypass reproductive barriers could enhance population viability. Moreover, this highlights the possibility that some hybrids may successfully adapt to new environments, potentially giving rise to a "super-genotype."

Chapter 3 explored the genetic regulation of flowering time, identifying *TERMINAL FLOWER 1* (*TFL1*) as a key factor influencing this trait. The study demonstrated that variation in flowering

time is not linked to major flowering genes like *FLOWERING LOCUS T (FT)* or *FLOWERING LOCUS C (FLC)*, but instead involves the antagonistic regulatory role of *TFL1*. This insight creates a base for future research into the genetic mechanisms controlling flowering time, branching, and reproductive success under natural environmental conditions, particularly in the face of climate change.

Together, these chapters illustrate the complexity of hybridization and survival in *Arabis* species. They point out the need for integrating ecological, genetic, and phenotypic approaches to uncover the mechanisms driving plant responses to environmental challenges. The findings also emphasize the importance of conducting experiments under field-like conditions to better replicate the complexity of natural habitats. By addressing the open questions and future research directions outlined in each chapter, subsequent studies can deepen our understanding of how plants adapt to rapidly changing environments. This thesis contributes to the broader understanding of plant evolution and adaptation, giving information about the ecological and genetic processes that shape species fitness in changing environments.

Bibliography

- 1. Abbott, R., D. Albach, S. Ansell, J. W. Arntzen, S. J.E. Baird, N. Bierne, J. Boughman, et al. 2013. "Hybridization and Speciation." *Journal of Evolutionary Biology*. https://doi.org/10.1111/j.1420-9101.2012.02599.x.
- 2. Abbott, Richard J. 2017. "Plant Speciation across Environmental Gradients and the Occurrence and Nature of Hybrid Zones." *Journal of Systematics and Evolution*. https://doi.org/10.1111/jse.12267.
- Adams, William W., Jared J. Stewart, Stephanie K. Polutchko, Christopher M. Cohu, Onno Muller, and Barbara Demmig-Adams. 2023. "Foliar Phenotypic Plasticity Reflects Adaptation to Environmental Variability." *Plants* 12 (10). https://doi.org/10.3390/plants12102041.
- Aguirre, Windsor E., Kerry Reid, Jessica Rivera, David C. Heins, Krishna R. Veeramah, and Michael A. Bell. 2022. "Freshwater Colonization, Adaptation, and Genomic Divergence in Threespine Stickleback." In *Integrative and Comparative Biology*. Vol. 62. https://doi.org/10.1093/icb/icac071.
- Albani, Maria C., Coral Vincent, Sara Bergonzi, Ming Luan, Yan Bai, Christiane Kiefer, Rosa Castillo, and George Coupland. 2011. "Aa Tfl1 Confers an Age-Dependent Response to Vernalization in Perennial Arabis Alpina." Plant Cell 23 (4). https://doi.org/10.1105/tpc.111.083451.
- Alonge, Michael, Ludivine Lebeigle, Melanie Kirsche, Katie Jenike, Shujun Ou, Sergey Aganezov, Xingang Wang, Zachary B. Lippman, Michael C. Schatz, and Sebastian Soyk. 2022. "Automated Assembly Scaffolding Using RagTag Elevates a New Tomato System for High-Throughput Genome Editing." *Genome Biology* 23 (1). https://doi.org/10.1186/s13059-022-02823-7.
- 7. Anderson, E., and G. L. Stebbins. 1954. "HYBRIDIZATION AS AN EVOLUTIONARY STIMULUS." *Evolution* 8 (4). https://doi.org/10.1111/j.1558-5646.1954.tb01504.x.
- 8. Anderson, Edgar. 2011. *Introgressive Hybridization*. *Introgressive Hybridization*. https://doi.org/10.5962/bhl.title.4553.
- 9. Anderson, Edgar, and Leslie Hubricht. 1938. "Hybridization in Tradescantia. III. The Evidence for Introgressive Hybridization." *American Journal of Botany* 25 (6). https://doi.org/10.2307/2436413.
- 10. Anderson, Jill T., Panetta, Anne Marie, Mitchell-Olds, Thomas. 2012. "Evolutionary and Ecological Responses to Anthropogenic Climate Change: Update on Anthropogenic

- Climate Change." *Plant Physiology* 160 (4): 1728–1740. https://doi.org/10.1104/pp.112.206219.
- 11. Andrés, Fernando, and George Coupland. 2012. "The Genetic Basis of Flowering Responses to Seasonal Cues." *Nature Reviews Genetics*. https://doi.org/10.1038/nrg3291.
- 12. Andrews, Simon. 2010. "FastQC: A Quality Control Tool for High Throughput Sequence Data. 2010." Retrieved from https://Www.Bioinformatics.Babraham.Ac.Uk/Projects/Fastqc/.
- 13. Anjum, Naser A., Sarvajeet S. Gill, Shahid Umar, Iqbal Ahmad, Armando C. Duarte, and Eduarda Pereira. 2012. "Improving Growth and Productivity of *Oleiferous Brassicas* under Changing Environment: Significance of Nitrogen and Sulphur Nutrition, and Underlying Mechanisms." *The Scientific World Journal*. https://doi.org/10.1100/2012/657808.
- 14. Anneberg, Thomas J., and Kari A. Segraves. 2020. "Nutrient Enrichment and Neopolyploidy Interact to Increase Lifetime Fitness of *Arabidopsis thaliana*." *Plant and Soil* 456 (1–2). https://doi.org/10.1007/s11104-020-04727-6.
- 15. Ballaré, Carlos L., and Ronald Pierik. 2017. "The Shade-Avoidance Syndrome: Multiple Signals and Ecological Consequences." *Plant Cell and Environment*. https://doi.org/10.1111/pce.12914.
- 16. Baucom, Regina S. 2019. "Evolutionary and Ecological Insights from Herbicide-Resistant Weeds: What Have We Learned about Plant Adaptation, and What Is Left to Uncover?" *New Phytologist*. https://doi.org/10.1111/nph.15723.
- 17. Becker, Matthias, Nicole Gruenheit, Mike Steel, Claudia Voelckel, Oliver Deusch, Peter B. Heenan, Patricia A. McLenachan, Olga Kardailsky, Jessica W. Leigh, and Peter J. Lockhart. 2013. "Hybridization May Facilitate in Situ Survival of Endemic Species through Periods of Climate Change." Nature Climate Change 3 (12). https://doi.org/10.1038/nclimate2027.
- 18. Benlloch, Reyes, Ana Berbel, Latifeh Ali, Gholamreza Gohari, Teresa Millán, and Francisco Madueño. 2015. "Genetic Control of Inflorescence Architecture in Legumes." *Frontiers in Plant Science*. https://doi.org/10.3389/fpls.2015.00543.
- 19. Bennett, Tom, and Laura E. Dixon. 2021. "Asymmetric Expansions of FT and TFL1 Lineages Characterize Differential Evolution of the EuPEBP Family in the Major Angiosperm Lineages." BMC Biology 19 (1). https://doi.org/10.1186/s12915-021-01128-8.

- 20. Blanckaert, Alexandre, Vedanth Sriram, and Claudia Bank. 2023. "In Search of the Goldilocks Zone for Hybrid Speciation II: Hard Times for Hybrid Speciation?" *Evolution* 77 (10). https://doi.org/10.1093/evolut/qpad125.
- 21. Bomblies, Kirsten, and Detlef Weigel. 2007. "Hybrid Necrosis: Autoimmunity as a Potential Gene-Flow Barrier in Plant Species." *Nature Reviews Genetics*. https://doi.org/10.1038/nrg2082.
- 22. Bontrager, Megan, and Amy L. Angert. 2019. "Gene Flow Improves Fitness at a Range Edge under Climate Change." *Evolution Letters* 3 (1). https://doi.org/10.1002/evl3.91.
- 23. Brandvain, Yaniv, Amanda M. Kenney, Lex Flagel, Graham Coop, and Andrea L. Sweigart. 2014. "Speciation and Introgression between *Mimulus Nasutus* and *Mimulus Guttatus*." *PLoS Genetics* 10 (6). https://doi.org/10.1371/journal.pgen.1004410.
- 24. Brauer, Chris J., Jonathan Sandoval-Castillo, Katie Gates, Michael P. Hammer, Peter J. Unmack, Louis Bernatchez, and Luciano B. Beheregaray. 2023. "Natural Hybridization Reduces Vulnerability to Climate Change." *Nature Climate Change* 13 (3). https://doi.org/10.1038/s41558-022-01585-1.
- Broman, Karl W., Hao Wu, Saunak Sen, and Gary A. Churchill. 2003. "R/Qtl: QTL Mapping in Experimental Crosses." *Bioinformatics* 19 (7). https://doi.org/10.1093/bioinformatics/btg112.
- 26. Buerkle, C. Alex, Robert J. Morris, Marjorie A. Asmussen, and Loren H. Rieseberg. 2000. "The Likelihood of Homoploid Hybrid Speciation." *Heredity* 84 (4). https://doi.org/10.1046/j.1365-2540.2000.00680.x.
- 27. Burmeier, Sandra, R. Lutz Eckstein, Tobias W. Donath, and Annette Otte. 2011. "Plant Pattern Development during Early Post-Restoration Succession in Grasslands-a Case Study of Arabis Nemorensis." *Restoration Ecology* 19 (5). https://doi.org/10.1111/j.1526-100X.2010.00668.x.
- 28. Cai, Zhe, Lian Zhou, Ning Ning Ren, Xun Xu, Rong Liu, Lei Huang, Xiao Ming Zheng, et al. 2019. "Parallel Speciation of Wild Rice Associated with Habitat Shifts." *Molecular Biology and Evolution* 36 (5). https://doi.org/10.1093/molbev/msz029.
- 29. Catchen, Julian, Paul A. Hohenlohe, Susan Bassham, Angel Amores, and William A. Cresko. 2013. "Stacks: An Analysis Tool Set for Population Genomics." *Molecular Ecology* 22 (11). https://doi.org/10.1111/mec.12354.
- 30. Ceballos, Gerardo, Paul R. Ehrlich, and Peter H. Raven. 2020. "Vertebrates on the Brink as Indicators of Biological Annihilation and the Sixth Mass Extinction." *Proceedings of the*

- National Academy of Sciences 117 (24): 13596–602. https://doi.org/10.1073/pnas.1922686117.
- 31. Cerise, Martina, Vítor da Silveira Falavigna, Gabriel Rodríguez-Maroto, Antoine Signol, Edouard Severing, He Gao, Annabel van Driel, et al. 2023. "Two Modes of Gene Regulation by *TFL1* Mediate Its Dual Function in Flowering Time and Shoot Determinacy of *Arabidopsis*." *Development (Cambridge)* 150 (23). https://doi.org/10.1242/DEV.202089.
- 32. Charlesworth, Brian. 2020. "How long does it take to fix a favorable mutation, and why should we care?" *The American Naturalist* 195(5): 753–771. https://doi.org/10.1086/708187.
- 33. Cheng, Haoyu, Gregory T. Concepcion, Xiaowen Feng, Haowen Zhang, and Heng Li. 2021. "Haplotype-Resolved de Novo Assembly Using Phased Assembly Graphs with Hifiasm." *Nature Methods* 18 (2). https://doi.org/10.1038/s41592-020-01056-5.
- 34. Cheng, Haoyu, Erich D. Jarvis, Olivier Fedrigo, Klaus Peter Koepfli, Lara Urban, Neil J. Gemmell, and Heng Li. 2022. "Haplotype-Resolved Assembly of Diploid Genomes without Parental Data." *Nature Biotechnology*. https://doi.org/10.1038/s41587-022-01261-x.
- 35. Cho, Lae Hyeon, Jinmi Yoon, and Gynheung An. 2017. "The Control of Flowering Time by Environmental Factors." *Plant Journal* 90 (4). https://doi.org/10.1111/tpj.13461.
- 36. Chunco, Amanda J. 2014. "Hybridization in a Warmer World." *Ecology and Evolution*. https://doi.org/10.1002/ece3.1052.
- 37. Cochrane, Sabine K.J., Jesper H. Andersen, Torsten Berg, Hugues Blanchet, Angel Borja, Jacob Carstensen, Michael Elliott, Herman Hummel, Nathalie Niquil, and Paul E. Renaud. 2016. "What Is Marine Biodiversity? Towards Common Concepts and Their Implications for Assessing Biodiversity Status." *Frontiers in Marine Science*. https://doi.org/10.3389/fmars.2016.00248.
- 38. Cooper, Brandon S., Alisa Sedghifar, W. Thurston Nash, Aaron A. Comeault, and Daniel R. Matute. 2018. "A Maladaptive Combination of Traits Contributes to the Maintenance of a *Drosophila* Hybrid Zone." *Current Biology* 28 (18). https://doi.org/10.1016/j.cub.2018.07.005.
- 39. Core Writing Team, H. Lee and J. Romero (eds.). 2022. "Climate Change 2023: Synthesis Report. Contribution of Working Groups I, II and III to the Sixth Assessment Report of the Intergovernmental Panel on Climate Change." *IPCC* 13 (3).
- 40. Corre, Valérie le, Fabrice Roux, and Xavier Reboud. 2002. "DNA Polymorphism at the *FRIGIDA* Gene in *Arabidopsis thaliana*: Extensive Nonsynonymous Variation Is

- Consistent with Local Selection for Flowering Time." *Molecular Biology and Evolution* 19 (8). https://doi.org/10.1093/oxfordjournals.molbev.a004187.
- 41. Coughlan, Jenn M., and Daniel R. Matute. 2020. "The Importance of Intrinsic Postzygotic Barriers throughout the Speciation Process: Intrinsic Barriers throughout Speciation." *Philosophical Transactions of the Royal Society B: Biological Sciences*. https://doi.org/10.1098/rstb.2019.0533.
- 42. Coulton, Alexander, Alexandra M. Przewieslik-Allen, Amanda J. Burridge, Daniel S. Shaw, Keith J. Edwards, and Gary L.A. Barker. 2020. "Segregation Distortion: Utilizing Simulated Genotyping Data to Evaluate Statistical Methods." *PLoS ONE* 15 (2). https://doi.org/10.1371/journal.pone.0228951.
- 43. Cowie, Robert H., Philippe Bouchet, and Benoît Fontaine. 2022. "The Sixth Mass Extinction: Fact, Fiction or Speculation?" *Biological Reviews* 97 (2). https://doi.org/10.1111/brv.12816.
- 44. Danecek, Petr, James K. Bonfield, Jennifer Liddle, John Marshall, Valeriu Ohan, Martin O. Pollard, Andrew Whitwham, Thomas Keane, Shane A. McCarthy, and Robert M. Davies. 2021. "Twelve Years of SAMtools and BCFtools." *GigaScience* 10 (2). https://doi.org/10.1093/gigascience/giab008.
- 45. Delaneau, Olivier, Halit Ongen, Andrew A. Brown, Alexandre Fort, Nikolaos I. Panousis, and Emmanouil T. Dermitzakis. 2017. "A Complete Tool Set for Molecular QTL Discovery and Analysis." *Nature Communications* 8. https://doi.org/10.1038/ncomms15452.
- 46. Didiano, Teresa J., Nash E. Turley, Georg Everwand, Hanno Schaefer, Michael J. Crawley, and Marc T.J. Johnson. 2014. "Experimental Test of Plant Defence Evolution in Four Species Using Long-Term Rabbit Exclosures." *Journal of Ecology* 102 (3). https://doi.org/10.1111/1365-2745.12227.
- 47. Dittberner, Hannes. 2019. "Evolutionary processes shaping natural variation in two *Brassicaceae* species." PhD thesis, Universität zu Köln. Retrieved from https://kups.ub.uni-koeln.de/10200/.
- 48. Dittberner, Hannes, Christian Becker, Wen Biao Jiao, Korbinian Schneeberger, Norbert Hölzel, Aurélien Tellier, and Juliette de Meaux. 2019. "Strengths and Potential Pitfalls of Hay Transfer for Ecological Restoration Revealed by RAD-Seq Analysis in Floodplain *Arabis* Species." *Molecular Ecology* 28 (17). https://doi.org/10.1111/mec.15194.
- 49. Dittberner, Hannes, Aurelien Tellier, and Juliette de Meaux. 2022. "Approximate Bayesian Computation Untangles Signatures of Contemporary and Historical Hybridization between

- Two Endangered Species." *Molecular Biology and Evolution* 39 (2). https://doi.org/10.1093/molbev/msac015.
- 50. Dobzhansky, Th. 1936. "STUDIES ON HYBRID STERILITY. II. LOCALIZATION OF STERILITY FACTORS IN *DROSOPHILA PSEUDOOBSCURA* HYBRIDS." *Genetics* 21 (2). https://doi.org/10.1093/genetics/21.2.113.
- 51. Dong, Huan, Xiaonan Ma, Pei Zhang, Huan Wang, Xiaoli Li, Jiaxing Liu, Ling Bai, and Chun peng Song. 2020. "Characterization of *Arabidopsis thaliana* Root-Related Mutants Reveals ABA Regulation of Plant Development and Drought Resistance." *Journal of Plant Growth Regulation* 39 (3). https://doi.org/10.1007/s00344-020-10076-6.
- 52. Eichenberg, David, Diana E. Bowler, Aletta Bonn, Helge Bruelheide, Volker Grescho, David Harter, Ute Jandt, Rudolf May, Marten Winter, and Florian Jansen. 2021. "Widespread Decline in Central European Plant Diversity across Six Decades." *Global Change Biology* 27 (5). https://doi.org/10.1111/gcb.15447.
- 53. Ellstrand, Norman C., and Kristina A. Schierenbeck. 2000. "Hybridization as a Stimulus for the Evolution of Invasiveness in Plants?" *Proceedings of the National Academy of Sciences of the United States of America*. https://doi.org/10.1073/pnas.97.13.7043.
- 54. Epskamp, Sacha, Angélique O.J. Cramer, Lourens J. Waldorp, Verena D. Schmittmann, and Denny Borsboom. 2012. "Qgraph: Network Visualizations of Relationships in Psychometric Data." *Journal of Statistical Software* 48. https://doi.org/10.18637/jss.v048.i04.
- 55. Ferguson, Laura, Gorka Sancho, Matthew T. Rutter, and Courtney J. Murren. 2016. "Root Architecture, Plant Size and Soil Nutrient Variation in Natural Populations of Arabidopsis Thaliana." *Evolutionary Ecology* 30 (1). https://doi.org/10.1007/s10682-015-9808-1.
- 56. Fishman, Lila, and Arpiar Saunders. 2008. "Centromere-Associated Female Meiotic Drive Entails Male Fitness Costs in Monkeyflowers." *Science* 322 (5907). https://doi.org/10.1126/science.1161406.
- 57. Geneious Prime® (2024.0.5). Retrieved from https://www.geneious.com/updates/geneious-prime-2024-0.
- 58. Goretti, Daniela, Marina Silvestre, Silvio Collani, Tobias Langenecker, Carla Méndez, Francisco Madueño, and Markus Schmid. 2020. "TERMINAL FLOWER1 Functions as a Mobile Transcriptional Cofactor in the Shoot Apical Meristem." Plant Physiology 182 (4). https://doi.org/10.1104/pp.19.00867.

- 59. Goulet, Benjamin E., Federico Roda, and Robin Hopkins. 2017. "Hybridization in Plants: Old Ideas, New Techniques." *Plant Physiology* 173 (1). https://doi.org/10.1104/pp.16.01340.
- 60. Haley, C. S., and S. A. Knott. 1992. "A Simple Regression Method for Mapping Quantitative Trait Loci in Line Crosses Using Flanking Markers." *Heredity* 69 (4). https://doi.org/10.1038/hdy.1992.131.
- 61. Han, Ting Shen, Chih Chieh Yu, Quan Jing Zheng, Seisuke Kimura, Renske E. Onstein, and Yao Wu Xing. 2024. "Synergistic Polyploidization and Long-Distance Dispersal Enable the Global Diversification of Yellowcress Herbs." *Global Ecology and Biogeography* 33 (3). https://doi.org/10.1111/geb.13798.
- 62. Hanano, Shigeru, and Koji Goto. 2011. "Arabidopsis Terminal Flower1 Is Involved in the Regulation of Flowering Time and Inflorescence Development through Transcriptional Repression." Plant Cell 23 (9). https://doi.org/10.1105/tpc.111.088641.
- 63. Hansen, Michael M., Isabelle Olivieri, Donald M. Waller, and Einar E. Nielsen. 2012. "Monitoring Adaptive Genetic Responses to Environmental Change." *Molecular Ecology*. https://doi.org/10.1111/j.1365-294X.2011.05463.x.
- 64. He, F., K. A. Steige, V. Kovacova, U. Göbel, M. Bouzid, P. D. Keightley, A. Beyer, and J. de Meaux. 2021. "Cis-Regulatory Evolution Spotlights Species Differences in the Adaptive Potential of Gene Expression Plasticity." *Nature Communications* 12 (1). https://doi.org/10.1038/s41467-021-23558-2.
- 65. He, Rui, Shi, Hang, Hu, Man, Zhou, Quan, Dang, Haishan, and Zhang, Quanfa. 2024. "Differential phenotypic plasticity of subalpine trees predicts trait integration under climate warming." *New Phytol* 244: 1074-1085. https://doi.org/10.1111/nph.20067.
- 66. Hedrick, Philip W. 2013. "Adaptive Introgression in Animals: Examples and Comparison to New Mutation and Standing Variation as Sources of Adaptive Variation." *Molecular Ecology*. https://doi.org/10.1111/mec.12415.
- 67. Hermans, Christian, John P. Hammond, Philip J. White, and Nathalie Verbruggen. 2006. "How Do Plants Respond to Nutrient Shortage by Biomass Allocation?" *Trends in Plant Science*. https://doi.org/10.1016/j.tplants.2006.10.007.
- 68. Ho, William Wing Ho, and Detlef Weigel. 2014. "Structural Features Determining Flower-Promoting Activity of *Arabidopsis FLOWERING LOCUS T." Plant Cell* 26 (2). https://doi.org/10.1105/tpc.113.115220.

- 69. Hölzel, Norbert. 2005. "Seedling Recruitment in Flood-Meadow Species: The Effects of Gaps, Litter and Vegetation Matrix." *Applied Vegetation Science* 8 (2). https://doi.org/10.1658/1402-2001(2005)008[0115:srifst]2.0.co;2.
- 70. Hooper, John N.A., John A. Kennedy, and Ronald J. Quinn. 2002. "Biodiversity 'Hotspots', Patterns of Richness and Endemism, and Taxonomic Affinities of Tropical Australian Sponges (*Porifera*)." *Biodiversity and Conservation* 11 (5). https://doi.org/10.1023/A:1015370312077.
- 71. Jalal, Arshad, Carlos Eduardo da Silva Oliveira, Fernando Shintate Galindo, Poliana Aparecida Leonel Rosa, Isabela Martins Bueno Gato, Bruno Horschut de Lima, and Marcelo Carvalho Minhoto Teixeira Filho. 2023. "Regulatory Mechanisms of Plant Growth-Promoting Rhizobacteria and Plant Nutrition against Abiotic Stresses in Brassicaceae Family." *Life*. https://doi.org/10.3390/life13010211.
- 72. Johanson, U., J. West, C. Lister, S. Michaels, R. Amasino, and C. Dean. 2000. "Molecular Analysis of *FRIGIDA*, a Major Determinant of Natural Variation in *Arabidopsis* Flowering Time." *Science* 290 (5490). https://doi.org/10.1126/science.290.5490.344.
- 73. Jung, Ji Yul, Ryoung Shin, and Daniel P. Schachtman. 2009. "Ethylene Mediates Response and Tolerance to Potassium Deprivation in *Arabidopsis*." *Plant Cell* 21 (2). https://doi.org/10.1105/tpc.108.063099.
- 74. Karl, Robert, and Marcus A. Koch. 2014. "Phylogenetic Signatures of Adaptation: The *Arabis hirsuta* Species Aggregate (*Brassicaceae*) Revisited." *Perspectives in Plant Ecology, Evolution and Systematics* 16 (5). https://doi.org/10.1016/j.ppees.2014.06.001.
- 75. Karthika, K. S., Prabha Susan Philip, and S. Neenu. 2020. "*Brassicaceae* Plants Response and Tolerance to Nutrient Deficiencies." In *The Plant Family Brassicaceae*. https://doi.org/10.1007/978-981-15-6345-4 11.
- 76. Kassambara, A. 2022. "Visualization of a Correlation Matrix Using 'Ggplot2." *Package* '*ggcorrplot*'.
- 77. Korfmann, Kevin, Marie Temple-Boyer, Thibaut Sellinger, and Aurélien Tellier. 2024. "Determinants of Rapid Adaptation in Species with Large Variance in Offspring Production." *Molecular Ecology* 33 (10). https://doi.org/10.1111/mec.16982.
- 78. Korves, Tonia M., Karl J. Schmid, Ana L. Caicedo, Charlotte Mays, John R. Stinchcombe, Michael D. Purugganan, and Johanna Schmitt. 2007. "Fitness Effects Associated with the Major Flowering Time Gene *FRIGIDA* in *Arabidopsis thaliana* in the Field." *The American Naturalist* 169 (5). https://doi.org/10.1086/513111.

- 79. Kreiner, Julia M., John R. Stinchcombe, and Stephen I. Wright. 2018. "Population Genomics of Herbicide Resistance: Adaptation via Evolutionary Rescue." *Annual Review of Plant Biology*. https://doi.org/10.1146/annurev-arplant-042817-040038.
- 80. Leeuwen, Casper H.A. van, Judith M. Sarneel, José van Paassen, Winnie J. Rip, and Elisabeth S. Bakker. 2014. "Hydrology, Shore Morphology and Species Traits Affect Seed Dispersal, Germination and Community Assembly in Shoreline Plant Communities." *Journal of Ecology* 102 (4). https://doi.org/10.1111/1365-2745.12250.
- 81. Leeuwen, Casper H.A. van, Merel B. Soons, Laura G.V.T.I. Vandionant, Andy J. Green, and Elisabeth S. Bakker. 2023. "Seed Dispersal by Waterbirds: A Mechanistic Understanding by Simulating Avian Digestion." *Ecography* 2023 (1). https://doi.org/10.1111/ecog.06470.
- 82. Lefebvre, Valérie, Seifollah Poormohammad Kiani, and Mylène Durand-Tardif. 2009. "A Focus on Natural Variation for Abiotic Constraints Response in the Model Species *Arabidopsis thaliana.*" *International Journal of Molecular Sciences*. https://doi.org/10.3390/ijms10083547.
- 83. Leijten, Willeke, Ronald Koes, Ilja Roobeek, and Giovanna Frugis. 2018. "Translating Flowering Time from *Arabidopsis thaliana* to *Brassicaceae* and *Asteraceae* Crop Species." *Plants*. https://doi.org/10.3390/plants7040111.
- 84. Levin, Simon A., Helene C. Muller-Landau, Ran Nathan, and Jérôme Chave. 2003. "The Ecology and Evolution of Seed Dispersal: A Theoretical Perspective." *Annual Review of Ecology, Evolution, and Systematics*. https://doi.org/10.1146/annurev.ecolsys.34.011802.132428.
- 85. Li, Heng, and Richard Durbin. 2009. "Fast and Accurate Short Read Alignment with Burrows-Wheeler Transform." *Bioinformatics* 25 (14). https://doi.org/10.1093/bioinformatics/btp324.
- 86. Li, Heng, Bob Handsaker, Alec Wysoker, Tim Fennell, Jue Ruan, Nils Homer, Gabor Marth, Goncalo Abecasis, and Richard Durbin. 2009. "The Sequence Alignment/Map Format and SAMtools." *Bioinformatics* 25 (16). https://doi.org/10.1093/bioinformatics/btp352.
- 87. Li, Juan, Molly Schumer, and Claudia Bank. 2022. "Imbalanced Segregation of Recombinant Haplotypes in Hybrid Populations Reveals Inter- and Intrachromosomal Dobzhansky-Muller Incompatibilities." *PLoS Genetics* 18 (3). https://doi.org/10.1371/journal.pgen.1010120.

- 88. Lososová, Zdeňka, Irena Axmanová, Milan Chytrý, Gabriele Midolo, Sylvain Abdulhak, Dirk Nikolaus Karger, Julien Renaud, Jérémie Van Es, Pascal Vittoz, and Wilfried Thuiller. 2023. "Seed Dispersal Distance Classes and Dispersal Modes for the European Flora." *Global Ecology and Biogeography* 32 (9). https://doi.org/10.1111/geb.13712.
- 89. Lu, H., J. Romero-Severson, and R. Bernardo. 2002. "Chromosomal Regions Associated with Segregation Distortion in Maize." *Theoretical and Applied Genetics* 105 (4). https://doi.org/10.1007/s00122-002-0970-9.
- 90. Lynch, Jonathan. 1995. "Root Architecture and Plant Productivity." *Plant Physiology*. https://doi.org/10.1104/pp.109.1.7.
- 91. Lynch, Jonathan P. 2019. "Root Phenotypes for Improved Nutrient Capture: An Underexploited Opportunity for Global Agriculture." *New Phytologist*. https://doi.org/10.1111/nph.15738.
- 92. Lynch, Jonathan P., Tania Galindo-Castañeda, Hannah M. Schneider, Jagdeep Singh Sidhu, Harini Rangarajan, and Larry M. York. 2023. "Root Phenotypes for Improved Nitrogen Capture." *Plant and Soil*. https://doi.org/10.1007/s11104-023-06301-2.
- 93. Lyttle, Terrence W. 1993. "Cheaters Sometimes Prosper: Distortion of Mendelian Segregation by Meiotic Drive." *Trends in Genetics* 9 (6). https://doi.org/10.1016/0168-9525(93)90120-7.
- 94. Ma, Yongpeng, Tobias Marczewski, Dan Xue, Zhikun Wu, Rongli Liao, Weibang Sun, and Jane Marczewski. 2019. "Conservation Implications of Asymmetric Introgression and Reproductive Barriers in a Rare *Primrose* Species." *BMC Plant Biology* 19 (1). https://doi.org/10.1186/s12870-019-1881-0.
- 95. Malik, Harmit S. 2005. "*Mimulus* Finds Centromeres in the Driver's Seat." *Trends in Ecology and Evolution*. https://doi.org/10.1016/j.tree.2005.01.014.
- 96. Mallet, James. 2007. "Hybrid Speciation." *Nature*. Nature Publishing Group. https://doi.org/10.1038/nature05706.
- 97. Mallet, James, Nora Besansky, and Matthew W. Hahn. 2016. "How Reticulated Are Species?" *BioEssays* 38 (2). https://doi.org/10.1002/bies.201500149.
- 98. Manrique-Carpintero, Norma C., Joseph J. Coombs, Richard E. Veilleux, C. Robin Buell, and David S. Douches. 2016. "Comparative Analysis of Regions with Distorted Segregation in Three Diploid Populations of Potato." G3: Genes, Genomes, Genetics 6 (8). https://doi.org/10.1534/g3.116.030031.

- 99. Maple, Robert, Pan Zhu, Jo Hepworth, Jia Wei Wang, and Caroline Dean. 2024. "Flowering Time: From Physiology, through Genetics to Mechanism." *Plant Physiology*. https://doi.org/10.1093/plphys/kiae109.
- 100. Marçais, Guillaume, and Carl Kingsford. 2011. "A Fast, Lock-Free Approach for Efficient Parallel Counting of Occurrences of k-Mers." *Bioinformatics* 27 (6): 764–70. https://doi.org/10.1093/bioinformatics/btr011.
- 101. Martin, Arnaud, and Virginie Orgogozo. 2013. "The Loci of Repeated Evolution: A Catalog of Genetic Hotspots of Phenotypic Variation." *Evolution* 67 (5). https://doi.org/10.1111/evo.12081.
- 102. Martin, Marcel. 2011. "Cutadapt Removes Adapter Sequences from High-Throughput Sequencing Reads." *EMBnet.Journal* 17 (1). https://doi.org/10.14806/ej.17.1.200.
- 103. Masly, John P., and Daven C. Presgraves. 2007. "High-Resolution Genome-Wide Dissection of the Two Rules of Speciation in *Drosophila*." *PLoS Biology* 5 (9). https://doi.org/10.1371/journal.pbio.0050243.
- 104. Mathar, Wanja, Till Kleinebecker, and Norbert Hölzel. 2015. "Environmental Variation as a Key Process of Co-Existence in Flood-Meadows." *Journal of Vegetation Science* 26 (3). https://doi.org/10.1111/jvs.12254.
- 105. Moore, Jean Sébastien, and Andrew P. Hendry. 2009. "Can Gene Flow Have Negative Demographic Consequences? Mixed Evidence from Stream Threespine Stickleback." *Philosophical Transactions of the Royal Society B: Biological Sciences* 364 (1523). https://doi.org/10.1098/rstb.2009.0007.
- Moran, Benjamin M., Cheyenne Y. Payne, Daniel L. Powell, Erik N.K. Iverson, Alexandra E. Donny, Shreya M. Banerjee, Quinn K. Langdon, et al. 2024. "A Lethal Mitonuclear Incompatibility in Complex I of Natural Hybrids." *Nature* 626 (7997). https://doi.org/10.1038/s41586-023-06895-8.
- 107. Muller, HJ J. 1942. "Isolating Mechanisms, Evolution and Temperature." *Biol. Symp*.
- 108. Nathan, Ran. 2006. "Long-Distance Dispersal of Plants." *Science*. https://doi.org/10.1126/science.1124975.
- 109. Nathan, Ran, Frank M. Schurr, Orr Spiegel, Ofer Steinitz, Ana Trakhtenbrot, and Asaf Tsoar. 2008. "Mechanisms of Long-Distance Seed Dispersal." *Trends in Ecology and Evolution*. https://doi.org/10.1016/j.tree.2008.08.003.

- 110. Nocchi, Gabriele, Jing Wang, Long Yang, Junyi Ding, Ying Gao, Richard J.A. Buggs, and Nian Wang. 2023. "Genomic Signals of Local Adaptation and Hybridization in Asian White Birch." *Molecular Ecology* 32 (3). https://doi.org/10.1111/mec.16788.
- 111. Ober, Eric S., Samir Alahmad, James Cockram, Cristian Forestan, Lee T. Hickey, Josefine Kant, Marco Maccaferri, et al. 2021. "Wheat Root Systems as a Breeding Target for Climate Resilience." *Theoretical and Applied Genetics*. https://doi.org/10.1007/s00122-021-03819-w.
- 112. Ohgushi, Takayuki. 2016. "Eco-Evolutionary Dynamics of Plant-Herbivore Communities: Incorporating Plant Phenotypic Plasticity." *Current Opinion in Insect Science*. https://doi.org/10.1016/j.cois.2016.01.006.
- 113. Olson-Manning, Carrie F., Maggie R. Wagner, and Thomas Mitchell-Olds. 2012. "Adaptive Evolution: Evaluating Empirical Support for Theoretical Predictions." *Nature Reviews Genetics*. https://doi.org/10.1038/nrg3322.
- 114. Owens, Gregory L., Marco Todesco, Natalia Bercovich, Jean Sébastien Légaré, Nora Mitchell, Kenneth D. Whitney, and Loren H. Rieseberg. 2021. "Standing Variation Rather than Recent Adaptive Introgression Probably Underlies Differentiation of the *Texanus* Subspecies of *Helianthus Annuus*." In *Molecular Ecology*. Vol. 30. https://doi.org/10.1111/mec.16008.
- 115. Peñalba, Joshua v., Anna Runemark, Joana I. Meier, Pooja Singh, Guinevere O.U. Wogan, Rosa Sánchez-Guillén, James Mallet, et al. 2024. "The Role of Hybridization in Species Formation and Persistence." *Cold Spring Harbor Perspectives in Biology*. https://doi.org/10.1101/cshperspect.a041445.
- 116. Pfennig, Karin S., Audrey L. Kelly, and Amanda A. Pierce. 2016. "Hybridization as a Facilitator of Species Range Expansion." *Proceedings of the Royal Society B: Biological Sciences*. https://doi.org/10.1098/rspb.2016.1329.
- 117. Powell, Daniel L., Mateo García-Olazábal, Mackenzie Keegan, Patrick Reilly, Kang Du, Alejandra P. Díaz-Loyo, Shreya Banerjee, et al. 2020. "Natural Hybridization Reveals Incompatible Alleles That Cause Melanoma in Swordtail Fish." *Science* 368 (6492). https://doi.org/10.1126/science.aba5216.
- 118. Presgraves, Daven C. 2010. "The Molecular Evolutionary Basis of Species Formation." *Nature Reviews Genetics*. https://doi.org/10.1038/nrg2718.
- 119. Ranallo-Benavidez, T. Rhyker, Kamil S. Jaron, and Michael C. Schatz. 2020. "GenomeScope 2.0 and Smudgeplot for Reference-Free Profiling of Polyploid Genomes." *Nature Communications* 11 (1). https://doi.org/10.1038/s41467-020-14998-3.

- 120. Ratcliffe, Oliver J., Iraida Amaya, Coral A. Vincent, Steven Rothstein, Rosemary Carpenter, Enrico S. Coen, and Desmond J. Bradley. 1998. "A Common Mechanism Controls the Life Cycle and Architecture of Plants." *Development* 125 (9). https://doi.org/10.1242/dev.125.9.1609.
- 121. Rhymer, Judith M., and Daniel Simberloff. 1996. "Extinction by Hybridization and Introgression." *Annual Review of Ecology and Systematics* 27. https://doi.org/10.1146/annurev.ecolsys.27.1.83.
- 122. Rich, Sarah M., Anton P. Wasson, Richard A. Richards, Trushna Katore, Renu Prashar, Ritika Chowdhary, D. C. Saxena, et al. 2016. "Wheats Developed for High Yield on Stored Soil Moisture Have Deep Vigorous Root Systems." *Functional Plant Biology* 43 (2). https://doi.org/10.1071/FP15182.
- 123. Rieseberg, Loren H., Olivier Raymond, David M. Rosenthal, Zhao Lai, Kevin Livingstone, Takuya Nakazato, Jennifer L. Durphy, Andrea E. Schwarzbach, Lisa A. Donovan, and Christian Lexer. 2003. "Major Ecological Transitions in Wild Sunflowers Facilitated by Hybridization." *Science* 301 (5637). https://doi.org/10.1126/science.1086949.
- 124. Rivera-Colón, Angel G., and Julian Catchen. 2022. "Population Genomics Analysis with RAD, Reprised: Stacks 2." In *Methods in Molecular Biology*. Vol. 2498. https://doi.org/10.1007/978-1-0716-2313-8_7.
- 125. Rosas, Ulises, Angelica Cibrian-Jaramillo, Daniela Ristova, Joshua A. Banta, Miriam L. Gifford, Angela Huihui Fan, Royce W. Zhou, et al. 2013. "Integration of Responses within and across *Arabidopsis* Natural Accessions Uncovers Loci Controlling Root Systems Architecture." *Proceedings of the National Academy of Sciences of the United States of America* 110 (37). https://doi.org/10.1073/pnas.1305883110.
- 126. Rosser, Neil, Fernando Seixas, Lucie M. Queste, Bruna Cama, Ronald Mori-Pezo, Dmytro Kryvokhyzha, Michaela Nelson, et al. 2024. "Hybrid Speciation Driven by Multilocus Introgression of Ecological Traits." *Nature* 628 (8009): 811–17. https://doi.org/10.1038/s41586-024-07263-w.
- 127. Schlaepfer, Martin A., and Joshua J. Lawler. 2023. "Conserving Biodiversity in the Face of Rapid Climate Change Requires a Shift in Priorities." *Wiley Interdisciplinary Reviews: Climate Change* 14 (1). https://doi.org/10.1002/wcc.798.
- 128. Schloerke, Barret, Di Cook, Joseph Larmarange, Francois Briatte, Moritz Marbach, Edwin Thoen, Amos Elberg, et al. 2020. "Ggally: Extension to Ggplot2." R Package Version 0.5.0. 2020.

- 129. Schmickl, Roswitha, Sarah Marburger, Sian Bray, and Levi Yant. 2017. "Hybrids and Horizontal Transfer: Introgression Allows Adaptive Allele Discovery." *Journal of Experimental Botany*. https://doi.org/10.1093/jxb/erx297.
- 130. Schneider, Hannah M., Lynch, Jonathan P. 2024. "Root Architecture and Nutrient Acquisition." In *Plant Roots The Hidden Half.* https://doi.org/10.1201/b23126.
- 131. Schnittler, M., and K. F. Günther. 1999. "Central European Vascular Plants Requiring Priority Conservation Measures An Analysis from National Red Lists and Distribution Maps." *Biodiversity and Conservation* 8 (7). https://doi.org/10.1023/A:1008828704456.
- 132. Schumer, Molly, and Yaniv Brandvain. 2016. "Determining Epistatic Selection in Admixed Populations." *Molecular Ecology* 25 (11). https://doi.org/10.1111/mec.13641.
- 133. Schumer, Molly, Rongfeng Cui, Daniel L. Powell, Rebecca Dresner, Gil G. Rosenthal, and Peter Andolfatto. 2014. "High-Resolution Mapping Reveals Hundreds of Genetic Incompatibilities in Hybridizing Fish Species." *ELife* 2014 (3). https://doi.org/10.7554/eLife.02535.
- 134. Schumer, Molly, Rongfeng Cui, Gil G. Rosenthal, and Peter Andolfatto. 2015. "Reproductive Isolation of Hybrid Populations Driven by Genetic Incompatibilities." *PLoS Genetics* 11 (3). https://doi.org/10.1371/journal.pgen.1005041.
- 135. Schumer, Molly, Chenling Xu, Daniel L. Powell, Arun Durvasula, Laurits Skov, Chris Holland, John C. Blazier, et al. 2018. "Natural Selection Interacts with Recombination to Shape the Evolution of Hybrid Genomes." *Science* 360 (6389). https://doi.org/10.1126/science.aar3684.
- 136. Seehausen, Ole. 2004. "Hybridization and Adaptive Radiation." *Trends in Ecology and Evolution*. https://doi.org/10.1016/j.tree.2004.01.003.
- 137. Serrano-Mislata, Antonio, Pedro Fernańdez-Nohales, María J. Domeńech, Yoshie Hanzawa, Desmond Bradley, and Francisco Maduenño. 2016. "Separate Elements of the *TERMINAL FLOWER 1* Cis-Regulatory Region Integrate Pathways to Control Flowering Time and Shoot Meristem Identity." *Development (Cambridge)* 143 (18). https://doi.org/10.1242/dev.135269.
- 138. Shalit, Akiva, Alexander Rozman, Alexander Goldshmidt, John P. Alvarez, John L. Bowman, Yuval Eshed, and Eliezer Lifschitz. 2009. "The Flowering Hormone Florigen Functions as a General Systemic Regulator of Growth and Termination." *Proceedings of the National Academy of Sciences of the United States of America* 106 (20). https://doi.org/10.1073/pnas.0810810106.

- 139. Siegmund, Jonatan F., Marc Wiedermann, Jonathan F. Donges, and Reik v. Donner. 2016. "Impact of Temperature and Precipitation Extremes on the Flowering Dates of Four German Wildlife Shrub Species." *Biogeosciences* 13 (19). https://doi.org/10.5194/bg-13-5541-2016.
- 140. Sim, Sheina B., Renee L. Corpuz, Tyler J. Simmonds, and Scott M. Geib. 2022. "HiFiAdapterFilt, a Memory Efficient Read Processing Pipeline, Prevents Occurrence of Adapter Sequence in PacBio HiFi Reads and Their Negative Impacts on Genome Assembly." *BMC Genomics* 23 (1). https://doi.org/10.1186/s12864-022-08375-1.
- 141. Singh, Amar Pal, Yulia Fridman, Neta Holland, Michal Ackerman-Lavert, Rani Zananiri, Yvon Jaillais, Arnon Henn, and Sigal Savaldi-Goldstein. 2018. "Interdependent Nutrient Availability and Steroid Hormone Signals Facilitate Root Growth Plasticity." *Developmental Cell* 46 (1). https://doi.org/10.1016/j.devcel.2018.06.002.
- 142. Smit, A F A, R Hubley, and P Grenn. 2015. "RepeatMasker Open-4.0." RepeatMasker Open-4.0.7.
- 143. Soppe, Wim J.J., Natanael Viñegra de la Torre, and Maria C. Albani. 2021. "The Diverse Roles of *FLOWERING LOCUS C* in Annual and Perennial *Brassicaceae* Species." *Frontiers in Plant Science*. https://doi.org/10.3389/fpls.2021.627258.
- 144. Staudinger, Michelle D, Nancy B Grimm, Amanda Staudt, Shawn F Carter, F Stuart Chapin, Peter Kareiva, Mary Ruckelshaus, and Bruce A Stein. 2012. "Impacts of Climate Change on Biodiversity, Ecosystems, and Ecosystem Services: Technical Input to the 2013 National Climate Assessment." Cooperative Report to the 2013 National Climate Assessment.
- 145. Stotz, Gisela C., Cristian Salgado-Luarte, Víctor M. Escobedo, Fernando Valladares, and Ernesto Gianoli. 2021. "Global Trends in Phenotypic Plasticity of Plants." *Ecology Letters* 24 (10). https://doi.org/10.1111/ele.13827.
- 146. Talbert, Paul B., and Steven Henikoff. 2020. "What Makes a Centromere?" *Experimental Cell Research* 389 (2). https://doi.org/10.1016/j.yexcr.2020.111895.
- 147. Taylor, Julian, and David Butler. 2017. "R Package ASMap: Efficient Genetic Linkage Map Construction and Diagnosis." *Journal of Statistical Software* 79. https://doi.org/10.18637/jss.v079.i06.
- 148. Tejada-Jiménez, Manuel, Ángel Llamas, Emanuel Sanz-Luque, Aurora Galván, and Emilio Fernández. 2007. "A High-Affinity Molybdate Transporter in Eukaryotes." *Proceedings of the National Academy of Sciences of the United States of America* 104 (50). https://doi.org/10.1073/pnas.0704646104.

- 149. Thawornwattana, Yuttapong, Fernando Seixas, Ziheng Yang, and James Mallet. 2023. "Major Patterns in the Introgression History of *Heliconius* Butterflies." *ELife* 12. https://doi.org/10.7554/eLife.90656.
- 150. Theissinger, Kathrin, Carlos Fernandes, Giulio Formenti, Iliana Bista, Paul R. Berg, Christoph Bleidorn, Aureliano Bombarely, et al. 2023. "How Genomics Can Help Biodiversity Conservation." *Trends in Genetics*. https://doi.org/10.1016/j.tig.2023.01.005.
- 151. Todesco, Marco, Gregory L. Owens, Natalia Bercovich, Jean Sébastien Légaré, Shaghayegh Soudi, Dylan O. Burge, Kaichi Huang, et al. 2020. "Massive Haplotypes Underlie Ecotypic Differentiation in Sunflowers." *Nature* 584 (7822). https://doi.org/10.1038/s41586-020-2467-6.
- 152. Todesco, Marco, Mariana A. Pascual, Gregory L. Owens, Katherine L. Ostevik, Brook T. Moyers, Sariel Hübner, Sylvia M. Heredia, et al. 2016. "Hybridization and Extinction." *Evolutionary Applications*. https://doi.org/10.1111/eva.12367.
- 153. Tun, Win, Jinmi Yoon, Jong Seong Jeon, and Gynheung An. 2021. "Influence of Climate Change on Flowering Time." *Journal of Plant Biology*. https://doi.org/10.1007/s12374-021-09300-x.
- 154. Wang, Renhou, Sara Farrona, Coral Vincent, Anika Joecker, Heiko Schoof, Franziska Turck, Carlos Alonso-Blanco, George Coupland, and Maria C. Albani. 2009. "PEP1 Regulates Perennial Flowering in *Arabis Alpina*." *Nature* 459 (7245). https://doi.org/10.1038/nature07988.
- 155. Wang, Richard J., Michael A. White, and Bret A. Payseur. 2015. "The Pace of Hybrid Incompatibility Evolution in House Mice." *Genetics* 201 (1). https://doi.org/10.1534/genetics.115.179499.
- 156. Wang, Shuang, Yiman Yang, Fadi Chen, and Jiafu Jiang. 2022. "Functional Diversification and Molecular Mechanisms of *FLOWERING LOCUS T/TERMINAL FLOWER 1* Family Genes in Horticultural Plants." *Molecular Horticulture*. https://doi.org/10.1186/s43897-022-00039-8.
- 157. Wells, Carolyn L., and Massimo Pigliucci. 2000. "Adaptive Phenotypic Plasticity: The Case of Heterophylly in Aquatic Plants." *Perspectives in Plant Ecology, Evolution and Systematics* 3 (1). https://doi.org/10.1078/1433-8319-00001.
- 158. White, Michael A., Brian Steffy, Tim Wiltshire, and Bret A. Payseur. 2011. "Genetic Dissection of a Key Reproductive Barrier between Nascent Species of House Mice." *Genetics* 189 (1). https://doi.org/10.1534/genetics.111.129171.

- 159. White, Michael A., Maria Stubbings, Beth L. Dumont, and Bret A. Payseur. 2012. "Genetics and Evolution of Hybrid Male Sterility in House Mice." *Genetics* 191 (3). https://doi.org/10.1534/genetics.112.140251.
- 160. Whitney, Kenneth D., Rebecca A. Randell, and Loren H. Rieseberg. 2010. "Adaptive Introgression of Abiotic Tolerance Traits in the Sunflower *Helianthus Annuus*." *New Phytologist* 187 (1). https://doi.org/10.1111/j.1469-8137.2010.03234.x.
- 161. Wickham, Hadley. 2011. "Ggplot2." *Wiley Interdisciplinary Reviews: Computational Statistics* 3 (2): 180–85. https://doi.org/10.1002/wics.147.
- 162. Wilczek, Amity M., Judith L. Roe, Mary C. Knapp, Martha D. Cooper, Cristina Lopez-Gallego, Laura J. Martin, Christopher D. Muir, et al. 2009. "Effects of Genetic Perturbation on Seasonal Life History Plasticity." *Science* 323 (5916). https://doi.org/10.1126/science.1165826.
- 163. Wu, Zeng Yuan, Richard I. Milne, Jie Liu, Ran Nathan, Richard T. Corlett, and De Zhu Li. 2023. "The Establishment of Plants Following Long-Distance Dispersal." *Trends in Ecology and Evolution*. https://doi.org/10.1016/j.tree.2022.11.003.
- 164. Yin, Jingjing, Weibo Ren, Ellen L. Fry, Ke Xu, Kairi Qu, Kairu Gao, Hailong Bao, and Fenghui Guo. 2024. "Clonal Transgenerational Effects of Parental Grazing Environment on Offspring Shade Avoidance" *Agronomy* 14 (5): 1085. https://doi.org/10.3390/agronomy14051085.
- 165. Zuellig, Matthew P., and Andrea L. Sweigart. 2018. "Gene Duplicates Cause Hybrid Lethality between Sympatric Species of *Mimulus*." *PLoS Genetics* 14 (4). https://doi.org/10.1371/journal.pgen.1007130.

Data Availability

All the codes and input data, including extensive tables of genotypic and phenotypic data for all three chapters, are available in a GitHub repository at the following link:

https://github.com/nedarahnama/Neda Rahnamae PhD Thesis Appendix

The genome assembly and *.fastq files containing raw reads for all individuals used in the analyses are available on the European Nucleotide Archive (ENA) under project number [PRJEB89863].